

Two-Stage Stochastic Mixed Integer Nonlinear Programming: Theory, Algorithms, and Applications

Yingqiu Zhang

Dissertation submitted to the Faculty of the
Virginia Polytechnic Institute and State University
in partial fulfillment of the requirements for the degree of

Doctor of Philosophy

in

Industrial and System Engineering

Manish Bansal, Chair

Douglas R. Bish

Adolfo R. Escobedo

Robert Hildebrand

Subhash C. Sarin

August 18, 2021

Blacksburg, Virginia

Keywords: Two-stage stochastic p -order conic mixed integer programming,
two-stage stochastic quadratic integer programs, scenario-based cuts, conic mixed
integer rounding, dual decomposition, stochastic load shed recovery

Copyright 2021, Yingqiu Zhang

Two-Stage Stochastic Mixed Integer Nonlinear Programming: Theory, Algorithms, and Applications

Yingqiu Zhang

(ABSTRACT)

With the rapidly growing need for long-term decision making in the presence of stochastic future events, it is important to devise novel mathematical optimization tools and develop computationally efficient solution approaches for solving them. Two-stage stochastic programming is one of the powerful modeling tools that allows probabilistic data parameters in mixed integer programming, a well-known tool for optimization modeling with deterministic input data. However, akin to the mixed integer programs, these stochastic models are theoretically intractable and computationally challenging to solve because of the presence of integer variables. This dissertation focuses on theory, algorithms and applications of two-stage stochastic mixed integer (non)linear programs and it has three-pronged plan. In the first direction, we study two-stage stochastic p -order conic mixed integer programs (TSS-CMIPs) with p -order conic terms in the second-stage objectives. We develop so called scenario-based (non)linear cuts which are added to the deterministic equivalent of TSS-CMIPs (a large-scale deterministic conic mixed integer program). We provide conditions under which these cuts are sufficient to relax the integrality restrictions on the second-stage integer variables without impacting the integrality of the optimal solution of the TSS-CMIP. We also introduce a multi-module capacitated stochastic facility location problem and TSS-CMIPs

with structured CMIPs in the second stage to demonstrate the significance of the foregoing results for solving these problems. In the second direction, we propose risk-neutral and risk-averse two-stage stochastic mixed integer linear programs for load shed recovery with uncertain renewable generation and demand. The models are implemented using a scenario-based approach where the objective is to maximize load shed recovery in the bulk transmission network by switching transmission lines and performing other corrective actions (e.g. generator re-dispatch) after the topology is modified. Experiments highlight how the proposed approach can serve as an offline contingency analysis tool, and how this method aids self-healing by recovering more load shedding. In the third direction, we develop a dual decomposition approach for solving two-stage stochastic quadratically constrained quadratic mixed integer programs. We also create a new module for an open-source package **DSP** (Decomposition for Structured Programming) to solve this problem. We evaluate the effectiveness of this module and our approach by solving a stochastic quadratic facility location problem.

Two-Stage Stochastic Mixed Integer Nonlinear Programming: Theory, Algorithms, and Applications

Yingqiu Zhang

(GENERAL AUDIENCE ABSTRACT)

With the rapidly growing need for long-term decision making in the presence of stochastic future events, it is important to devise novel mathematical optimization tools and develop computationally efficient solution approaches for solving them. Two-stage stochastic programming is one of the powerful modeling tools that allows two-stages of decision making where the first-stage strategic decisions (such as deciding the locations of facilities or topology of a power transmission network) are taken before the realization of uncertainty, and the second-stage operational decisions (such as transportation decisions between customers and facilities or power flow in the transmission network) are taken in response to the first-stage decision and a realization of the uncertain (demand) data. This modeling tool is gaining wide acceptance because of its applications in healthcare, power systems, wildfire planning, logistics, and chemical industries, among others. Though intriguing, two-stage stochastic programs are computationally challenging. Therefore, it is crucial to develop theoretical results and computationally efficient algorithms, so that these models for real-world applied problems can be solved in a realistic time frame. In this dissertation, we consider two-stage stochastic mixed integer (non)linear programs, provide theoretical and algorithmic results for them, and introduce their applications in logistics and power systems. First,

we consider a two-stage stochastic mixed integer program with p -order conic terms in the objective that has applications in facility location problem, power system, portfolio optimization, and many more. We provide a so-called second-stage convexification technique which greatly reduces the computational time to solve a facility location problem, in comparison to solving it directly with a state-of-the-art solver, CPLEX, with its default settings. Second, we introduce risk-averse and risk-neutral two-stage stochastic models to deal with uncertainties in power systems, as well as the risk preference of decision makers. We leverage the inherent flexibility of the bulk transmission network through the systematic switching of transmission lines in/out of service while accounting for uncertainty in generation and demand during an emergency. We provide abundant computational experiments to quantify our proposed models, and justify how the proposed approach can serve as an offline contingency analysis tool. Third, we develop a new solution approach for two-stage stochastic mixed integer programs with quadratic terms in the objective function and constraints and implement it as a new module for an open-source package DSP. We perform computational experiments on a stochastic quadratic facility location problem to evaluate the performance of this module.

Dedication

To my parents.

Acknowledgments

This research is funded by National Science Foundation Grant CMMI- 1824897 and Junior Faculty Award of Institute for Critical Technology and Applied Science at Virginia Tech, which are gratefully acknowledged. I am also thankful to INTERN (Non-Academic Research Internships for Graduate Students) supplemental program of National Science Foundation for funding my internship (off-site GRA) at Argonne National Laboratory. This dissertation would not have been possible without help, support and guidance from many people. I would like to express my gratitude for all of them.

First and foremost, my heartfelt gratitude goes to my advisor, Dr. Manish Bansal, for his encouragement, patience, support, and advice. His passion and attitude always motivated me to improve myself and conquer difficulties. Dr. Bansal always gave me valuable advice and suggestions about research and life. During my hardest time, Dr. Bansal told me “Challenges are a part of life, so it is important to learn how to deal with them.” I will always remember his word. I was fortune to have Dr. Bansal as my advisor, and I am forever grateful for his inspiration and support.

I also thank the rest of my committee members: Dr. Douglas R. Bish, Dr. Adolfo R. Escobedo, Dr. Robert Hildebrand, and Dr. Subhash C. Sarin, for give me valuable and insightful feedback to improve this dissertation.

I would like to express my gratitude to the ISE department faculty and staff for providing a great research environment. I would also thank my friends: Fangzhou,

Guangrui, Jie, Jing, Shuyuan, Wenjing, Yi, and many more, and my lab mates Kartik and Parshin, for making my years at Virginia Tech an enjoyable experience. Finally, I thank my mother Yandong Yin and my father Hui Zhang for their everlasting love and support throughout my life, which endowed me with power and energy to overcome difficulties.

Contents

List of Figures	xv
List of Tables	xvii
1 Introduction	1
1.1 State-of-the-Art Mathematical Optimization Tools	2
1.2 Two-Stage Stochastic p -order Conic Mixed Integer Programming . . .	6
1.3 Two-Stage Stochastic Mixed Integer Quadratically Constrained Quadratic Programming	8
1.4 Applications of TSS-MILP in Power Systems	10
1.5 Outline and Contributions of This Dissertation	11
2 Necessary Background	14
2.1 Convex Hull and Partial Convex Hull	14
2.1.1 Convex Hull	14
2.1.2 Partial Convex Hull	16
2.2 Cut-Generation Procedures	17
2.3 Dual Decomposition Method for TSS-MILPs	19

2.3.1	Lagrangian Relaxation of TSS-MILP	20
2.3.2	Dual Search Method: Cutting-Plane Method	22
3	Scenario-based Cuts for Two-stage Stochastic p-order Conic Mixed Integer Programs	24
3.1	Introduction	24
3.1.1	Deterministic Polyhedral Conic Mixed Integer Sets	26
3.1.2	Structured Two-Stage Stochastic and Distributionally Robust p -Order Conic Mixed Integer Programs	27
3.1.3	Multi-Module Capacitated Stochastic Facility Location Problem with Subcontracting	29
3.1.4	Organization of This Chapter	32
3.2	Literature Review	33
3.2.1	Literature Review on Special Cases of TSS-CMIP and TSDR-CMIP	33
3.2.2	Brief literature review on CMIPs	36
3.3	(Partial) Convex Hull for Deterministic Polyhedral Conic Mixed Integer Sets	37
3.4	Reformulation of Second Stage of TSS-CMIPs and TSDR-CMIPs	41
3.5	Scenario-Based Cuts for Extensive Formulation of TSS-CMIPs	43

3.6	Structured Two-Stage Stochastic and Distributionally Robust p -Order Conic Mixed Integer Programs	45
3.6.1	Tight Second Stage Formulations for Structured TSS-CMIPs and TSDR-CMIPs	45
3.6.2	Scenario-Based Cuts for Extensive Formulation of Structured TSS-CMIPs	59
3.6.3	Tight Second Stage Formulation and Partial Convex Hull for the Extensive Formulation of MM-SFLP-S	62
3.7	Computational Experiments	64
3.7.1	Generation of MM-SFLP-S and MM-DRFLP-S Test Instances	64
3.7.2	Generation of Structured TSS-CMIP Test Instances	65
3.7.3	Computational Framework	68
3.8	Conclusion	77
4	Risk-Neutral and Risk-Averse Transmission Switching for Load Shed Recovery	79
4.1	Introduction	79
4.2	Stochastic Optimal Load Shed Recovery	86
4.2.1	Risk-Neutral Stochastic DC Optimal Load Shed Recovery With Transmission Switching	86

4.2.2	Risk-Averse Stochastic DC Optimal Load Shed Recovery with Transmission Switching	91
4.3	Evaluation of Stochastic Models for LSR	93
4.3.1	Evaluation of Risk-Neutral LSR Solution	94
4.3.2	An Illustrative Example: A 6-bus System	95
4.3.3	Evaluation of Risk-Averse CVaR-LSR Solution	97
4.4	Computational Experiments	97
4.4.1	Test Cases and Instance Generation	98
4.4.2	Test Cases and Instance Generation	98
4.4.3	Experimental Framework	101
4.5	Results and Analysis	102
4.5.1	Computational Results for Risk-Neutral Stochastic LSR	102
4.5.2	Computational Results of Risk-Averse CVaR-Based LSR	107
4.5.3	Computational Results using Larger Number of Scenarios	109
4.5.4	Practical Implications	110
4.6	Conclusion	113
5	Two-stage Stochastic Mixed-integer Quadratically Constrained Quadratic Programming	115
5.1	Introduction	115

5.2	Literature Review: TSS-MIQCQP	116
5.3	Dual Decomposition for TSS-MIQCQP	118
5.4	An Open-source Package: Decomposition of Structured Programs (DSP)	120
5.4.1	DSP: Review	121
5.4.2	Extension of DSP	122
5.5	Stochastic Quadratic Capacitated Facility Location Problem	124
5.5.1	Literature of Quadratic Facility Location Problem	125
5.5.2	Generation of SQCFL Test Instances	128
5.5.3	Computational Framework of SQCFL Test Instances	129
5.6	Conclusion	130
6	Conclusion	132
	Appendices	135
A	Appendix for Chapter 3	136
A.1	Proof of Theorem 3.8	136
A.2	Tight Second Stage Formulations for Structured TSS-CMIPs	139
A.2.1	Proof of Corollary 3.10	139

A.3	Partial Convex Hull for Extensive Formulation of Structured TSS- CMIPs	140
A.3.1	Proof of Corollary 3.13	140
A.3.2	Proof of Corollary 3.14	140
A.3.3	Proof of Corollary 3.15	141
A.4	Deterministic Polyhedral Conic Mixed Integer Sets	141
A.4.1	Proof of Theorem 3.4	141
A.4.2	Proof of Theorem 3.5	142
A.4.3	Proof of Theorem 3.6	142
	Bibliography	144

List of Figures

1.1	Sequential Decision-Making using TSSP.	4
2.1	Set S_1 and its linear programming relaxation.	15
2.2	Convex hull of set S_1	15
2.3	A partial convex hull of set S_1 , i.e., $S_{1,\text{pch}}$: Two red vertical line segments	16
2.4	A partial convex hull of set S_1 , i.e., $\bar{S}_{1,\text{pch}}$: Two red horizontal line segments and a point.	17
2.5	MIR cuts.	18
2.6	CMIR cuts.	20
4.1	Decision making process for stochastic LSR.	87
4.2	A 6-bus system.	95
4.3	%LSR with different switching limits for IEEE 118-bus test case.	103
4.4	VSS for RN-LSR with different switching limits for IEEE 118-bus test case.	103
4.5	BD time with number of scenarios for IEEE 14-bus test case	105
4.6	%LSR with number of scenarios for IEEE 14-bus test case	105

5.1	SolverInterface Class	122
5.2	Model class.	123
5.3	Sovler Class	123

List of Tables

3.1	Details of TSS-CMIP Instances with $p = 1$ and E_{ω}^j is network flow matrix	67
3.2	Details of TSS-CMIP Instances with $p = 2$ and $E_{\omega}^j = \mathbf{I}$	67
3.3	Details of TSS-CMIP Instances with $p = 2$ and E_{ω}^j is network flow matrix	67
3.4	Results of Computational Experiments for the MM-SFLP-S Instances	71
3.5	Results of Computational Experiments for the MM-DRFLP-S Instances	72
3.6	Results of Computational Experiments for TSS-CMIPs with $p = 1$ and E_{ω}^j for all $j \in J$ are network flow matrices	73
3.7	Results of Computational Experiments for TSS-CMIPs with $p = 2$ and $E_{\omega}^j = \mathbf{I}$	74
3.8	Results of Computational Experiments for TSDR-CMIPs with $p = 2$ and $E_{\omega}^j = \mathbf{I}$	76
3.9	Computational Results for TSS-CMIPs where $p = 2$ and E_{ω}^j for $j \in J$ are network flow matrices	77
4.1	Deterministic demand and two scenarios of stochastic demand for the 6-bus system (in MW)	96

4.2	A List of Contingencies for IEEE 118-bus Test Case	101
4.3	Results for Computational Experiments with Different Risk Coefficient and Confidence Interval	108
4.4	Computational Results for RN-LSR and CVaR-LSR Models	110
5.1	Computational results of SQCFL random generated instances	130

Chapter 1

Introduction

Mathematical Optimization toolbox provides a variety of algebraic methods to formulate optimization problems in science, military, engineering, and business. During World War II, the need to efficiently manage scarce resources led to the origin of an algebraic modeling tool, referred to as linear programming (or linear optimization). Since then, the mathematical optimization toolbox has been evolving to address various optimization problems arising in applications such as production and inventory planning, logistics, healthcare, wildfire planning, power systems, bioinformatics, chemical industries, and many more. Currently, this toolbox includes nonlinear programming, mixed integer (non)linear programming, stochastic optimization, and distributionally robust optimization, among others. It allows a decision maker to handle decisions of discrete nature, nonlinear objective functions and constraints, probabilistic input data parameters, and adjustments based on the level of risk-aversion of the decision maker. As a consequence, better (or optimal) decisions can be made to save lives, time, and money.

With the rapidly growing need to make long-term policy planning with probabilistic (future demand or cost) data, stochastic programming in two-stage setting is gaining wide acceptance. This is because it allows two-stages of decision making where the first-stage strategic decisions (such as deciding the locations of facilities

or topology of a power transmission network) are taken before the realization of uncertainty, and the second-stage operational decisions (such as transportation decisions between customers and facilities or power flow in the transmission network) are taken in response to the first-stage decision and a realization of the uncertain (demand) data. Though intriguing, two-stage stochastic programs are computationally challenging. Therefore, it is crucial to develop theoretical results and computationally efficient algorithms, so that these models for real-world applied problems can be solved in a realistic timeframe. In this dissertation, we consider two-stage stochastic mixed integer (non)linear programs, provide theoretical and algorithmic results for them, and introduce their applications in logistics and power systems.

1.1 State-of-the-Art Mathematical Optimization Tools

A mathematical optimization problem involves minimizing (or maximizing) an objective function of a set of decision variables subject to constraints on the decision variables. Generally, it is defined as follows:

$$\text{minimize } f_0(x) \tag{1.1a}$$

$$\text{s.t. } f_i(x) \leq 0, \quad i = 1, \dots, m, \tag{1.1b}$$

where $x = (x_1, \dots, x_n) \in \mathbb{R}^n$ is a vector of n decision variables, and $f_i : \mathbb{R}^n \rightarrow \mathbb{R}$, $i = 0, 1, \dots, m$, are functions of x . In this formulation, inequalities (1.1b) and

function f_0 are referred to as constraints and objective function, respectively.

Based on the properties of objective function, constraints, and decision variables, Problem (1.1) can be classified into different categories:

- (i) Linear Program (LP): Problem (1.1) is referred to as a linear program when the objective function and constraints are of linear form, i.e., $f_0(x) := c^\top x$ and $f_i(x) := a_i x$ where $c \in \mathbb{R}^n$ and $a_i \in \mathbb{R}^n$ for $i \in \{1, \dots, m\}$.
- (ii) Nonlinear Program (NLP): Problem (1.1) with at least one nonlinear function $f_i(x)$, for $i \in \{0, 1, \dots, m\}$, is referred to as a nonlinear program.
- (iii) Mixed Integer Linear Program (MILP): A linear program with additional integrality restrictions on a subset of the decision variables, i.e., $x \in \mathbb{R}^{n-m} \times \mathbb{Z}^m$ where $m > 0$, is referred to as mixed integer linear program.
- (iv) Mixed Integer Nonlinear Program (MINLP): Similar to MILP, a nonlinear program with additional integrality restrictions on a subset of the decision variables is referred to as mixed integer nonlinear program. MINLPs can be further categorized. Two categories of MINLPs, pertinent to this dissertation, are as follows: mixed integer p -order conic program (for $p \geq 1$) and mixed integer quadratically constrained quadratic program, where the objective function and/or constraints have l_p norm or quadratic terms, respectively.

All aforementioned tools provide powerful deterministic modeling frameworks for decision-making, assuming that all input data parameters are known. However in reality, decisions are not always made under deterministic conditions. For an example, manufacturing companies have to make decisions to procure different types

of raw material to produce products, even with incomplete information of products' demand, which is uncertain. Failure to incorporate the uncertainties may result in poor planning and hence, high expected cost. Two-stage stochastic programming (TSSP) [27] is a well-known framework for sequential decision-making that allows uncertain data parameters represented by a random vector whose probability distribution is known. The decision process is shown in Figure 1.1, where ω denotes a realization/scenario of the random vector ξ defined over a sample space Ω :

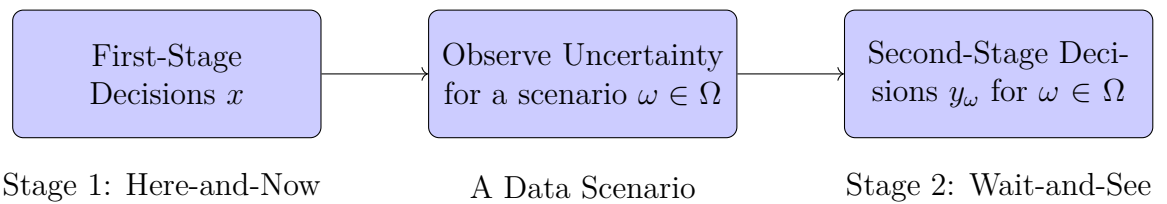


Figure 1.1: Sequential Decision-Making using TSSP.

According to Figure 1.1, the first subset of decisions x is made using available data and before the realization of uncertainties, which is referred to as the first-stage (or here-and-now) decisions; whereas the remaining decisions i.e., y_ω for $\omega \in \Omega$, referred to as the second-stage (or wait-and-see) decisions that depend on the first-stage decisions, are made after the information is received on the realization of the random vector ξ . In TSSPs, the cost of second-stage decisions (or corrective actions) is measured as a recourse function, and we seek a solution that optimizes the expected value of the objective function for the probability distribution followed by the uncertain parameters. Applications of TSSPs exist in numerous domains, such as facility location [138], health care [81], unit commitment [80], optimal power flow [141], supply chain [145], and many more.

Dantzig [43] introduced two-stage stochastic linear programs (TSS-LPs) to tackle

uncertainty in input parameters of a linear program. Researchers have further extended this framework to introduce two-stage stochastic mixed integer programs [2, 27, 28, 83, 84], which is defined as follows.

$$z = \min \{c^\top x + \mathbb{E}_\xi[\mathcal{Q}_\omega(x)] : Ax \geq b, x \in \mathbb{Z}^{\bar{n}_1} \times \mathbb{R}^{n_1 - \bar{n}_1}\} \quad (1.2)$$

where for each scenario ω of $\boldsymbol{\xi}$, the recourse function of the second stage problem is given by:

$$\mathcal{Q}_\omega(x) := \min g_\omega^\top y_\omega \quad (1.3a)$$

$$\text{s.t. } W_\omega y_\omega \geq h_\omega - T_\omega x \quad (1.3b)$$

$$y_\omega \in \mathbb{Z}^{\bar{n}_2} \times \mathbb{R}^{n_2 - \bar{n}_2}. \quad (1.3c)$$

Here, y_ω is the vector of second-stage decisions corresponding to scenario $\omega \in \Omega$, W_ω is referred to as the recourse matrix, and T_ω is referred to as the technology matrix. For TSS-MILPs with finite sample space Ω where probability of the occurrence of scenario $\omega \in \Omega$ is p_ω , the deterministic equivalent formulation (DEF) of problem (1.2) is given by

$$z = \min c^\top x + \sum_{\omega \in \Omega} p_\omega g_\omega^\top y_\omega \quad (1.4)$$

$$\text{s.t. } W_\omega y_\omega \geq h_\omega - T_\omega x, \quad \omega \in \Omega, \quad (1.5)$$

$$x \in \mathbb{Z}^{\bar{n}_1} \times \mathbb{R}^{n_1 - \bar{n}_1}, y_\omega \in \mathbb{Z}^{\bar{n}_2} \times \mathbb{R}^{n_2 - \bar{n}_2}, \quad \omega \in \Omega. \quad (1.6)$$

The DEF is a large-scale (block-angular structured) mixed-integer program whose size (number of variables and constraints) increases with the increase in the number

of scenarios.

In this dissertation, we propose to study two generalizations of the TSS-MILPs, i.e., two-stage stochastic p -order conic mixed integer programs (TSS-CMIPs) and two-stage stochastic mixed integer quadratically constrained quadratic programming (TSS-MIQCQPs). Since the foregoing problems involve discrete variables, uncertain data parameters, and nonlinear terms, they are computationally more challenging than TSS-MILPs. Therefore, it is crucial to develop efficient solution approaches (cutting planes and decomposition algorithms) for the TSS-CMIPs and TSS-MIQCQPs (refer to Sections 1.2 and 1.3, respectively). Furthermore, we introduce TSS-MILP models for load shed recovery in power systems with uncertain renewable generation and demand (refer to Section 1.4).

1.2 Two-Stage Stochastic p -order Conic Mixed Integer Programming

A p -order conic mixed-integer program is a nonlinear nonconvex problem whose feasible region is defined by linear constraints, p -order conic constraints, and integrality constraints. It generalizes various optimization frameworks such as MILP and quadratically constrained convex quadratic mixed integer program, and arises in applications ranging from portfolio optimization to machine learning [4, 94]. We study TSS-CMIPs where the first stage problem has pure integer variables and the second stage problems have the sum of l_p -norms in the objective function along

with integer variables. More specifically, the TSS-CMIP is defined as follows:

$$\min \{c^\top x + \mathbb{E}_\xi[\overline{\mathcal{Q}}_\omega(x)] : Ax \geq b, x \in \mathbb{Z}^{n_1}\}, \quad (1.7)$$

where the random variable ξ follows a known probability distribution P with a finite sample space Ω , and for a given x and a scenario $\omega \in \Omega$ with \bar{p}_ω probability of occurrence:

$$\overline{\mathcal{Q}}_\omega(x) := \min \left\{ g_\omega^\top y_\omega + \sum_{j \in J} \hat{g}_\omega^j \|E_\omega^j y_\omega^j + F_\omega^j x - h_\omega^j\|_p : \right. \\ \left. W_\omega y_\omega \geq r_\omega - T_\omega x, y_\omega^j \in \mathbb{Z}^q, j \in J \right\},$$

which is equivalent to

$$\overline{\mathcal{Q}}_\omega(x) := \min g_\omega^\top y_\omega + \sum_{j \in J} \hat{g}_\omega^j d_{\omega,0}^j \quad (1.8a)$$

$$\text{s.t. } W_\omega y_\omega \geq r_\omega - T_\omega x, \quad (1.8b)$$

$$\|E_\omega^j y_\omega^j + F_\omega^j x - h_\omega^j\|_p \leq d_{\omega,0}^j, \quad j \in J, \quad (1.8c)$$

$$y_\omega^j \in \mathbb{Z}^q, d_{\omega,0}^j \in \mathbb{R}_+, \quad j \in J. \quad (1.8d)$$

Here, $\|\cdot\|_p$ denotes l_p -norm, i.e., $\|y\|_p = (\sum_k |y_k|^p)^{1/p}$ for $p \geq 1$, $c \in \mathbb{R}^{n_1}$, $A \in \mathbb{R}^{m_1 \times n_1}$, $b \in \mathbb{R}^{m_1}$, and for each $\omega \in \Omega$ and $j \in J := \{1, \dots, |J|\}$, $g_\omega \in \mathbb{R}^{|J|}$, $\hat{g}_\omega^j \in \mathbb{R}$, $E_\omega^j \in \mathbb{R}^{m_2 \times q}$, $F_\omega^j \in \mathbb{R}^{m_2 \times n_1}$, $h_\omega^j \in \mathbb{R}^{m_2}$, $W_\omega \in \mathbb{R}^{m_3 \times q|J|}$, $T_\omega \in \mathbb{R}^{m_3 \times n_1}$, and $r_\omega \in \mathbb{R}^{m_3}$.

We note that by setting $J = \emptyset$, our proposed TSS-CMIP becomes TSS-MILP. Hence, TSS-MILP is a special case of TSS-CMIP. Moreover, the deterministic

equivalent of TSS-CMIP is given by:

$$\min c^\top x + \sum_{\omega \in \Omega} \bar{p}_\omega \left(g_\omega^\top y_\omega + \sum_{j \in J} \hat{g}_\omega^j d_{\omega,0}^j \right) \quad (1.9a)$$

$$\text{s.t. } Ax \geq b, \quad T_\omega x + W_\omega y_\omega \geq r_\omega, \quad \omega \in \Omega, \quad (1.9b)$$

$$\|F_\omega^j x + E_\omega^j y_\omega^j - h_\omega^j\|_p \leq d_{\omega,0}^j, \quad j \in J, \quad \omega \in \Omega, \quad (1.9c)$$

$$(x, y, d) \in \mathbb{Z}^{n_1} \times (\mathbb{Z}^{q_1} \times \mathbb{R}^{q-q_1})^{|\Omega| \times |J|} \times \mathbb{R}_+^{|\Omega| \times |J|}, \quad (1.9d)$$

which is a large-scale p -order conic mixed integer program.

1.3 Two-Stage Stochastic Mixed Integer Quadratically Constrained Quadratic Programming

Mixed integer quadratically constrained quadratic program (MIQCQP) is a nonlinear nonconvex optimization problem that involves discrete variables and quadratic terms in both objective functions and constraints. MIQCQP is hard to solve due to its nonlinear and nonconvex properties. Nevertheless, MIQCQPs have been widely applied to applications in power system [47, 88], portfolio selection problem [42], process system [106, 120], transportation problem [32, 38], and many more. In this dissertation, we propose to study a two-stage stochastic variant of the MIQCQP, which is denoted by TSS-MIQCQP and is defined as follows:

$$\min \left\{ \frac{1}{2} x^\top P^{xx} x + c^\top x + \mathbb{E}_\xi[\mathcal{Q}_\omega(x)] : Ax \geq b, x \in X \right\} \quad (1.10)$$

where ξ is observed with probability p_ω for a scenario ω from a finite sample space

Ω . For $\omega \in \Omega$, the recourse function is defined as,

$$\mathcal{Q}_\omega(x) := \min \frac{1}{2} y_\omega^\top P_{\omega,0}^{yy} y_\omega + x^\top P_{\omega,0}^{xy} y_\omega + q_{\omega,0}^\top y_\omega \quad (1.11)$$

$$\text{s.t. } \frac{1}{2} [x; y_\omega]^\top P_{\omega,i} [x; y_\omega] + q_{\omega,i}^\top [x; y_\omega] + d_\omega^i \leq 0, \quad i = 1, \dots, I \quad (1.12)$$

$$y_\omega \in Y \quad (1.13)$$

where sets $X \subseteq \mathbb{R}^{n_1}$ and $Y \subseteq \mathbb{R}^{n_2}$ represent integer or binary restrictions on some or all of the decision variables x and y_ω for $\omega \in \Omega$, respectively. In the first stage problem (1.10), we have parameters $A \in \mathbb{R}^{m_1 \times n_1}$, $b \in \mathbb{R}^{m_1}$, and P^{xx} is a $n_1 \times n_1$ positive semidefinite matrix. In the second stage problem (1.11)-

(1.13), for $\omega \in \Omega$ and $i = 1, \dots, I$, we have $P_{\omega,i} = \begin{bmatrix} P_{\omega,i}^{xx} & P_{\omega,i}^{xy} \\ P_{\omega,i}^{yx} & P_{\omega,i}^{yy} \end{bmatrix} \in \mathbb{R}^{(n_1+n_2) \times (n_1+n_2)}$,

$q_{\omega,i} = \begin{bmatrix} q_{\omega,i}^x \\ q_{\omega,i}^y \end{bmatrix} \in \mathbb{R}^{1 \times (n_1+n_2)}$, and $d_\omega^i \in \mathbb{R}$; $P_{\omega,i}^{xx}$ and $P_{\omega,i}^{yy}$ are $n_1 \times n_1$ and $n_2 \times n_2$

submatrices of $P_{\omega,i}$, respectively; $q_{\omega,i}^x$ and $q_{\omega,i}^y$ are vectors in \mathbb{R}^{n_1} and \mathbb{R}^{n_2} space, respectively. Constraints (1.12) can be written as

$$\frac{1}{2} x^\top P_{\omega,i}^{xx} x + \frac{1}{2} y_\omega^\top P_{\omega,i}^{yy} y_\omega + \frac{1}{2} x^\top P_{\omega,i}^{xy} y_\omega + \frac{1}{2} y_\omega^\top P_{\omega,i}^{yx} x^\top + q_{\omega,i}^{x\top} x + q_{\omega,i}^{y\top} y_\omega + d_\omega^i \leq 0.$$

We assume $P^{xx} \succ 0$, $P_{\omega,0}^{yy} \succ 0$, and $P_{\omega,i} \succeq 0$ for $i = 1, \dots, I$ and $\omega \in \Omega$, to ensure that the extensive formulation of the problem obtained after relaxing integrality restrictions in TSS-MIQCQP is convex. We note that when $P^{xx} = 0$ and $P_{\omega,i} = 0$ for $i = 0, 1, \dots, I$, the TSS-MIQCQP reduces to TSS-MILP.

1.4 Applications of TSS-MILP in Power Systems

Maintaining a reliable source of power is a fundamental goal of large electrical networks. Unfortunately, disruption events continuously pose risks to the system and can ultimately trigger power outages, i.e., short-term or long-term electric power disconnections of certain areas/customers. Imbalances in total energy supply and demand are among the main causes of power outages, at times forcing electric utilities to interrupt service in certain areas by automatic and/or manual disconnection or shedding of loads. An outage must be recovered within 90 minutes as requested by Federal Energy Regulatory Commission (FERC) [52], because the damages of power outages become more severe as the recovery time lengthens. Even though self-healing capabilities of today's smart grid can minimize blackouts by performing continuous self-assessments to detect, analyze, respond to, and as needed, restore grid components or network sections [111], power outages still affect everyday life and cause huge losses in the U.S. Power outages caused more than \$1 trillion worth of damage due to weather from 1980 to 2014 [34] and annual financial losses of \$44 billion in 2015 [1] in the U.S. Indeed, each U.S. electricity user experienced an average of 1.3 electrical outage events, or equivalently 250 minutes of disconnected service, in 2016.

One of the main desired capabilities of the smart grid is “self-healing”, which is the ability to quickly restore power after a disturbance. Due to critical outage events, customer demand or load is at times disconnected or shed temporarily. While deterministic optimization models have been devised to help operators expedite load shed recovery by harnessing the flexibility of the grid's topology (i.e., transmission switching), an important issue that remains unaddressed is how to cope with the

uncertainty in generation and demand encountered during the recovery process. In this research direction, we introduce two-stage stochastic models to deal with these uncertain parameters, and one of them incorporates conditional value-at-risk to measure the risk level of the unrecovered load shed.

1.5 Outline and Contributions of This Dissertation

In this dissertation, we develop scenario-based valid inequalities and efficient algorithms to solve two important generalizations of TSS-MILP, i.e., TSS-CMIP and TSS-MIQCQP. We also intend to develop a package for our proposed algorithms based on the open-source software: DSP (Decomposition for Structured Programming) [80] and packages maintained by COIN-OR [96]. Furthermore, we study the application of TSS-MIP in power systems. In the rest of this section, we present an outline of this dissertation along with more details about its contributions.

In Chapter 2, we introduce some concepts and algorithms known in the literature to build a background necessary to explain results presented in this dissertation. We present the definition of convex hull and partial convex hull, two cut-generation procedures: mixed integer rounding and conic mixed integer rounding, and dual decomposition method for solving TSS-MILPs.

In Chapter 3, we introduce two-stage stochastic p -order conic mixed integer programs (denoted by TSS-CMIPs) in which the second stage problems have p -order conic constraints along with integer variables. First, we present sufficient condi-

tions under which the addition of sparse nonlinear cuts in the extensive formulation of TSS-CMIPs is sufficient to relax the integrality restrictions on the second stage integer variables without impacting the integrality of the optimal solution of the TSS-CMIP. We also consider TSS-CMIPs with structured p -order CMIPs in the second stage and derive classes of globally valid parametric (non)-linear cuts for them. These cuts provide conic linear (or convex) programming equivalent, under certain conditions, for the second stage CMIPs. Our cuts for TSS-CMIPs with $p = 1$ satisfy the aforementioned sufficient conditions. We also perform extensive computational experiments by solving randomly generated structured TSS-CMIPs with polyhedral CMIPs and second-order CMIPs in the second stage, i.e. $p = 1$ and $p = 2$, respectively, and observe that there is a significant reduction in the total time taken to solve these problems after adding our sparse cuts. Finally, we demonstrate the significance of our results for TSS-CMIP in deriving (partial) convex hull for deterministic multi-constraint conic mixed integer sets with multiple integer variables. This study extends the result of Atamtürk and Narayanan [7] for a simple polyhedral conic mixed integer set with a single constraint and one integer variable.

In Chapter 4, we introduce stochastic load shed recovery models (S-LSR) to handle the uncertainty of generation and demand, and incorporate conditional value-at-risk (CVaR) for measuring the risk level of unrecovered load in power systems. This paper builds on the previous work of Escobedo, Moreno-Centeno, and Hedman [51] on deterministic models where data parameters are assumed to be fixed and known. We leverage the inherent flexibility of the bulk transmission network through the systematic switching of transmission lines in/out of service while ac-

counting for uncertainty in generation and demand during an emergency. These stochastic models are implemented using a scenario-based approach where the objective is to maximize load shed recovery in the bulk transmission network by switching transmission lines and performing other corrective actions (e.g., generator re-dispatch) after the topology is modified. The benefits of the proposed stochastic programming models are quantified via comparisons with a deterministic mean-value model, using the IEEE 14-bus and 118-bus test cases. Experiments and discussions highlight how the proposed approach can serve as an offline contingency analysis tool.

In Chapter 5, we study two-stage stochastic quadratically constrained quadratic programs (TSS-MIQCQPs). More specifically, we present dual decomposition for TSS-MIQCQPs, and add new features to open-source package DSP to implement extensive formulation and dual decomposition for solving TSS-MIQCQPs. We also introduce a stochastic quadratic facility location problem and perform computational experiments on this problem using the aforementioned new feature in DSP. The computational results illustrate the significance of our extension of DSP.

Chapter 2

Necessary Background

In this chapter, we introduce some concepts and algorithms known in the literature to build a background necessary to explain results presented in this dissertation. We present the definition of convex hull and partial convex hull [19], two cut-generation procedures: mixed integer rounding [113] and conic mixed integer rounding [7], and dual decomposition method [35] for solving TSS-MILPs.

2.1 Convex Hull and Partial Convex Hull

2.1.1 Convex Hull

The convex hull of a set S is the inclusion-wise minimal convex set that contains S , which is denoted as $\text{conv}(S)$. Suppose there are N points, i.e., $\hat{x}_i \in S$, for $i = 1, \dots, N$, then $\text{conv}(S)$ is defined as follows,

$$\text{conv}(S) = \left\{ \sum_{i=1}^N \lambda_i \hat{x}_i : \sum_{i=1}^N \lambda_i = 1, \lambda_i \geq 0, \hat{x}_i \in S, \forall i = 1, \dots, N \right\}.$$

In other words, every convex combination of points in set S must be in set $\text{conv}(S)$. We provide an example integer set $S_1 := \{(x_1, x_2) \in \mathbb{Z}_+^2 : 3x_1 + 2x_2 \leq 5\}$, which is

equivalent to set of five integer points $\{(1, 0), (0, 0), (0, 1), (0, 2), (1, 1)\}$ as shown in Figure 2.1. The linear programming relaxation of set S_1 , i.e., $\text{LPrelax}(S_1) := \{(x_1, x_2) \in \mathbb{R}_+^2 : 3x_1 + 2x_2 \leq 5\}$, is color (red) filled triangle in the figure. We observe that set S_1 is nonconvex and noncontinuous.

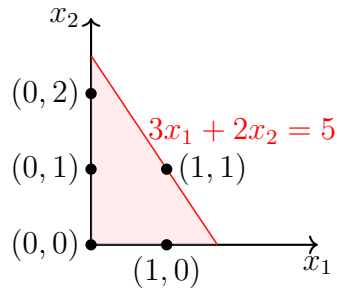


Figure 2.1: Set S_1 and its linear programming relaxation.

The convex hull of this set is blue region with boundaries in Figure 2.2, which is convex and continuous, i.e., $\text{conv}(S_1) = \{(x_1, x_2) \in \mathbb{R}_+ \times \mathbb{R}_+ : x_1 \leq 1, x_1 + x_2 \leq 2\}$. In order to solve a mixed integer program $\min\{c^\top x : x \in S\}$ where c is a real vector with the same dimension as x , it is sufficient to solve a linear program $\min\{c^\top x : x \in \text{conv}(S)\}$, where the feasible region of this linear program is the convex relaxation of set S .

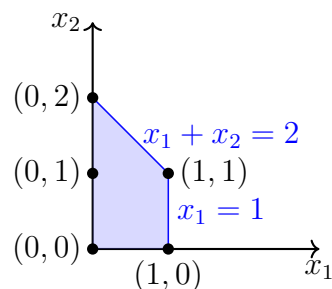


Figure 2.2: Convex hull of set S_1 .

2.1.2 Partial Convex Hull

Definition 2.1. [Bansal et al. [19]] A partial convex hull of a mixed integer set S is another mixed integer set S_{pch} such that $S \subseteq S_{\text{pch}} \subseteq \text{conv}(S) = \text{conv}(S_{\text{pch}})$.

The set S_{pch} is a subset of convex hull of the set S and has a lesser number of integrality constraints (but possibly more linear or nonlinear inequalities) than S . Whereas in comparison to $\text{conv}(S)$, S_{pch} might have fewer inequalities but more integrality constraints. We provide a partial convex hull of the aforementioned set S_1 in Figure 2.3 (represented by two red line segments), and denote it by $S_{1,\text{pch}} = \{(x_1, x_2) \in \mathbb{Z}_+ \times \mathbb{R}_+ : x_1 \leq 1, x_1 + x_2 \leq 2\}$. Observe that $S_{1,\text{pch}}$ has one more linear constraint compared with S_1 , i.e., $x_1 \leq 1$, and the integrality restriction on x_2 is relaxed, but x_1 is still an integer variable. Moreover, $S_1 \subseteq S_{1,\text{pch}} \subseteq \text{conv}(S_1) \subseteq \text{conv}(S_{1,\text{pch}})$.

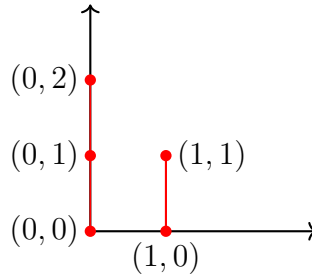


Figure 2.3: A partial convex hull of set S_1 , i.e., $S_{1,\text{pch}}$: Two red vertical line segments

Unlike convex hull, a mixed integer set can have multiple different partial convex hulls. For example, another partial convex hull of S_1 is $\bar{S}_{1,\text{pch}} = \{(x_1, x_2) \in \mathbb{R}_+ \times \mathbb{Z}_+ : x_1 \leq 1, x_1 + x_2 \leq 2\}$, which is represented in Figure 2.4 by two red line segments and one point $(0, 2)$. For $\bar{S}_{1,\text{pch}}$, the integrality restriction on x_1 has been relaxed, but x_2 remains to be integral.

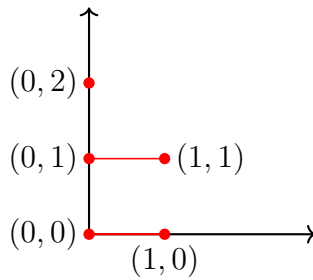


Figure 2.4: A partial convex hull of set S_1 , i.e., $\bar{S}_{1,\text{pch}}$: Two red horizontal line segments and a point.

2.2 Cut-Generation Procedures

An inequality of the form $\pi^\top x \geq \pi_0$, where $\pi \in \mathbb{R}^n$ and $\pi_0 \in \mathbb{R}$, is valid for set $S \subseteq \mathbb{R}^n$ if it is satisfied for every point in S , i.e., $\pi^\top \hat{x} \geq \pi_0$ for all $\hat{x} \in S$ or $S \subseteq S \cap \{x \in \mathbb{R}^n : \pi^\top x \geq \pi_0\}$. Such inequalities are referred to as valid inequalities for the set. To solve mixed integer (non)linear programs, valid inequalities are added to their continuous relaxation in order to cut off the fractional extreme points of the continuous relaxation and obtain a tighter continuous relaxation. This procedure is referred to as the cutting plane method and therefore, the valid inequalities are also referred to as cuts or cutting planes. In this section, we will introduce two cut-generation procedures: mixed integer rounding (MIR) cuts [147] and conic mixed integer rounding (CMIR) cuts [7] for mixed integer linear programs and conic mixed integer programs, respectively. To develop these cut-generation procedures, researchers studied polyhedral structures of simple (conic) mixed integer sets.

Mixed Integer Rounding Cuts. Consider a simple mixed integer set with single constraint and one integer variable, $Z = \{(\nu, s) \in \mathbb{R}_+ \times \mathbb{Z} : s - \nu \leq \rho\}$, where $\rho \in \mathbb{R}$. The convex hull of Z is obtained by adding the following so-called MIR

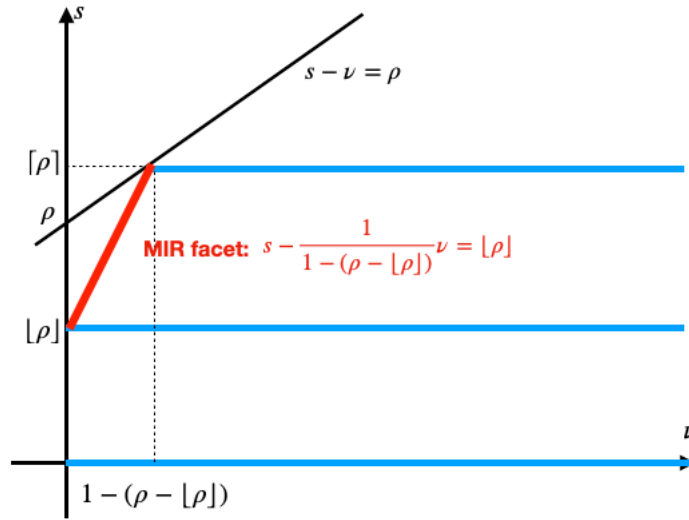


Figure 2.5: MIR cuts.

cut to the linear programming relaxation of Z [113, 147]:

$$s - \frac{1}{1 - (\rho - \lfloor \rho \rfloor)} \nu \leq \lfloor \rho \rfloor. \quad (2.1)$$

In Figure 2.5, set Z is presented in blue and the hyperplane corresponding to the MIR cut is in red.

Various generalizations of MIR cut-generation procedure includes mixed MIR [65], continuous mixing [143], n -step MIR [77], continuous multi-mixing MIR [14, 16], and mingled n -step mixing MIR [15], among many others. These generalizations have been derived by analyzing the polyhedral structure and developing facet-defining valid inequalities for multi-constraint mixed integer sets with multiple integer variables and continuous variables in each constraints (reader can refer to Bansal and Kianfar [15] for more details).

Conic Mixed Integer Rounding Cuts. To generalize MIR cuts for MINLPs,

Atamtürk and Narayanan [7] consider a single-constraint conic mixed integer set with one integer variable, i.e., $\bar{Z} := \{(\sigma, v, \rho_0) \in \mathbb{Z} \times \mathbb{R}_+^2 : \sqrt{(\sigma - \beta)^2 + v^2} \leq \rho_0\}$, where $\beta \in \mathbb{R}$. By adding additional continuous variables, set \bar{Z} can be reformulated as,

$$Z := \{(\sigma, v, \rho_0, \rho_1, \rho_2) \in \mathbb{Z} \times \mathbb{R}_+^4 : |\sigma - \beta| \leq \rho_1, |v| \leq \rho_2, \sqrt{\rho_1^2 + \rho_2^2} \leq \rho_0\}.$$

Let $Z_1 = \{(\sigma, \rho_1) \in \mathbb{Z} \times \mathbb{R}_+ : |\sigma - \beta| \leq \rho_1\}$, $Z_2 = \{(v, \rho_2) \in \mathbb{Z} \times \mathbb{R}_+ : |v| \leq \rho_2\}$, and $Z_3 = \{(\rho_1, \rho_2) \in \mathbb{R}_+^2 : \sqrt{\rho_1^2 + \rho_2^2} \leq \rho_0\}$. Note that $Z = Z_1 \cap Z_2 \cap Z_3$. The conic MIR inequality

$$(1 - 2\beta^{(1)}) (\sigma - \lfloor \beta \rfloor) + \beta^{(1)} \leq \rho_1 \quad (2.2)$$

where $\beta^{(1)} = \beta - \lfloor \beta \rfloor$, is a facet defining inequality for Z_1 . Figure 2.6 illustrates set Z_1 and CMIR cuts (2.2). The fractional point $(\beta, 0)$ of the linear relaxation of Z_1 is cut off by adding inequality (2.2). Hence, the convex hull of Z_1 is

$$\text{conv}(Z_1) = \{(\sigma, \rho_1) \in \mathbb{R} \times \mathbb{R}_+ : |\sigma - \beta| \leq \rho_1, (1 - 2\beta^{(1)}) (\sigma - \lfloor \beta \rfloor) + \beta^{(1)} \leq \rho_1\}.$$

2.3 Dual Decomposition Method for TSS-MILPs

In this section, we present Lagrangian relaxation based approach (referred to as dual decomposition method) of Carøe and Schultz [35] to derive a lower bound for TSS-MILP with mixed integer variables in both stages. In [35], a branch-

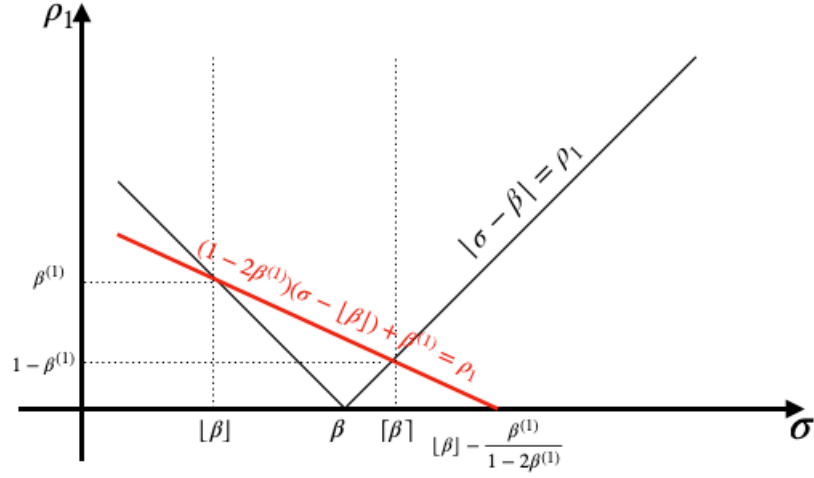


Figure 2.6: CMIR cuts.

and-bound method to solve TSS-MILP has also been provided, which utilizes this bounding procedure at each node.

2.3.1 Lagrangian Relaxation of TSS-MILP

For the dual decomposition method, we derive a Lagrangian relaxation of TSS-MILP as follows. Let $\Omega := \{\omega_1, \dots, \omega_{|\Omega|}\}$. We add auxiliary variables $x_{\omega_1}, x_{\omega_2}, \dots, x_{\omega_{|\Omega|}} \in \mathbb{Z}^{\bar{n}_1} \times \mathbb{R}^{n_1 - \bar{n}_1}$ and constraints $x_{\omega_1} = x_{\omega_2} = \dots = x_{\omega_{|\Omega|}} = x$ in problem (1.3) to get an equivalent reformulation

$$z = \min \sum_{\omega \in \Omega} p_{\omega} (c^{\top} x_{\omega} + g_{\omega}^{\top} y_{\omega}) \quad (2.3a)$$

$$\text{s.t. } W_{\omega} y_{\omega} \geq h_{\omega} - T_{\omega} x_{\omega}, \quad \omega \in \Omega, \quad (2.3b)$$

$$x_{\omega_i} - x_{\omega_{i+1}} = \mathbf{0}, \quad i \in \{1, \dots, |\Omega| - 1\}, \quad (2.3c)$$

$$x_{\omega} \in \mathbb{Z}^{\bar{n}_1} \times \mathbb{R}^{n_1 - \bar{n}_1}, y_{\omega} \in \mathbb{Z}^{\bar{n}_2} \times \mathbb{R}^{n_2 - \bar{n}_2}, \quad \omega \in \Omega. \quad (2.3d)$$

Constraints (2.3c) are referred to as nonanticipativity constraints and in compact form are written as $\sum_{\omega \in \Omega} H_\omega x_\omega = \mathbf{0}$ where $\mathbf{0}$ denotes zero vector of appropriate dimensions. A Lagrangian relaxation of (2.3) is obtained by dualizing constraints (2.3c) using dual variable $\lambda \in \mathbb{R}^{(|\Omega|-1) \times n_1}$, which is given by

$$D(\lambda) = \min \sum_{\omega \in \Omega} p_\omega c^\top x_\omega + \sum_{\omega \in \Omega} p_\omega g_\omega^\top y_\omega + \sum_{\omega \in \Omega} \lambda^\top H_\omega x_\omega \quad (2.4a)$$

$$\text{s.t. } W_\omega y_\omega \geq h_\omega - T_\omega x_\omega, \quad \omega \in \Omega, \quad (2.4b)$$

$$x_\omega \in \mathbb{Z}^{\bar{n}_1} \times \mathbb{R}^{n_1 - \bar{n}_1}, y_\omega \in \mathbb{Z}^{\bar{n}_2} \times \mathbb{R}^{n_2 - \bar{n}_2}, \quad \omega \in \Omega. \quad (2.4c)$$

Observe that $D(\lambda) = \sum_{\omega \in \Omega} D_\omega(\lambda)$ where for each scenario $\omega \in \Omega$,

$$D_\omega(\lambda) = \min p_\omega c^\top x_\omega + p_\omega g_\omega^\top y_\omega + \lambda^\top H_\omega x_\omega \quad (2.5a)$$

$$\text{s.t. } W_\omega y_\omega \geq h_\omega - T_\omega x_\omega, \quad (2.5b)$$

$$x_\omega \in \mathbb{Z}^{\bar{n}_1} \times \mathbb{R}^{n_1 - \bar{n}_1}, y_\omega \in \mathbb{Z}^{\bar{n}_2} \times \mathbb{R}^{n_2 - \bar{n}_2}. \quad (2.5c)$$

For any λ , the Lagrangian dual function, i.e., $D(\lambda)$, provides a lower bound of Problem (2.3). Hence, we aim to find the best lower bound by maximizing this function over λ , i.e.,

$$z_{LD} = \max_{\lambda} \left\{ D(\lambda) = \sum_{\omega \in \Omega} D_\omega(\lambda) \right\}. \quad (2.6)$$

This maximization problem is referred to as Lagrangian dual problem.

2.3.2 Dual Search Method: Cutting-Plane Method

To solve problem (2.6), there are various dual search methods known in the literature such as subgradient methods [35, 80], cutting-plane methods [75, 80, 98], and column-generation methods [98, 99]. In this dissertation, we utilize cutting-plane methods that provide outer approximations of the Lagrangian dual problem by iteratively adding cutting planes. A pseudocode of this approach is given in Algorithm 1.

Algorithm 1 Dual Decomposition Algorithm

- 1: **Initialization:** Set iteration counter $k \leftarrow 0$, dual variable $\lambda = \lambda^0 = \mathbf{0}$, $z_{LB} = -\infty$, and $z_{UB}^k = \infty$;
 - 2: **while** $z_{UB}^k > z_{LB}$ **do**
 - 3: **for all** $\omega \in \Omega$ **do**
 - 4: Compute $D_\omega(\lambda^k)$ by solving Lagrangian subproblems (2.5) for $\lambda = \lambda^k$ and storing its optimal solution (x_ω^k, y_ω^k) ;
 - 5: Using $\lambda^k, D_\omega(\lambda^k)$ and x_ω^k , derive cut (2.7b), i.e.,

$$\theta_\omega \leq D_\omega(\lambda^k) + (H_\omega x_\omega^k)^\top (\lambda - \lambda^k)$$
 and add it to the master problem (2.7);
 - 6: **end for**
 - 7: Solve problem (2.7) to obtain z_{UB}^{k+1} and optimal solution $(\theta^{k+1}, \lambda^{k+1})$;
 - 8: Update lower bound $z_{LB} = \max\{z_{LB}, \sum_{\omega \in \Omega} D_\omega(\lambda^k)\}$;
 - 9: $k \leftarrow k + 1$;
 - 10: **end while**
-

To initialize Algorithm 1, we set iteration counter $k = 0$, dual variable $\lambda = \lambda^0 = \mathbf{0}$ for the first iteration, lower bound $z_{LB} = -\infty$, and upper bound $z_{UB}^k = \infty$ (Line 1). Until the termination condition is satisfied, i.e., $z_{UB}^k \leq z_{LB}$, the following steps are performed in each iteration. For each scenario $\omega \in \Omega$, problem (2.5) is solved for a given values of dual variables in the k -th iteration, i.e., λ^k , and its optimal solution value $D_\omega(\lambda^k)$ and optimal solution (x_ω^k, y_ω^k) are stored (Line 4). Using

λ^k , $D_\omega(\lambda^k)$, and x_ω^k , an affine function $D_\omega(\lambda^k) + (H_\omega x_\omega^k)^\top (\lambda - \lambda^k)$ is derived to obtain an upper bound approximation of $D_\omega(\lambda)$, thereby leading to a so-called Lagrangian master problem:

$$z_{UB}^{k+1} = \max \sum_{\omega \in \Omega} \theta_\omega \quad (2.7a)$$

$$\text{s.t. } \theta_\omega \leq D_\omega(\lambda^j) + (H_\omega x_\omega^j)^\top (\lambda - \lambda^j), \quad j = 0, \dots, k, \quad \omega \in \Omega, \quad (2.7b)$$

that provides an upper bound for z_{LD} such that $z_{LD} \leq z_{UB}^{k+1} \leq z_{UB}^k$ (7). Let $(\theta^{k+1}, \lambda^{k+1})$ be an optimal solution of (2.7). In iteration $k + 1$, we set $\lambda = \lambda^{k+1}$. The best-known lower bound for Problem (2.3) is updated in Line 8 using $z_{LB} = \max\{z_{LB}, \sum_{\omega \in \Omega} D_\omega(\lambda^k)\}$. Notice that $D_\omega(\lambda)$ is a piecewise linear concave function and it is supported by the linear hyperplane (2.7b). As a result, this approach converges to an optimal solution of the Lagrangian dual problem (2.6) after finite iterations.

Chapter 3

Scenario-based Cuts for Two-stage Stochastic p -order Conic Mixed Integer Programs

3.1 Introduction

In this chapter, we study TSS-CMIPs, as defined in section 1.2, under the following assumptions:

- (A1) $T_\omega \in \mathbb{Z}^{m_3 \times n_1}$ and $F_\omega^j \in \mathbb{Z}^{m_2 \times n_1}$ for all $\omega \in \Omega$ and $j \in J$ (w.l.o.g.),
- (A2) $X := \{x : Ax \geq b, x \in \mathbb{Z}^{n_1}\}$ is non-empty,
- (A3) Relatively complete recourse, i.e. $\bar{\mathcal{K}}_\omega(x) := \{(y_\omega, d_{\omega,0}) : (1.8c)-(1.8d)\} \neq \emptyset$
for $(x, \omega) \in X \times \Omega$.

Recall the deterministic equivalent of TSS-CMIPs is defined as follows:

$$\min \left\{ cx + \sum_{\omega \in \Omega} \bar{p}_\omega \left(g_\omega y_\omega + \sum_{j \in J} \hat{g}_\omega^j d_{\omega,0}^j \right) \right\} : \quad (3.1)$$

This chapter is from paper: M. Bansal, Y. Zhang, Scenario-based cuts for two-stage stochastic and distributionally robust p -order conic mixed integer programs, Journal on Global Optimization (1-42), 2021. <https://doi.org/10.1007/s10898-020-00986-w>

$$(x, y, d) \in \mathbb{Z}^{n_1} \times (\mathbb{Z}^{q_1} \times \mathbb{R}^{q-q_1})^{|\Omega| \times |J|} \times \mathbb{R}_+^{|\Omega| \times |J|}, \quad (3.2)$$

$$Ax \geq b, \quad T_\omega x + W_\omega y_\omega \geq r_\omega, \quad \omega \in \Omega, \quad (3.3)$$

$$\left\| F_\omega^j x + E_\omega^j y_\omega^j - h_\omega^j \right\|_p \leq d_{\omega,0}^j, \quad j \in J, \omega \in \Omega \Big\}, \quad (3.4)$$

in which the first stage has pure integer variables and the second stage problems have sum of l_p -norms in the objective function along with integer variables. We present sufficient conditions under which by adding scenario-based nonlinear cuts in $(x, y_\omega, d_{\omega,0})$ space to the deterministic equivalent of TSS-CMIP, the integrality constraints on the y_ω integer variables can be relaxed without impacting the integrality of the optimal solution of the problem. We present examples of TSS-CMIPs and derive scenario-based cuts for them which satisfy these conditions. Moreover, we provide (partial) convex hull (see Definition 3.1) for deterministic multi-constraint polyhedral conic mixed integer sets with multiple integer variable, and present an application of our results by solving stochastic capacitated facility location problem. In the following subsections, we discuss other contributions of this research, in particular, (partial) convex hulls for deterministic multi-constraint polyhedral conic mixed integer sets with multiple integer variables, conic/linear programming equivalent or approximation for structured CMIPs in the second stage of TSS-CMIPs and their distributionally robust generalizations, and application of the foregoing results for solving stochastic capacitated facility location problem.

Definition 3.1. A partial convex hull of a conic mixed integer set \mathfrak{N} is another conic mixed integer set \mathfrak{N}_{pch} such that $\mathfrak{N} \subseteq \mathfrak{N}_{pch} \subseteq \text{conv}(\mathfrak{N}) = \text{conv}(\mathfrak{N}_{pch})$. Note that \mathfrak{N}_{pch} has lesser number of integrality constraints (but possibly more linear or

nonlinear inequalities) than \mathfrak{N} . Whereas in comparison to $\text{conv}(\mathfrak{N})$, \mathfrak{N}_{pch} might have lesser inequalities but more integrality constraints.

3.1.1 Deterministic Polyhedral Conic Mixed Integer Sets

Atamtürk and Narayanan [7] generalize the well-known mixed integer rounding (MIR) inequalities of Nemhauser and Wolsey [113] by studying a polyhedral (or first-order) conic mixed integer set defined by a single conic constraint and one integer variable, i.e., $Z^{1,1} := \{(\sigma, \rho_1) \in \mathbb{Z} \times \mathbb{R}_+ : |\sigma - \beta| \leq \rho_1\}$. They introduce so-called conic MIR cut for $Z^{1,1}$ which is facet-defining for the convex hull of $Z^{1,1}$, denoted by $\text{conv}(Z^{1,1})$. The conic MIR cut along with defining and nonnegativity constraints are sufficient to describe $\text{conv}(Z^{1,1})$. Moreover, they demonstrate how this cut can be utilized to develop strong cutting planes for general conic mixed integer programs (CMIPs), thereby providing an effective approach to solve them. We introduce four new deterministic multi-constraint polyhedral conic mixed integer sets with multiple integer variables, derive conic MIR cuts for them, and provide conditions under which addition of these cuts is sufficient to provide the convex hull or a partial convex hull of the sets. More specifically, we study the following generalizations of the set $Z^{1,1}$:

(i) Set I:

$$S_K^{m,n} := \left\{ (\sigma, \rho, \rho_0) \in \mathbb{Z}^{nK} \times \mathbb{R}_+^{mK} \times \mathbb{R}_+^K : \mathcal{A}\sigma \geq b, \right. \\ \left. \left| \sum_{t=1}^n g_{kt}^i \sigma_{kt} - \beta_{ik} \right| \leq \rho_i^k, i = 1, \dots, m, k = 1, \dots, K \right\}$$

where $\beta \in \mathbb{R}^{mK}$, $\mathcal{A} \in \mathbb{R}^{m_3 \times nK}$ and $\mathcal{G}^k = (g_{kt}^i) \in \mathbb{R}^{m \times n}$ for $k = 1, \dots, K$.

(ii) Set II:

$$U_K^{m,n,u} := \left\{ (\eta, \sigma, \rho, \rho_0) \in \mathbb{Z}^u \times \mathbb{Z}^{nK} \times \mathbb{R}_+^{mK} \times \mathbb{R}_+^K : \mathcal{A}_1 \eta + \mathcal{A} \sigma \geq b, \right. \\ \left. \|\rho^k\|_1 \leq \rho_0^k, \left| \sum_{t=1}^u c_{kt}^i \eta_t + \sum_{t=1}^n g_{kt}^i \sigma_{kt} - \beta_{ik} \right| \leq \rho_i^k, i = 1, \dots, m, k = 1, \dots, K \right\}$$

where $\beta \in \mathbb{R}^{mK}$, $\mathcal{A} \in \mathbb{R}^{m_3 \times nK}$, and $\mathcal{G}^k = (g_{kt}^i) \in \mathbb{R}^{m \times n}$ for $k = 1, \dots, K$.

We assume that matrices \mathcal{A}_1 and $\mathcal{C}^k = (c_{kt}^i)$, for $k = 1, \dots, K$, are integral. We also study sets $S_K^{m,n}$ and $U_K^{m,n,u}$ with $n = 1$ and $g_{k1}^i = 1$ for all (i, k) .

3.1.2 Structured Two-Stage Stochastic and Distributionally Robust p -Order Conic Mixed Integer Programs

We introduce TSS-CMIPs with structured multi-constraint p -order conic mixed integer sets having multiple integer variables in the second stage. We derive scenario-based cuts for these second stage structured CMIPs using conic MIR and prove that these cuts provide a convex programming equivalent or approximation, in particular, a conic/linear program, for the second stage CMIPs. The foregoing second stage convexification results also hold for distributionally robust generalizations of TSS-CMIPs where we seek a solution that optimizes the expected value of the objective function for the worst case probability distribution within a prescribed (ambiguity) set of distributions that may be followed by the uncertain parameters [22, 26, 33, 46, 49, 58, 74, 103, 119, 123, 129, 148, 151]. The two-stage distributionally robust p -order conic mixed integer program (TSDR-CMIP) is defined as

follows:

$$\min \left\{ cx + \max_{P \in \mathfrak{P}} \mathbb{E}_{\xi_P} [\bar{Q}_\omega(x)] \mid x \in X \right\}, \quad (3.5)$$

where complete information about the probability distribution P followed by the random variable ξ_P is not known but it belongs to a set of distributions \mathfrak{P} (referred to as the ambiguity set). In addition, we derive scenario-based valid inequalities for the extensive formulation of distributionally robust variants of the aforementioned structured TSS-CMIPs, i.e.,

$$\min \left\{ cx + \theta \mid \sum_{\omega \in \Omega} \bar{p}_\omega \left(g_\omega y_\omega + \sum_{j \in J} \hat{g}_\omega^j d_{\omega,0}^j \right) \leq \theta, \quad \{\bar{p}_\omega\}_{\omega \in \Omega} \in \mathfrak{P}; \right. \\ \left. (3.2) - (3.4) \text{ hold} \right\}. \quad (3.6)$$

For $|\mathfrak{P}| = 1$, these cuts provide partial convex hull for the extensive formulation with no integrality restrictions on the second-stage integer variables.

We also perform computational experiments to evaluate the effectiveness of scenario based cuts by solving structured TSS-CMIPs where $p = 1$ or $p = 2$, and TSDR-CMIPs with $p = 2$. We observe that after adding the scenario-based cuts, there is a significant reduction in the number of the second stage integer variables for instances where $p = 1$ and tightening of second stage feasible region for instances where $p = 2$, thereby leading to reduction in the total solution time taken to solve the TSS-CMIP and TSDR-CMIP instances. For instance, CPLEX 12.70 (with default settings) could not solve 85 out of 290 TSS-CMIP instances within a time limit of 3 hours and the allocated memory of 24 GB RAM. In contrast,

after adding the scenario-based cuts at the root node, CPLEX could solve 82 out of these 85 (unsolvable) instances within 8.2 minutes (on average). For TSDR-CMIP instances with finite $|\mathfrak{P}|$, CPLEX 12.70 (with its default settings) could not solve 4 out of 9 instances within the time limit. After adding the cuts, CPLEX solved all these instances in 4.8 minutes (on average).

3.1.3 Multi-Module Capacitated Stochastic Facility Location Problem with Subcontracting

To illustrate the significance of the aforementioned structured TSS-CMIPs, we introduce a multi-module capacitated stochastic facility location problem with subcontracting (denoted as MM-SFLP-S), which is defined as follows. Given a set $P = \{1, \dots, m\}$ of facilities, a set $P' = \{1, \dots, m'\}$ of retailers, per unit transportation cost t_{ij} for each $i \in P$ and $j \in P'$, machines of capacity α_k , $k \in \{1, \dots, n\}$, that can be installed at facility $i \in P$ at the cost c_k^i , and per unit subcontracting cost g_i at facility $i \in P$, we formulate the MM-SFLP-S as a TSS-CMIP:

$$\min \sum_{i \in P} \sum_{k=1}^n c_k^i x_{ik} + \sum_{i \in P} \sum_{j \in P'} t_{ij} z_{ij} + \sum_{i \in P} g_i u_i + \sum_{\omega \in \Omega} \bar{p}_\omega Q_\omega(x, z, u) \quad (3.7)$$

$$\text{s.t.} \quad \sum_{k=1}^n x_{ik} \leq s_i, \quad i \in P, \quad (3.8)$$

$$\sum_{j \in P'} z_{ij} \leq \sum_{k=1}^n \alpha_k x_{ik} + u_i, \quad i \in P, \quad (3.9)$$

$$\sum_{i \in P} u_i \leq r, \quad (3.10)$$

$$x_{ik}, u_i, z_{ij} \in \mathbb{Z}_+, \quad i \in P, j \in P', k = 1, \dots, n, \quad (3.11)$$

where x_{ik} denotes the number of machines of capacity α_k installed at facility i , z_{ij} denotes the number of items transported from facility $i \in P$ to retailer $j \in P'$, and u_i denotes the number of items subcontracted by facility $i \in P$. Here, an item represents either a single entity or a packet of uncountable commodity in liquid or powder form. Constraints (3.8) restrict the number of machines installed at facility i to be at most s_i . Constraints (3.9) restrict the total number of items transported from facility i to all retailers to be no more than the sum of the total capacity of installed machines and number of items subcontracted at the facility. Constraint (3.10) limits the total number of items subcontracted by all facilities to be at most r . Let $\mathcal{X} := \{(x, z, u) : (3.8)-(3.11) \text{ hold}\}$. The objective (3.7) of MM-SFLP-S is to minimize the total machines' installation cost, transportation cost, subcontracting cost, and the expected (second-stage) transportation cost, inventory cost at facilities, and penalty cost after the realization of uncertain demand. Note that the penalty cost is incurred for shipping both more or less than a retailer's demand because in case of supplying more than the demand, the retailer has to incur inventory cost. Specifically, for $(x, u, z) \in \mathcal{X}$ and $\omega \in \Omega$, the second-stage problem is defined by,

$$Q_\omega(x, z, u) := \min \sum_{i \in P} w_{inv}^i \left(\sum_{k=1}^n \alpha_k x_{ik} + u_i - \sum_{j \in P'} (z_{ij} + y_\omega^{ij}) \right) + w_{sc} \sum_{j \in P'} \sum_{i \in P} t_{ij} y_\omega^{ij} + w_{pen} \sum_{j \in P'} \left| \sum_{i \in P} (y_\omega^{ij} + z_{ij}) - \zeta_\omega^j \right| \quad (3.12)$$

$$\text{s.t.} \quad \sum_{j \in P'} (z_{ij} + y_\omega^{ij}) \leq \sum_{k=1}^n \alpha_k x_{ik} + u_i, \quad i \in P, \quad (3.13)$$

$$y_\omega \in \mathbb{Z}_+^{|P| \times |P'|}, \quad (3.14)$$

where y_ω^{ij} denotes the number of items transported from facility $i \in P$ to retailer $j \in P'$ after realization of demand $\zeta_\omega^j \geq 0$ in response to a last minute order and constraints (3.13) ensure that the total number of items (including the last minute order) transported from each facility to all retailers is not greater than the sum of total capacity of machines installed at the facility and number of items subcontracted from the facility. We denote per unit inventory cost at facility i by w_{inv}^i , per unit surcharge on transportation cost for any last minute order by w_{sc} , and per unit penalty cost for either falling short of a retailer's demand or supplying more than the demand (thereby incurring inventory cost for the retailer) by w_{pen} . The second-stage objective (3.12) is to minimize the inventory cost at facilities, transportation cost for the last minute orders, and the penalty cost for shortage or surplus at each retailer's end. In this research, we derive linear programming equivalent for the second stage CMIP using scenario-based conic MIR cuts and perform computational experiments which demonstrate that these cuts significantly reduce time taken to solve the MM-SFLP-S instances.

We also consider distributionally robust variant of the MM-SFLP-S which is denoted by MM-DRFLP-S and defined as follows:

$$\min \sum_{i \in P} \sum_{k=1}^n c_i^k x_{ik} + \sum_{i \in P} \sum_{j \in P'} t_{ij} z_{ij} + \sum_{i \in P} g_i u_i + \max_{\{\bar{p}_\omega\}_{\omega \in \Omega} \in \mathfrak{P}} \sum_{\omega \in \Omega} \bar{p}_\omega Q_\omega(x, z, u)$$

where $(x, u, z) \in \mathcal{X}$, $Q_\omega(x, z, u)$ is defined by (3.12)-(3.14). We utilize the scenario-based CMIR cuts in solving the extensive formulation of the MM-DRFLP-S with finite $|\mathfrak{P}|$ and observe that these cuts are computationally effective.

3.1.4 Organization of This Chapter

In Section 3.2, we review literature related to TSS-CMIP, TSDR-CMIP, and deterministic CMIP. In Section 3.3, we first review the conic MIR cut [7], and then provide conditions under which addition of cuts derived using conic MIR for the aforementioned deterministic polyhedral conic mixed integer sets is sufficient to provide convex hull or partial convex hull of these sets. In Section 3.4, we provide a reformulation of the second stage CMIP using additional continuous variables, and describe feasible region of the reformulated second stage problem (exactly/approximately) as the intersection of convex hull of a polyhedral conic mixed integer set and a set of p -order cones. In Section 3.5, we present conditions under which the scenario-based nonlinear cuts provide partial convex hulls for the feasible set of the deterministic equivalent of TSS-CMIPs. To provide special cases of TSS-CMIPs and cutting planes which satisfy these conditions, in Section 3.6, we introduce TSS-CMIPs (and TSDR-CMIPs) with structured CMIPs in the second stage, derive scenario-based cuts for them using conic MIR, and prove that these cuts provide conic/linear programming equivalent or approximation for the second-stage CMIPs. We also demonstrate the applicability of these results for solving the MM-SFLP-S and MM-DRFLP-S. In Section 3.7, we explore the computational effectiveness of the scenario-based cuts by solving instances of MM-SFLP-S, and MM-DRFLP-S, and randomly generated structured TSS-CMIPs and TSDR-CMIPs. We provide concluding remarks in Section 3.8.

3.2 Literature Review

We review literature on special cases of TSS-CMIP and TSDR-CMIP in Section 3.2.1 and on cutting planes for deterministic CMIPs in Section 3.2.2.

3.2.1 Literature Review on Special Cases of TSS-CMIP and TSDR-CMIP

One of the most extensively studied special cases of TSS-CMIP is the class of two-stage stochastic mixed integer linear programs (TSS-MILPs), i.e., (1.7) with $J = \emptyset$ (refer to [83] for a comprehensive survey on TSS-MILPs), which includes the problems whose second stage are pure integer programs [2, 82, 130], mixed binary programs [36, 55, 84, 115, 132, 135], or mixed integer programs [19, 132, 133, 136]. To solve TSS-MILP, many researchers have been using globally valid linear scenario-based cuts in (x, y_ω) space, for each scenario $\omega \in \Omega$, to tighten the second stage problems with binary or integer variables, which are then embedded within Benders' decomposition algorithm [24] to solve TSS-MILP. These cuts are of the form $\gamma_\omega y_\omega \geq \gamma_{\omega,0} - \gamma_{\omega,1}x$, where x is a first-stage feasible solution, and γ_ω , $\gamma_{\omega,0}$, and $\gamma_{\omega,1}$ are real-vectors, and are referred to as the “scenario-based” or “parametric” (linear) cuts. For instance, Sherali and Fraticelli [135] derive parametric linear cuts using the reformulation-linearization technique to solve TSS-MILP with $|\Omega| = 1$, only binary variables in the first-stage, and mixed binary programs in the second stage. Likewise, Gade et al. [55] utilize parametric Gomory fractional cuts for solving TSS-MILPs with only binary variables in the first stage and non-negative integer variables in the second stage. Similarly, Bodur et al. [29] use parametric

cuts based on split disjunctions to solve TSS-MILP with mixed integer first stage and continuous second stage variables.

In the aforementioned studies, the parametric cuts are developed/added sequentially in the algorithms. Recently, Kim and Mehrotra [81] formulate an integrated staffing and scheduling problem under demand uncertainty as a TSS-MILP with the second stage MIPs having a certain structure and utilize parametric mixed integer rounding inequalities (added a priori) to obtain a linear programming equivalent of the second stage MIPs. Bansal et al. [19] generalize their observation to the general TSS-MILPs and show that under suitable conditions, the second stage MIPs can be convexified by adding parametric cuts a priori. As special cases, the authors consider structured parameterized mixed integer sets or convex objective integer program (COIP) in the second stage. In particular, they extend the results of Miller and Wolsey [105] for deterministic mixed integer sets and COIP to the two-stage stochastic framework, and consider TSS-MILPs with the parametrized version of two special cases of the continuous multi-mixing set [14, 15] in the second stage. In this research, we further generalize their results for TSS-CMIPs, which is equivalent to TSS-MILPs with parametric p -order conic constraints in the second stage. We utilize parametric cutting planes to obtain a conic/linear programming equivalent or approximation for some structured second stage CMIPs in TSS-CMIPs.

Another special case of TSS-CMIP is two-stage stochastic convex quadratic integer program (TSS-QIP). Özaltın et al. [117] study TSS-QIPs with only stochastic right-hand sides in the second stage along with deterministic quadratic objective functions, linear constraints, and only integer variables in both stages. They re-

formulate this problem using value functions for quadratic integer programs, and present a global branch-and-bound algorithm and a level-set approach to solve the problem. Mijangos [104] present a branch-and-fix coordination based algorithm to solve TSS-QIP with quadratic terms in the second stage objective function and two-stage stochastic convex problems where the objective function and constraints are nonlinear; both of these problems have binary and continuous variables in the first stage and only continuous variables in the second stage.

The TSDR-CMIPs generalize the two-stage distributionally robust mixed binary programs with general ambiguity set, studied by [20], where both stages have linear constraints and integer variables are bounded between 0 and 1. Another special case of TSDR-CMIPs are TSDR linear programs where $|J| = 0$ and both stages have continuous variables [20, 30, 31, 125]. In literature, the ambiguity sets are defined using: linear constraints on the first two moments of the distribution [25, 49, 123, 129], conic constraints to describe the set of distributions with moments [26, 46], Kantorovich distance or Wasserstein metric [58, 103, 119, 148], ζ -structure metrics [151], and χ^2 distance and Kullback-Leibler divergence [22, 33, 74, 97, 144, 149]. Recently, Luo and Mehrotra [100] propose a decomposition algorithm to solve general TSDR-CMIP, where the first stage variables are pure binary and the second stage has mixed integer variables. They use branch-and-cut algorithm to solve second stage CMIPs, and generate optimality cuts using disjunctive programming techniques and distribution separation algorithm [20]. In contrast, we consider TSDR-CMIPs with pure integer variables in the first stage and provide conic/linear programming equivalent or approximation for structured CMIPs in the second stage.

3.2.2 Brief literature review on CMIPs

In the last two decades, researchers have extended various classes of cutting planes derived for mixed integer linear programs (MILPs) to mixed integer nonlinear programs (MINLP). It includes extensions of Gomory mixed integer cuts, MIR cuts, split cuts [40], and n -step MIR inequalities [77] for MIPs to solve MINLPs [152], second-order CMIPs [7], second-order conic mixed integer sets [108], and polyhedral CMIPs [128], respectively. Additionally, attempts have been made to derive the convex hull description of (structured) conic mixed integer sets (see [7, 62, 79, 107] for few examples). In this research, we consider TSS-CMIPs and TSDR-CMIPs with (structured) p -order CMIPs in the second stage. Among all papers on deterministic CMIPs, the work in [7] is most closely related to our work. As mentioned before, Atamtürk and Narayanan [7] generalize the MIR inequalities [113] by studying a conic mixed integer set defined by a single second-order conic constraint and one integer variable. They introduce conic MIR cuts which are non-linear in the original space and linear in higher dimensional space. Vinal and Krokhmal [142] extend the conic MIR [7] and lifted conic MIR cuts [8] for second-order CMIPs to derive valid inequalities for p -order CMIPs. In this research, we introduce TSS-CMIPs with multi-constraint p -order conic mixed integer sets having multiple integer variables in the second stage and describe the convex hull or tighter approximation of these sets using parametric conic MIR inequalities.

3.3 (Partial) Convex Hull for Deterministic Polyhedral Conic Mixed Integer Sets

In this section, we first briefly review the conic MIR cut generation procedure [7] which we will use in the proofs of the subsequent theorems. Atamtürk and Narayanan [7] study a single-constraint conic mixed integer set with one integer variable, i.e., $\bar{Z} := \{(\sigma, v, \rho_0) \in \mathbb{Z} \times \mathbb{R}_+^2 : \sqrt{(\sigma - \beta)^2 + v^2} \leq \rho_0\}$, where $\beta \in \mathbb{R}$. They reformulated set \bar{Z} by using additional continuous variables to get

$$Z := \{(\sigma, v, \rho_0, \rho_1, \rho_2) \in \mathbb{Z} \times \mathbb{R}_+^4 : |\sigma - \beta| \leq \rho_1, |v| \leq \rho_2, \sqrt{\rho_1^2 + \rho_2^2} \leq \rho_0\}. \quad (3.15)$$

Proposition 3.2 ([7]). *The conic MIR inequality*

$$(1 - 2\beta^{(1)}) (\sigma - \lfloor \beta \rfloor) + \beta^{(1)} \leq \rho_1 \quad (3.16)$$

where $\beta^{(1)} = \beta - \lfloor \beta \rfloor$, is a facet defining inequality for $Z^{1,1}$.

Proposition 3.3 ([7]). *The convex hull of \bar{Z} is obtained by adding*

$$\sqrt{((1 - 2\beta^{(1)}) (\sigma - \lfloor \beta \rfloor) + \beta^{(1)})^2 + v^2} \leq \rho_0$$

to the continuous relaxation of \bar{Z} .

Let $R_K^m := \{(\sigma, \rho, \rho_0) \in \mathbb{Z}^K \times \mathbb{R}_+^{mK} \times \mathbb{R}_+^K : \mathcal{A}\sigma \geq b, |\sigma_k - \beta_{ik}| \leq \rho_i^k, i = 1, \dots, m, k = 1, \dots, K\}$ and

$$T_K^{m,u} := \left\{ (\eta, \sigma, \rho, \rho_0) \in \mathbb{Z}^u \times \mathbb{Z}^K \times \mathbb{R}_+^{mK} \times \mathbb{R}_+^K : \mathcal{A}_1\eta + \mathcal{A}\sigma \geq b, \right.$$

$$\|\rho^k\|_1 \leq \rho_0^k, \left\{ \sum_{t=1}^u c_{kt}^i \eta_t + \sigma_k - \beta_{ik} \right\} \leq \rho_i^k, i = 1, \dots, m, k = 1, \dots, K \},$$

where $\beta \in \mathbb{R}^{mK}$ and $\mathcal{A} \in \mathbb{R}^{m_3 \times K}$, be special cases of $S^{m,n}$ and $U_K^{m,n,u}$, respectively, with $n = 1$ and $g_{k1}^i = 1$ for all (i, k) . Using the conic MIR cut generation procedure on each defining conic inequality of the sets R_K^m , $S^{m,n}$, $T_K^{m,u}$, and $U_K^{m,n,u}$, in Theorems 3.4, 3.5, and 3.6, we provide (partial) convex hull description of these sets, under certain conditions. The proofs of these theorems are provided in Appendix A.4. Note that $Z^{1,1}$ is equivalent to R_1^1 , $S_1^{1,1}$, $T_1^{1,0}$, and $U_1^{1,1,0}$ where \mathcal{A} and b are zero vectors, and $g_{11}^1 = 1$. We denote the fractional part of β_{ik} by $\beta_{ik}^{(1)} := \beta_{ik} - \lfloor \beta_{ik} \rfloor$.

Motivation behind studying these structured CMIPs comes from the work of Miller and Wolsey [105] who introduced various structured mixed integer linear sets and utilized MIR inequalities of Nemhauser and Wolsey [113] to provide convex hull of these sets. Their results led to a new direction of research in which polyhedral structure of more generalized mixed integer sets have been studied, thereby resulting in new cut-generation approaches for MILPs (see [13, 14, 15] for details). Moreover, these sets arise as substructure in the mixed integer programming formulations of variety of applied problems such as production planning, facility location, and network design problems. Likewise, we extend the results of [7] for conic mixed integer sets with a single constraint and one integer variable and consider structured conic mixed integer sets that have not been studied in the literature. Our results will provide a stepping stone for future polyhedral studies on more generalized conic mixed integer sets, thereby leading to new cut generation approaches for general CMIPs.

First, we consider a multi-constraint generalization of the simple polyhedral conic mixed integer set $Z_{1,1}$, denoted by $R^{m,k} := \{(\sigma_k, \rho^k) \in \mathbb{Z} \times \mathbb{R}^m : |\sigma_k - \beta_{ik}| \leq \rho_i^k, i = 1, \dots, m\}$ for $k \in \{1, \dots, K\}$. Set $R^{m,k}$ has m polyhedral conic constraints with one nonnegative continuous variable in each constraint and an integer variable that is common among all these constraints. In Theorem 3.4, we derive convex hull of $R_K^m := \bigcap_{k=1}^K R^{m,k} \cap \{\sigma : \mathcal{A}\sigma \geq b\}$ using conic MIR cuts.

Theorem 3.4. *If \mathcal{A} is a totally unimodular (TU) matrix and b is integral, then the convex hull of the set R_K^m is given by*

$$\left\{ (\sigma, \rho, \rho_0) \in \mathbb{R}^K \times \mathbb{R}_+^{mK} \times \mathbb{R}_+^K : \right. \\ \left. \begin{aligned} &\mathcal{A}\sigma \geq b, \quad |\sigma_k - \beta_{ik}| \leq \rho_i^k, \quad i = 1, \dots, m, k = 1, \dots, K, \\ &(1 - 2\beta_{ik}^{(1)}) (\sigma_k - \lfloor \beta_{ik} \rfloor) + \beta_{ik}^{(1)} \leq \rho_i^k, \quad i = 1, \dots, m, \quad k = 1, \dots, K \end{aligned} \right\}.$$

Proof. Refer to Appendix A.4.1 □

Next, in Theorem 3.5, we consider a multi-integer generalization of the sets $R^{m,k}$ and R_K^m where each polyhedral conic constraint has n integer variables. We denote this set by $S_K^{m,n}$, and note that for $n = 1$, $S_K^{m,n}$ reduces to R_K^m . We provide conditions under which addition of conic MIR cuts is sufficient to describe the convex hull of $S_K^{m,n}$. In addition, we utilize the foregoing results to demonstrate that under the same conditions, the conic MIR cuts also provide a partial convex hull of a generalization of set $S_K^{m,n}$, i.e., $U_K^{m,n,u}$, that has $n + u$ number of integer variables in each conic constraint.

Theorem 3.5. *If either of the following conditions is satisfied, i.e.,*

- (i) \mathcal{A} and $\mathcal{G}^k = (g_{kt}^i)$ for $k = 1, \dots, K$, are network flow matrices,
- (ii) \mathcal{A} is a zero matrix and $\mathcal{G}^k = (g_{kt}^i)$ for $k = 1, \dots, K$, are TU matrices,
- (iii) \mathcal{A} is an identity matrix and $\mathcal{G}^k = (g_{kt}^i)$ for $k = 1, \dots, K$, are TU matrices,

and b is integral, then the following results hold: (a) the convex hull of the set $S_K^{m,n}$ is obtained by adding inequalities,

$$\left(1 - 2\beta_{ik}^{(1)}\right) \left(\sum_{t=1}^n g_{kt}^i \sigma_{kt} - \lfloor \beta_{ik} \rfloor\right) + \beta_{ik}^{(1)} \leq \rho_i^k, \quad i = 1, \dots, m, k = 1, \dots, K,$$

to the continuous relaxation of $S_K^{m,n}$; and (b) a partial convex hull of the set $U_K^{m,n,u}$ is given by

$$\begin{aligned} U_{K,pch}^{m,n,u} := & \left\{ (\eta, \sigma, \rho, \rho_0) \in \mathbb{Z}^u \times \mathbb{R}^{nK} \times \mathbb{R}_+^{mK} \times \mathbb{R}_+^K : \mathcal{A}_1 \eta + \mathcal{A} \sigma \geq b, \right. \\ & \|\rho^k\|_1 \leq \rho_0^k, \quad \left| \sum_{t=1}^u c_{kt}^i \eta_t + \sum_{t=1}^n g_{kt}^i \sigma_{kt} - \beta_{ik} \right| \leq \rho_i^k, \quad i = 1, \dots, m, k = 1, \dots, K, \\ & \left. \left(1 - 2\beta_{ik}^{(1)}\right) \left(\sum_{t=1}^u c_{kt}^i \eta_t + \sum_{t=1}^n g_{kt}^i \sigma_{kt} - \lfloor \beta_{ik} \rfloor\right) + \beta_{ik}^{(1)} \leq \rho_i^k, \quad i = 1, \dots, m, k = 1, \dots, K \right\}. \end{aligned}$$

Proof. Refer to Appendix A.4.2 □

In Theorem 3.6, we derive a partial convex hull of the set $U_K^{m,n,u}$ for $n = 1$, denoted by $T_K^{m,u}$, using conic MIR cuts under the condition that matrix \mathcal{A} is TU (which is not considered in Theorem 3.5).

Theorem 3.6. *If \mathcal{A} is a TU matrix and b is integral, then a partial convex hull*

of the set $T_K^{m,u}$ is given by

$$T_{K,pch}^{m,u} := \left\{ (\eta, \sigma, \rho, \rho_0) \in \mathbb{Z}^u \times \mathbb{R}^K \times \mathbb{R}_+^{mK} \times \mathbb{R}_+^K : \mathcal{A}_1 \eta + \mathcal{A} \sigma \geq b, \right. \\ \left. \|\rho^k\|_1 \leq \rho_0^k, \quad \left| \sum_{t=1}^u c_{kt}^i \eta_t + \sigma_k - \beta_{ik} \right| \leq \rho_i^k, \quad i = 1, \dots, m, k = 1, \dots, K, \right. \\ \left. \left(1 - 2\beta_{ik}^{(1)}\right) \left(\sum_{t=1}^u c_{kt}^i \eta_t + \sigma_k - \lfloor \beta_{ik} \rfloor \right) + \beta_{ik}^{(1)} \leq \rho_i^k, \quad i = 1, \dots, m, k = 1, \dots, K \right\}.$$

Proof. Refer to Appendix A.4.3 □

3.4 Reformulation of Second Stage of TSS-CMIPs and TSDR-CMIPs

We reformulate the second stage problem $\bar{\mathcal{Q}}_\omega(x)$ of the TSS-CMIP and TSDR-CMIP using additional continuous variables, as follows:

$$\mathcal{Q}_\omega(x) := \min g_\omega y_\omega + \sum_{j \in J} \hat{g}_\omega^j d_{\omega,0}^j \quad (3.17)$$

$$\text{s.t. } W_\omega y_\omega \geq r_\omega - T_\omega x, \quad (3.18)$$

$$|e_{\omega,i}^j y_\omega + f_{\omega,i}^j x - h_{\omega,i}^j| \leq d_{\omega,i}^j, \quad i = 1, \dots, m_2, j \in J, \quad (3.19)$$

$$\|d_\omega^j\|_p \leq d_{\omega,0}^j, \quad j \in J, \quad (3.20)$$

$$y_\omega^j \in \mathbb{Z}^{q_1} \times \mathbb{R}^{q-q_1}, d_{\omega,i}^j \in \mathbb{R}_+, \quad i = 0, 1, \dots, m_2, j \in J, \quad (3.21)$$

where $d_\omega^j := (d_{\omega,1}^j, \dots, d_{\omega,m_2}^j) \in \mathbb{R}_+^{m_2}$ for $j \in J$, $e_{\omega,i}^j$ and $f_{\omega,i}^j$ denote the i th row of matrices E_ω^j and F_ω^j , respectively, and $h_{\omega,i}^j$ denotes the i th element of real vector

h_ω^j . We define the feasible region of the reformulated second stage program by $\mathcal{K}_\omega(x) := \{(y_\omega, d_\omega) : (3.18) - (3.21) \text{ hold}\}$ for $x \in X$ and $\omega \in \Omega$. We note that $\bar{\mathcal{K}}_\omega(x)$ is in lower dimensional space by rewriting (3.19) and (3.20).

Next, we describe the feasible region of the reformulated second stage problem (exactly/approximately) as intersection of convex hull of a polyhedral conic mixed integer set and a set of p -order cones. Let $\mathcal{K}_\omega(x) = \mathcal{K}_\omega^1(x) \cap \mathcal{K}_\omega^2(x)$ where $\mathcal{K}_\omega^1(x) := \{(y_\omega, d_\omega) \in (\mathbb{Z}^{q_1} \times \mathbb{R}^{q-q_1})^{|J|} \times \mathbb{R}_+^{m_2|J|+|J|} : (3.18) - (3.19) \text{ hold}\}$ is a polyhedral conic mixed integer set and $\mathcal{K}_\omega^2(x) := \{(y_\omega, d_\omega) \in \mathbb{R}^{q|J|} \times \mathbb{R}_+^{m_2|J|+|J|} : (3.20) \text{ holds}\}$ is an intersection of $|J|$ number of p -order cones. In Theorem 3.7, we provide a relation between the convex hull of $\mathcal{K}_\omega(x)$ and the convex hull of $\mathcal{K}_\omega^1(x)$.

Theorem 3.7. *For each $x \in X$ and $\omega \in \Omega$, if $p = 1$,*

$$\text{conv}(\mathcal{K}_\omega(x)) = \text{conv}(\mathcal{K}_\omega^1(x)) \cap \mathcal{K}_\omega^2(x), \quad (3.22)$$

and if $p \geq 2$, $\text{conv}(\mathcal{K}_\omega(x)) \subseteq \text{conv}(\mathcal{K}_\omega^1(x)) \cap \mathcal{K}_\omega^2(x)$.

Proof. For $x \in X$ and $\omega \in \Omega$, $\mathcal{K}_\omega(x) = \mathcal{K}_\omega^1(x) \cap \mathcal{K}_\omega^2(x)$. Therefore,

$$\text{conv}(\mathcal{K}_\omega(x)) \subseteq \text{conv}(\mathcal{K}_\omega^1(x)) \cap \mathcal{K}_\omega^2(x). \quad (3.23)$$

Now, for $p = 1$, assume that a point $\hat{\eta}_\omega = \left(\hat{y}_\omega, \{\hat{d}_{\omega,0}^j\}_{j \in J}\right)$ belongs to $\text{conv}(\mathcal{K}_\omega^1(x)) \cap \mathcal{K}_\omega^2(x)$, i.e. $\hat{\eta}_\omega \in \text{conv}(\mathcal{K}_\omega^1(x))$ and $\hat{\eta}_\omega \in \mathcal{K}_\omega^2(x)$ or $\hat{d}_{\omega,0}^j - \sum_{i=1}^{m_2} \hat{d}_{\omega,i}^j \geq 0$. Since $\hat{\eta}_\omega \in \text{conv}(\mathcal{K}_\omega^1(x))$, $\hat{\eta}_\omega$ can be written as convex combination of a finite number of points $\bar{\eta}_\omega^k = \left(\bar{y}_\omega^k, \{\bar{d}_{\omega,0}^{j,k}, \bar{d}_{\omega,i}^{j,k}\}_{j \in J}\right) \in \mathcal{K}_\omega^1(x)$, where we define $\bar{d}_{\omega,0}^{j,k} = \hat{d}_{\omega,0}^j + \sum_{i=1}^{m_2} \left(\bar{d}_{\omega,i}^{j,k} - \hat{d}_{\omega,i}^j\right)$ for $j \in J$ and $k \in \{1, 2, \dots, q|J| + 1 + (m_2 + 1)|J|\}$,

i.e., for $\lambda_k \in [0, 1]$ and $\sum_k \lambda_k = 1$, $\sum_k \lambda_k \bar{\eta}_\omega^k = \hat{\eta}_\omega$. Observe that for all (j, k) , $\bar{d}_{\omega,0}^{j,k} \geq 0$ as $\hat{d}_{\omega,0}^j - \sum_{i=1}^{m_2} \hat{d}_{\omega,i}^j \geq 0$ and $\bar{d}_{\omega,i}^{j,k} \geq 0$ for all $i = 1, \dots, m_2$. Also, note that $\bar{\eta}_\omega^k \in \mathcal{K}_\omega^2(x)$ as $\bar{d}_{\omega,0}^{j,k} = \hat{d}_{\omega,0}^j + \sum_{i=1}^{m_2} (\bar{d}_{\omega,i}^{j,k} - \hat{d}_{\omega,i}^j) \geq \sum_{i=1}^{m_2} \bar{d}_{\omega,i}^{j,k}$. Hence, $\bar{\eta}_\omega^k \in \mathcal{K}_\omega^1(x) \cap \mathcal{K}_\omega^2(x)$ for all k . This implies $\sum_k \lambda_k \bar{\eta}_\omega^k = \hat{\eta}_\omega \in \text{conv}(\mathcal{K}_\omega^1(x) \cap \mathcal{K}_\omega^2(x)) = \text{conv}(\mathcal{K}_\omega(x))$, and therefore, $\text{conv}(\mathcal{K}_\omega^1(x)) \cap \mathcal{K}_\omega^2(x) \subseteq \text{conv}(\mathcal{K}_\omega(x))$. Hence, for $p = 1$, we get

$$\text{conv}(\mathcal{K}_\omega(x)) = \text{conv}(\mathcal{K}_\omega^1(x) \cap \mathcal{K}_\omega^2(x)). \quad (3.24)$$

and this completes the proof. \square

3.5 Scenario-Based Cuts for Extensive Formulation of TSS-CMIPs

In this section, we present sufficient conditions under which the integrality restrictions on the second stage integer variables of the TSS-CMIPs can be relaxed (without impacting the integrality of the optimal solution) by adding scenario-based nonlinear inequalities in (x, y_ω, d_ω) space to the extensive formulation of TSS-CMIPs. In other words, using these scenario-based cuts, we derive “partial convex hull(s)” for $\bar{\mathcal{P}}$, which is the feasible region of the deterministic equivalent of TSS-CMIPs. Given a nonempty set $\Gamma \subseteq \Omega$, we define a partial convex hull of $\bar{\mathcal{P}}$ by another conic mixed integer set,

$$\begin{aligned} \bar{\mathcal{P}}_{pch} &:= \{T_\omega x + W_\omega y_\omega \geq r_\omega, & \omega \in \Omega, \\ & \|E_\omega^j y_\omega^j + F_\omega^j x - h_\omega^j\|_p \leq d_{\omega,0}^j, & j \in J, \omega \in \Omega, \end{aligned}$$

$$\begin{aligned}
\left\| \overline{E}_{\omega,l}^j y_\omega^j + \overline{F}_{\omega,l}^j x - \overline{h}_{\omega,l}^j \right\|_p &\leq d_{\omega,0}^j, & l \in \mathcal{L}, j \in J, \omega \in \Gamma, \\
x \in X, d \in \mathbb{R}_+^{|\mathcal{J}| \times |\Omega|}, y_\omega^j \in \mathbb{R}^q, & & j \in J, \omega \in \Gamma, \\
y_\omega^j \in \mathbb{Z}^q, & & j \in J, \omega \in \Omega \setminus \Gamma,
\end{aligned}$$

where for each $l \in \mathcal{L}$, $j \in J$, and $\omega \in \Gamma$, $\overline{E}_{\omega,l}^j$, $\overline{F}_{\omega,l}^j$, $\overline{h}_{\omega,l}^j$ are matrices (or vectors) corresponding to scenario-based cuts in (x, y_ω, d_ω) space added a priori to $\overline{\mathcal{P}}$, such that $\overline{\mathcal{P}} \subseteq \overline{\mathcal{P}}_{pch} \subseteq \text{conv}(\overline{\mathcal{P}}) = \text{conv}(\overline{\mathcal{P}}_{pch})$. Note that $\overline{\mathcal{P}}_{pch}$ has fewer number of integrality constraints (but possibly more linear or nonlinear inequalities) than $\overline{\mathcal{P}}$. Whereas in comparison to $\text{conv}(\mathcal{P})$, \mathcal{P}_{pch} might have lesser inequalities but more integrality constraints.

Theorem 3.8. *Given a nonempty set $\Gamma \subseteq \Omega$, if $\text{conv}(\overline{\mathcal{K}}_\omega(x)) = \overline{\mathcal{K}}_{tight}^\omega(x)$ for all $x \in X$ and $\omega \in \Gamma$, where*

$$\begin{aligned}
\overline{\mathcal{K}}_{tight}^\omega(x) &:= \{(y_\omega, d_\omega) \in \mathbb{R}^{q|J|} \times \mathbb{R}_+^{|\mathcal{J}|} : W_\omega y_\omega \geq r_\omega - T_\omega x, \\
&\quad \left\| E_\omega^j y_\omega^j + F_\omega^j x - h_\omega^j \right\|_p \leq d_{\omega,0}^j, \quad j \in J, \\
&\quad \left\| \overline{E}_{\omega,l}^j y_\omega^j + \overline{F}_{\omega,l}^j x - \overline{h}_{\omega,l}^j \right\|_p \leq d_{\omega,0}^j, \quad l \in \mathcal{L}, j \in J\},
\end{aligned}$$

then $\overline{\mathcal{P}}_{pch}$ is a partial convex hull of $\overline{\mathcal{P}}$, i.e., $\overline{\mathcal{P}} \subseteq \overline{\mathcal{P}}_{pch} \subseteq \text{conv}(\overline{\mathcal{P}}) = \text{conv}(\overline{\mathcal{P}}_{pch})$.

Proof. Refer to Appendix A.1. □

Remark 3.9. Theorem 3.8 for TSS-CMIP extends the results (Lemma 1 and Theorem 3) of [19] for TSS-MILP, i.e., TSS-CMIP with $|J| = 0$, with linear parametric cuts. In Section 3.6, we introduce structured TSS-CMIPs and derive classes of cutting planes for them which satisfy the conditions stated in Theorem 3.8.

3.6 Structured Two-Stage Stochastic and Distributionally Robust p -Order Conic Mixed Integer Programs

In this section, we introduce TSS-CMIPs and TSDR-CMIPs with structured p -order CMIPs in the second stage, derive scenario-based cuts using conic MIR for them, and prove that these cuts along with the defining constraints provide conic/linear programming equivalent or approximation for the second stage CMIPs. We also demonstrate the applicability of these results for solving MM-SFLP-S. Specifically, we consider the following three structured CMIPs in the second stage, i.e. $\overline{\mathcal{Q}}_\omega(x)$ (or $\mathcal{Q}_\omega(x)$) where

- (a) $E_\omega = \mathbf{I}_2$, $F_\omega^j = [1, 0]^T$ for $j \in J$, and $m_3 = 0$ (Corollary 3.10);
- (b) $E_\omega^j = \mathbf{1}$ for $j \in J$ and W_ω is TU (Theorem 3.11);
- (c) E_ω^j for all $j \in J$, and W_ω are network flow matrices (Theorem 3.12(i));
- (d) E_ω^j for all $j \in J$ are TU matrices, and $W_\omega = \mathbf{I}_{m_3}$ or $W_\omega = \mathbf{0}$ (Theorem 3.12(ii)).

3.6.1 Tight Second Stage Formulations for Structured TSS-CMIPs and TSDR-CMIPs

We derive classes of parametric (non)-linear inequalities using conic MIR to get conic/linear programming equivalent or approximation for the second stage problems. It is important to note that for structured TSS-CMIP (a), we utilize the

result of [7] for \bar{Z} in Corollary 3.10; whereas for structures (b), (c), and (d), no result is known for multi-constraint and multi-variable generalizations of \bar{Z} or Z_1 , except Theorems 1-3. We introduce case (a) mainly to present a simple example that illustrates how parametric nonlinear inequalities can be used to get conic programming equivalent of the second stage CMIP of TSS-CMIPs and TSDR-CMIPs.

Corollary 3.10. *In TSS-CMIP (1.7) and TSDR-CMIP (3.5), let*

$$\bar{Q}_\omega(x) := \min g_\omega^1 y_{\omega,1} + g_\omega^2 y_{\omega,2} + \hat{g}_\omega d_{\omega,0} \quad (3.25)$$

$$s.t. \sqrt{(y_{\omega,1} + f_\omega x - h_\omega)^2 + (y_{\omega,2})^2} \leq d_{\omega,0}, \quad (3.26)$$

$$y_{\omega,1} \in \mathbb{Z}, y_{\omega,2} \in \mathbb{R}_+, d_{\omega,0} \in \mathbb{R}_+. \quad (3.27)$$

The convex hull of the feasible region of $\bar{Q}_\omega(x)$ for all $x \in X$ is given by

$$\left\{ (y_{\omega,1}, y_{\omega,2}, d_{\omega,0}) \in \mathbb{R} \times \mathbb{R}_+^2 : (3.26) \text{ and } \sqrt{((1 - 2\mu_\omega)(y_{\omega,1} + f_\omega x - h_\omega) + \mu_\omega)^2 + (y_{\omega,2})^2} \leq d_{\omega,0} \right\},$$

where $\mu_\omega = h_\omega - \lfloor h_\omega \rfloor$. Furthermore, in higher dimensional space $\bar{Q}_\omega(x)$ can be reformulated as:

$$\mathcal{Q}_\omega(x) := \min \left\{ g_\omega^1 y_{\omega,1} + g_\omega^2 y_{\omega,2} + \hat{g}_\omega d_{\omega,0} : |y_{\omega,1} + f_\omega x - h_\omega| \leq d_{\omega,1}, \right. \\ \left. |y_{\omega,2}| \leq d_{\omega,2}, \sqrt{d_{\omega,1}^2 + d_{\omega,2}^2} \leq d_{\omega,0}, \right. \\ \left. y_{\omega,1} \in \mathbb{Z}, y_{\omega,2} \in \mathbb{R}_+, d_{\omega,i} \in \mathbb{R}_+, i = 0, 1, 2 \right\}.$$

Then, for all $x \in X$, the convex hull of the feasible region of $\mathcal{Q}_\omega(x)$, denoted

by $\mathcal{K}_\omega(x)$, is obtained by adding the following parametric linear inequality to the continuous relaxation of $\mathcal{K}_\omega(x)$:

$$(1 - 2\mu_\omega)(y_{\omega,1} - \lfloor h_\omega \rfloor + f_\omega x) + \mu_\omega \leq d_{\omega,1}.$$

Proof. Refer to Appendix A.2.1. □

As mentioned before, the motivation behind the ensuing theorems is to extend the results of Bansal et al. [19] for structured TSS-MILPs to structured TSS-CMIPs and TSDR-CMIPs. More specifically, in [19], the authors considered structured mixed integer sets studied by Miller and Wolsey [105] and two special cases of the continuous multi-mixing set [14, 15] in the second stage of TSS-MILPs, and provide linear programming equivalent for the second stage programs. We also obtain a conic/linear programming equivalent or approximation for aforementioned structured second stage CMIPs in TSS-CMIPs and TSDR-CMIPs, thereby extending our results for deterministic CMIPs (Theorems 3.4 and 3.5 for R_K^m and $S_K^{m,n}$, respectively) to stochastic CMIPs. In Theorem 3.11, we consider second stage problems with $|J|$ conic constraints (3.30) where each constraint has only one integer variables $y_\omega^j \in \mathbb{Z}$ associated to it and these integer variables $y_\omega = (y_\omega^1, y_\omega^2, \dots, y_\omega^{|J|}) \in \mathbb{Z}^{|J|}$ are connected with linear constraints (3.29).

Theorem 3.11. *In TSS-CMIP (1.7) and TSDR-CMIP (3.5), let*

$$\bar{\mathcal{Q}}_\omega(x) := \min g_\omega y_\omega + \sum_{j \in J} \hat{g}_\omega^j d_{\omega,0}^j \tag{3.28}$$

$$s.t. W_\omega y_\omega \geq r_\omega - T_\omega x, \tag{3.29}$$

$$\|\mathbf{1}y_\omega^j + F_\omega^j x - h_\omega^j\|_p \leq d_{\omega,0}^j, \quad j \in J, \tag{3.30}$$

$$y_\omega^j \in \mathbb{Z}, d_{\omega,0}^j \in \mathbb{R}_+, \quad j \in J, \quad (3.31)$$

where W_ω is a TU matrix and r_ω is integral. For $p = 1$ or $p \geq 2$, the convex hull or an approximation, respectively, of the feasible region of $\overline{\mathcal{Q}}_\omega(x)$ for all $x \in X$ are given by

$$\left\{ (y_\omega, d_{\omega,0}) \in \mathbb{R}^{|J|} \times \mathbb{R}_+^{|J|} : (3.29), (3.30), \text{ and} \right. \\ \left. \left\| \overline{E}_{\omega,l}^j y_\omega^j + \overline{F}_{\omega,l}^j x - \overline{h}_{\omega,l}^j \right\|_p \leq d_{\omega,0}^j, \quad l \in \mathcal{L}, j \in J \right\},$$

where the i th element of $\overline{E}_{\omega,l}^j y_\omega^j + \overline{F}_{\omega,l}^j x - \overline{h}_{\omega,l}^j$ is either $y_\omega^j + f_{\omega,i}^j x - h_{\omega,i}^j$ or $(1 - 2\mu_{\omega,i}^j) (y_\omega^j - \lfloor h_{\omega,i}^j \rfloor + f_{\omega,i}^j x) + \mu_{\omega,i}^j$, and $\mu_{\omega,i}^j = h_{\omega,i}^j - \lfloor h_{\omega,i}^j \rfloor$. Furthermore, in higher dimensional space $\overline{\mathcal{Q}}_\omega(x)$ can be reformulated as:

$$\mathcal{Q}_\omega(x) := \min \left\{ g_\omega y_\omega + \sum_{j \in J} \hat{g}_\omega^j d_{\omega,0}^j : (3.29), \text{ and} \right. \quad (3.32)$$

$$|y_\omega^j + f_{\omega,i}^j x - h_{\omega,i}^j| \leq d_{\omega,i}^j, \quad i = 1, \dots, m_2, \quad j \in J, \quad (3.33)$$

$$\|d_\omega^j\|_p \leq d_{\omega,0}^j, \quad j \in J, \quad (3.34)$$

$$y_\omega^j \in \mathbb{Z}, d_{\omega,0}^j \in \mathbb{R}_+, d_\omega^j \in \mathbb{R}_+^{m_2} \quad j \in J \left. \right\}. \quad (3.35)$$

Then, for all $x \in X$, the convex hull (for $p = 1$) and an approximation (for $p \geq 2$) of the feasible region of $\mathcal{Q}_\omega(x)$, denoted by $\mathcal{K}_\omega(x)$, are obtained by adding $m_2 \times |J|$ number of the following parametric linear inequalities (in the higher dimensional space) to the continuous relaxation of $\mathcal{K}_\omega(x)$: $(1 - 2\mu_{\omega,i}^j) (y_\omega^j - \lfloor h_{\omega,i}^j \rfloor + f_{\omega,i}^j x) + \mu_{\omega,i}^j \leq d_{\omega,i}^j$, $i = 1, \dots, m_2, j \in J$.

Proof. Let

$$\mathcal{K}_\omega^1(x) = \left\{ (y_\omega, d_\omega) \in \mathbb{Z}^{|J|} \times \mathbb{R}_+^{m_2|J|+|J|} : \right. \quad (3.36)$$

$$W_\omega y_\omega \geq r_\omega - T_\omega x, \quad (3.37)$$

$$\left. |y_\omega^j + f_{\omega,i}^j x - h_{\omega,i}^j| \leq d_{\omega,i}^j, \quad i = 1, \dots, m_2, j \in J \right\} \quad (3.38)$$

for all $x \in X$. First we apply Proposition 3.2 to each defining inequality (3.38) of $\mathcal{K}_\omega^1(x)$. In other words, we substitute $\sigma = y_\omega^j$, $\beta = h_{\omega,i}^j - f_{\omega,i}^j x$, and $\rho_1 = d_{\omega,i}^j$ in Z_1 and get the following valid parametric conic MIR inequalities (3.16) for $\mathcal{K}_\omega^1(x)$:

$$(1 - 2\mu_{\omega,i}^j) (y_\omega^j - \lfloor h_{\omega,i}^j - f_{\omega,i}^j x \rfloor) + \mu_{\omega,i}^j \leq d_{\omega,i}^j, \quad i = 1, \dots, m_2, j \in J. \quad (3.39)$$

Since $f_{\omega,i}^j x$ is integral for all $x \in X$, $\lfloor f_{\omega,i}^j x \rfloor = f_{\omega,i}^j x$ and therefore, inequality (3.39) is equivalent to

$$(1 - 2\mu_{\omega,i}^j) (y_\omega^j - \lfloor h_{\omega,i}^j \rfloor + f_{\omega,i}^j x) + \mu_{\omega,i}^j \leq d_{\omega,i}^j, \quad i = 1, \dots, m_2, j \in J. \quad (3.40)$$

Thus,

$$\text{conv}(\mathcal{K}_\omega^1(x)) \subseteq \mathcal{K}_\omega^3(x) := \left\{ (y_\omega, d_\omega) \in \mathbb{R}^{|J|} \times \mathbb{R}_+^{m_2|J|+|J|} : (3.37), (3.38), (3.40) \text{ hold} \right\} \quad (3.41)$$

for all $x \in X$. Notice that we can rewrite the set $\mathcal{K}_\omega^3(x)$ as

$$\mathcal{K}_\omega^3(x) = \left\{ (y_\omega, d_\omega) \in \mathbb{R}^{|J|} \times \mathbb{R}_+^{m_2|J|+|J|} : W_\omega y_\omega \geq r_\omega - T_\omega x, \right.$$

$$d_{\omega,i}^j \geq y_\omega^j - (h_{\omega,i}^j - f_{\omega,i}^j x), \quad i = 1, \dots, m_2, j \in J, \quad (3.42)$$

$$d_{\omega,i}^j \geq (h_{\omega,i}^j - f_{\omega,i}^j x) - y_\omega^j, \quad i = 1, \dots, m_2, j \in J, \quad (3.43)$$

$$d_{\omega,i}^j \geq (1 - 2\mu_{\omega,i}^j) (y_{\omega}^j - \lfloor h_{\omega,i}^j \rfloor + f_{\omega,i}^j x) + \mu_{\omega,i}^j, i = 1, \dots, m_2, j \in J \}.$$

Now let $\mathcal{K}_{\omega}^4(x)$ be a bounded face of $\text{Proj}_{y_{\omega}, d_1, \dots, d_{|\Omega|}} \mathcal{K}_{\omega}^3(x)$ with maximum possible dimension. Since $\mathcal{K}_{\omega}^4(x)$ is a bounded face, for all points $(y_{\omega}, d_1, \dots, d_{|\Omega|}) \in \mathcal{K}_{\omega}^4(x)$, $d_{\omega,i}^j \leq \hat{d}_{\omega,i}^j$ for $i = 1, \dots, m_2$ and $j \in J$, where $(\hat{y}_{\omega}, \hat{d}_1, \dots, \hat{d}_{|\Omega|}) \in \text{Proj}_{y_{\omega}, d_1, \dots, d_{|\Omega|}} \mathcal{K}_{\omega}^3(x)$. Thus, for $i = 1, \dots, m_2$ and $j \in J$, we have

$$d_{\omega,i}^j = \max \left\{ y_{\omega}^j - (h_{\omega,i}^j - f_{\omega,i}^j x), (h_{\omega,i}^j - f_{\omega,i}^j x) - y_{\omega}^j, (1 - 2\mu_{\omega,i}^j) (y_{\omega}^j - \lfloor h_{\omega,i}^j \rfloor + f_{\omega,i}^j x) + \mu_{\omega,i}^j \right\}.$$

Moreover, if $h_{\omega,i}^j \in \mathbb{Z}$ for all $j \in J$ then $\mu_{\omega,i}^j = 0$, and as a result inequality (3.40) reduces to inequality (3.42). However, when $h_{\omega,i}^j \notin \mathbb{Z}$ for $j \in J$, then there are three possible cases:

Case I. $d_{\omega,i}^j = y_{\omega}^j - (h_{\omega,i}^j - f_{\omega,i}^j x)$: This case will happen if and only if $y_{\omega}^j - (h_{\omega,i}^j - f_{\omega,i}^j x) \geq (h_{\omega,i}^j - f_{\omega,i}^j x) - y_{\omega}^j$ and $y_{\omega}^j - (h_{\omega,i}^j - f_{\omega,i}^j x) \geq (1 - 2\mu_{\omega,i}^j) (y_{\omega}^j - \lfloor h_{\omega,i}^j \rfloor + f_{\omega,i}^j x) + \mu_{\omega,i}^j$, which are equivalent to $y_{\omega}^j \geq h_{\omega,i}^j - f_{\omega,i}^j x$ and $y_{\omega}^j \geq \lfloor h_{\omega,i}^j \rfloor - f_{\omega,i}^j x$, respectively. Note that the last inequality is stronger than the second last inequality. Therefore, we can claim that $d_{\omega,i}^j = y_{\omega}^j - (h_{\omega,i}^j - f_{\omega,i}^j x)$ if and only if $y_{\omega}^j \geq \lfloor h_{\omega,i}^j \rfloor - f_{\omega,i}^j x$.

Case II. $d_{\omega,i}^j = h_{\omega,i}^j - f_{\omega,i}^j x - y_{\omega}^j$: This case will happen if and only if $h_{\omega,i}^j - f_{\omega,i}^j x - y_{\omega}^j \geq y_{\omega}^j - (h_{\omega,i}^j - f_{\omega,i}^j x)$ and $h_{\omega,i}^j - f_{\omega,i}^j x - y_{\omega}^j \geq (1 - 2\mu_{\omega,i}^j) (y_{\omega}^j - \lfloor h_{\omega,i}^j \rfloor + f_{\omega,i}^j x) + \mu_{\omega,i}^j$, which are equivalent to $y_{\omega}^j \leq h_{\omega,i}^j - f_{\omega,i}^j x$ and $y_{\omega}^j \leq \lfloor h_{\omega,i}^j \rfloor - f_{\omega,i}^j x$, respectively, as $\mu_{\omega,i}^j \leq 1$. Again, note that the last inequality is stronger than the second last

inequality. Therefore, $d_{\omega,i}^j = h_{\omega,i}^j - f_{\omega,i}^j x - y_{\omega}^j$ if and only if $y_{\omega}^j \leq \lfloor h_{\omega,i}^j \rfloor - f_{\omega,i}^j x$.

Case III. $d_{\omega,i}^j = (1 - 2\mu_{\omega,i}^j) (y_{\omega}^j - \lfloor h_{\omega,i}^j \rfloor + f_{\omega,i}^j x) + \mu_{\omega,i}^j$: This case will happen if and only if $(1 - 2\mu_{\omega,i}^j) (y_{\omega}^j - \lfloor h_{\omega,i}^j \rfloor + f_{\omega,i}^j x) + \mu_{\omega,i}^j \geq h_{\omega,i}^j - f_{\omega,i}^j x - y_{\omega}^j$ and $(1 - 2\mu_{\omega,i}^j) (y_{\omega}^j - \lfloor h_{\omega,i}^j \rfloor + f_{\omega,i}^j x) + \mu_{\omega,i}^j \geq y_{\omega}^j - (h_{\omega,i}^j - f_{\omega,i}^j x)$, which are equivalent to $y_{\omega}^j \geq \lfloor h_{\omega,i}^j \rfloor - f_{\omega,i}^j x$ and $y_{\omega}^j \leq \lceil h_{\omega,i}^j \rceil - f_{\omega,i}^j x$, respectively. Therefore, $d_{\omega,i}^j = (1 - 2\mu_{\omega,i}^j) (y_{\omega}^j - \lfloor h_{\omega,i}^j \rfloor + f_{\omega,i}^j x) + \mu_{\omega,i}^j$ if and only if $\lfloor h_{\omega,i}^j \rfloor - f_{\omega,i}^j x \leq y_{\omega}^j \leq \lceil h_{\omega,i}^j \rceil - f_{\omega,i}^j x$.

Next, for each $j \in J$, we partition the set $\mathcal{I} := \{1, \dots, m_2\}$ into the sets \mathcal{I}_1^j , \mathcal{I}_2^j , and \mathcal{I}_3^j , i.e. $\mathcal{I} = \mathcal{I}_1^j \cup \mathcal{I}_2^j \cup \mathcal{I}_3^j$, such that

$$\mathcal{I}_1^j := \{i \in \mathcal{I} : d_{\omega,i}^j = y_{\omega}^j - (h_{\omega,i}^j - f_{\omega,i}^j x)\}, \quad (3.44)$$

$$\mathcal{I}_2^j := \{i \in \mathcal{I} : d_{\omega,i}^j = (h_{\omega,i}^j - f_{\omega,i}^j x) - y_{\omega}^j\}, \text{ and} \quad (3.45)$$

$$\mathcal{I}_3^j := \left\{ i \in \mathcal{I} : d_{\omega,i}^j = (1 - 2\mu_{\omega,i}^j) (y_{\omega}^j - \lfloor h_{\omega,i}^j \rfloor + f_{\omega,i}^j x) + \mu_{\omega,i}^j \right\}. \quad (3.46)$$

Therefore, in the light of the above discussed cases, we can rewrite $\mathcal{K}_{\omega}^4(x)$ as

$$\begin{aligned} \mathcal{K}_{\omega}^4(x) = & \left\{ (y_{\omega}, d_{\omega}) \in \mathbb{R}^{|J|} \times \mathbb{R}_+^{m_2|J|+|J|} : W_{\omega} y_{\omega} \geq r_{\omega} - T_{\omega} x, \right. \\ & y_{\omega}^j \geq \lfloor h_{\omega,i}^j \rfloor - f_{\omega,i}^j x, \quad d_{\omega,i}^j = y_{\omega}^j - (h_{\omega,i}^j - f_{\omega,i}^j x), \quad i \in \mathcal{I}_1^j, j \in J, \\ & y_{\omega}^j \leq \lfloor h_{\omega,i}^j \rfloor - f_{\omega,i}^j x, \quad d_{\omega,i}^j = (h_{\omega,i}^j - f_{\omega,i}^j x) - y_{\omega}^j, \quad i \in \mathcal{I}_2^j, j \in J, \\ & \lfloor h_{\omega,i}^j \rfloor - f_{\omega,i}^j x \leq y_{\omega}^j \leq \lceil h_{\omega,i}^j \rceil - f_{\omega,i}^j x, \quad i \in \mathcal{I}_3^j, j \in J, \\ & \left. d_{\omega,i}^j = (1 - 2\mu_{\omega,i}^j) (y_{\omega}^j - \lfloor h_{\omega,i}^j \rfloor + f_{\omega,i}^j x) + \mu_{\omega,i}^j, \quad i \in \mathcal{I}_3^j, j \in J \right\}. \end{aligned}$$

The compact form $\mathcal{K}_\omega^4(x)$ can be written as

$$\begin{aligned} \mathcal{K}_\omega^4(x) = \{ & (y_\omega, d_\omega) \in \mathbb{R}^{|J|} \times \mathbb{R}_+^{m_2|J|+|J|} : W_\omega y_\omega \geq r_\omega - T_\omega x, \\ & d_{\omega,i}^j = \theta_{\omega,i}^j y_\omega^j + \sigma_{\omega,i}^j, l_\omega^j \leq y_\omega^j \leq \bar{u}_\omega^j, i = 1, \dots, m_2, j \in J \}, \end{aligned}$$

where $\theta_{\omega,i}^j, \sigma_{\omega,i}^j \in \mathbb{R}$ and $l_\omega^j, \bar{u}_\omega^j \in \mathbb{Z} \cup \{-\infty, +\infty\}$ for $j \in J$ and $i = 1, \dots, m_2$. Since W_ω is a TU matrix (by assumption), transpose of $(W_\omega^T, \mathbf{I}, -\mathbf{I})$ is also a TU matrix. Therefore, each bounded face $\mathcal{K}_\omega^4(x)$ of $\text{Proj}_{y_\omega, d_1, \dots, d_{|\Omega|}} \mathcal{K}_\omega^3(x)$, for $x \in X$, has extreme points with integral y_ω^j as $r_\omega - T_\omega x$ is integral. Since $\mathcal{K}_\omega^3(x)$ is a subset of the continuous relaxation of $\mathcal{K}_\omega^1(x)$, and all bounded faces of $\mathcal{K}_\omega^3(x)$ have extreme points with integral y_ω components, $\mathcal{K}_\omega^3(x) \subseteq \text{conv}(\mathcal{K}_\omega^1(x))$. Hence, $\text{conv}(\mathcal{K}_\omega^1(x)) = \mathcal{K}_\omega^3(x)$ for all $x \in X$ because of (3.41).

Finally, because of Theorem 3.7, $\text{conv}(\mathcal{K}_\omega^1(x)) \cap \mathcal{K}_\omega^2(x) \subseteq \mathcal{K}_\omega^3(x) \cap \mathcal{K}_\omega^2(x)$ where $\mathcal{K}_\omega^2(x) := \{(y_\omega, d_\omega) \in \mathbb{R}^{|J|} \times \mathbb{R}_+^{m_2|J|+|J|} : \|d_\omega^j\|_p \leq d_{\omega,0}^j, j \in J\}$, provides the convex hull (for $p = 1$) or an approximation (for $p \geq 2$) for $(\mathcal{K}_\omega(x))$. In other words, we obtain the convex hull (for $p = 1$) or an approximation (for $p \geq 2$) of $\mathcal{K}_\omega(x)$ by adding $m_2 \times |J|$ number of linear inequalities:

$$d_{\omega,i}^j \geq (1 - 2\mu_{\omega,i}^j) (y_\omega^j - \lfloor h_{\omega,i}^j x \rfloor + f_{\omega,i}^j) + \mu_{\omega,i}^j, \quad i = 1, \dots, m_2, j \in J, \quad (3.47)$$

to the continuous relaxation of $\mathcal{K}_\omega(x)$. Moreover, $\mathcal{K}_\omega^3(x) \cap \mathcal{K}_\omega^2(x)$ when projected to $(y_\omega, d_{\omega,0})$ space gives the convex hull of the feasible region of $\bar{\mathcal{Q}}_\omega(x)$, i.e.

$$\left\{ (y_\omega, d_{\omega,0}) \in \mathbb{R}^{|J|} \times \mathbb{R}_+^{|J|} : (3.29), (3.30), \text{ and} \right.$$

$$\left\{ \left\| \bar{E}_{\omega,l}^j y_{\omega}^j + \bar{F}_{\omega,l}^j x - \bar{h}_{\omega,l}^j \right\|_p \leq d_{\omega,0}^j, \quad l \in \mathcal{L}, j \in J \right\},$$

where the i th row of $\bar{E}_{\omega,l}^j y_{\omega}^j + \bar{F}_{\omega,l}^j x - \bar{h}_{\omega,l}^j$ is either $y_{\omega}^j + f_{\omega,i}^j x - h_{\omega,i}^j$ or $(1 - 2\mu_{\omega,i}^j)(y_{\omega}^j - \lfloor h_{\omega,i}^j \rfloor + f_{\omega,i}^j x) + \mu_{\omega,i}^j$. This completes the proof. \square

Next, we consider multi-integer generalization of the second stage problem studied in Theorem 3.11. More specifically, we again consider second stage problems with $|J|$ conic constraints (3.50), but each constraint has q integer variables $y_{\omega}^j \in \mathbb{Z}^q$ associated to it and these integer variables $y_{\omega} = (y_{\omega}^1, y_{\omega}^2, \dots, y_{\omega}^{|J|}) \in \mathbb{Z}^{q|J|}$ are also connected with linear constraints (3.49).

Theorem 3.12. *In TSS-CMIP (1.7) and TSDR-CMIP (3.5), let*

$$\bar{Q}_{\omega}(x) := \min g_{\omega} y_{\omega} + \sum_{j \in J} \hat{g}_{\omega}^j d_{\omega,0}^j \quad (3.48)$$

$$\text{s.t. } W_{\omega} y_{\omega} \geq r_{\omega} - T_{\omega} x, \quad (3.49)$$

$$\left\| E_{\omega}^j y_{\omega}^j + F_{\omega}^j x - h_{\omega}^j \right\|_p \leq d_{\omega,0}^j, \quad j \in J, \quad (3.50)$$

$$y_{\omega}^j \in \mathbb{Z}^q, d_{\omega,0}^j \in \mathbb{R}_+, \quad j \in J, \quad (3.51)$$

where r_{ω} is integral and either of following conditions is satisfied:

(i) E_{ω}^j for $j \in J$ and W_{ω} are network flow matrices;

(ii) E_{ω}^j for $j \in J$ are TU matrices, and $W_{\omega} = \mathbf{I}_{m_3}$ or $W_{\omega} = \mathbf{0}$.

For $p = 1$ or $p \geq 2$, the convex hull or an approximation, respectively, of the

feasible region of $\overline{\mathcal{Q}}_\omega(x)$ for all $x \in X$ are given by

$$\left\{ (y_\omega, d_{\omega,0}) \in \mathbb{R}^{q|J|} \times \mathbb{R}_+^{|J|} : (3.49), (3.50), \text{ and} \right. \\ \left. \left\| \overline{E}_{\omega,l}^j y_\omega^j + \overline{F}_{\omega,l}^j x - \overline{h}_{\omega,l}^j \right\|_p \leq d_{\omega,0}^j, \quad l \in \mathcal{L}, j \in J \right\},$$

where the i th element of $\overline{E}_{\omega,l}^j y_\omega^j + \overline{F}_{\omega,l}^j x - \overline{h}_{\omega,l}^j$ is either $e_{\omega,i}^j y_\omega^j + f_{\omega,i}^j x - h_{\omega,i}^j$ or $(1 - 2\mu_{\omega,i}^j) (e_{\omega,i}^j y_\omega^j - \lfloor h_{\omega,i}^j \rfloor + f_{\omega,i}^j x) + \mu_{\omega,i}^j$, and $\mu_{\omega,i}^j = h_{\omega,i}^j - \lfloor h_{\omega,i}^j \rfloor$. Furthermore, in higher dimensional space $\overline{\mathcal{Q}}_\omega(x)$ can be reformulated as:

$$\mathcal{Q}_\omega(x) := \min \left\{ g_\omega y_\omega + \sum_{j \in J} \hat{g}_\omega^j d_{\omega,0}^j : (3.49), \text{ and} \right. \quad (3.52)$$

$$\left. |e_{\omega,i}^j y_\omega^j + f_{\omega,i}^j x - h_{\omega,i}^j| \leq d_{\omega,i}^j, \quad i = 1, \dots, m_2, \quad j \in J, \quad (3.53)$$

$$\left. \|d_\omega^j\|_p \leq d_{\omega,0}^j, \quad j \in J, \quad (3.54)$$

$$\left. y_\omega^j \in \mathbb{Z}^q, d_{\omega,0}^j \in \mathbb{R}_+, d_\omega^j \in \mathbb{R}_+^{m_2} \quad j \in J \right\}. \quad (3.55)$$

Then, for all $x \in X$, the convex hull (for $p = 1$) and an approximation (for $p \geq 2$) of the feasible region of $\mathcal{Q}_\omega(x)$, denoted by $\mathcal{K}_\omega(x)$, is obtained by adding $m_2 \times |J|$ number of the following linear inequalities (in the higher dimensional space) to the continuous relaxation of $\mathcal{K}_\omega(x)$:

$$(1 - 2\mu_{\omega,i}^j) (e_{\omega,i}^j y_\omega^j - \lfloor h_{\omega,i}^j \rfloor + f_{\omega,i}^j x) + \mu_{\omega,i}^j \leq d_{\omega,i}^j, \quad i = 1, \dots, m_2, \quad j \in J.$$

Proof. Let

$$\mathcal{K}_\omega^1(x) = \left\{ (y_\omega, d_\omega) \in \mathbb{R}^{q|J|} \times \mathbb{R}_+^{m_2|J|+|J|} : \right.$$

$$W_\omega y_\omega \geq r_\omega - T_\omega x, \quad (3.56)$$

$$\left. |e_{\omega,i}^j y_\omega^j + f_{\omega,i}^j x - h_{\omega,i}^j| \leq d_{\omega,i}^j, \quad i = 1, \dots, m_2, \quad j \in J \right\} \quad (3.57)$$

for all $x \in X$. Since E_ω^j is either a network flow matrix, or a TU matrix, $e_{\omega,i}^j y_\omega^j$ is integral. Similar to the proof of the previous theorem, we again apply Proposition 3.2 to each defining inequality (3.57) of $\mathcal{K}_\omega^1(x)$. In this case we substitute $\sigma = e_{\omega,i}^j y_\omega^j \in \mathbb{Z}$, $\beta = h_{\omega,i}^j - f_{\omega,i}^j x$, and $\rho_1 = d_{\omega,i}^j$ in Z_1 and get the following valid parametric conic MIR inequalities (3.16) for $\mathcal{K}_\omega^1(x)$: $(1 - 2\mu_{\omega,i}^j) (e_{\omega,i}^j y_\omega^j - [h_{\omega,i}^j - f_{\omega,i}^j x]) + \mu_{\omega,i}^j \leq d_{\omega,i}^j$, for $i = 1, \dots, m_2$ and $j \in J$, which is equivalent to

$$(1 - 2\mu_{\omega,i}^j) (e_{\omega,i}^j y_\omega^j - [h_{\omega,i}^j] + f_{\omega,i}^j x) + \mu_{\omega,i}^j \leq d_{\omega,i}^j, \quad (3.58)$$

for $i = 1, \dots, m_2$ and $j \in J$, as $f_{\omega,i}^j x$ is integral for all $x \in X$. Thus, $\text{conv}(\mathcal{K}_\omega^1(x)) \subseteq \mathcal{K}_\omega^3(x)$ for all $x \in X$, where

$$\mathcal{K}_\omega^3(x) = \left\{ (y_\omega, d_\omega) \in \mathbb{R}^{q|J|} \times \mathbb{R}_+^{m_2|J|+|J|} : W_\omega y_\omega \geq r_\omega - T_\omega x, \right.$$

$$d_{\omega,i}^j \geq e_{\omega,i}^j y_\omega^j - (h_{\omega,i}^j - f_{\omega,i}^j x), \quad i = 1, \dots, m_2, j \in J, \quad (3.59)$$

$$d_{\omega,i}^j \geq (h_{\omega,i}^j - f_{\omega,i}^j x) - e_{\omega,i}^j y_\omega^j, \quad i = 1, \dots, m_2, j \in J, \quad (3.60)$$

$$\left. d_{\omega,i}^j \geq (1 - 2\mu_{\omega,i}^j) (e_{\omega,i}^j y_\omega^j - [h_{\omega,i}^j] + f_{\omega,i}^j x) + \mu_{\omega,i}^j, i = 1, \dots, m_2, j \in J \right\}.$$

Notice that $\mathcal{K}_\omega^3(x)$ is a subset of the continuous relaxation of $\mathcal{K}_\omega^1(x)$, and there is no restriction on variables $d_{\omega,0}$ for all $\omega \in \Omega$. Therefore, if we can prove that all bounded faces of $\text{Proj}_{y_\omega, d_1, \dots, d_{|\Omega|}}(\mathcal{K}_\omega^3(x))$ have extreme points with integral y_ω component, then it will imply that $\mathcal{K}_\omega^3(x) \subseteq \text{conv}(\mathcal{K}_\omega^1(x))$ for all $x \in X$. So,

we now consider a bounded face of $\mathcal{K}_\omega^3(x)$ with maximum possible dimension, denoted by $\mathcal{K}_\omega^4(x)$, and on this face, $d_{\omega,i}^j$, $i = 1, \dots, m_2$ and $j \in J$, is minimal, i.e. $d_{\omega,i}^j = \max \{z_{\omega,i}^j - h_{\omega,i}^j, h_{\omega,i}^j - z_{\omega,i}^j, (1 - 2\mu_{\omega,i}^j)(z_{\omega,i}^j - \lfloor h_{\omega,i}^j \rfloor) + \mu_{\omega,i}^j\}$ where $z_{\omega,i}^j = e_{\omega,i}^j y^j + f_{\omega,i}^j x \in \mathbb{Z}$. Now if $h_{\omega,i}^j \in \mathbb{Z}$ for any $j \in J$, then $\mu_{\omega,i}^j = 0$ and as a result inequality (3.58) reduces to inequality (3.59). However, when $h_{\omega,i}^j \notin \mathbb{Z}$ for some $j \in J$, then again there are three possible cases:

Case I. $d_{\omega,i}^j = z_{\omega,i}^j - h_{\omega,i}^j$: This case will happen if and only if $z_{\omega,i}^j - h_{\omega,i}^j \geq h_{\omega,i}^j - z_{\omega,i}^j$ and $z_{\omega,i}^j - h_{\omega,i}^j \geq (1 - 2\mu_{\omega,i}^j)(z_{\omega,i}^j - \lfloor h_{\omega,i}^j \rfloor) + \mu_{\omega,i}^j$, which are equivalent to $z_{\omega,i}^j \geq h_{\omega,i}^j$ and $z_{\omega,i}^j \geq \lceil h_{\omega,i}^j \rceil$, respectively. Therefore, we can claim that $d_{\omega,i}^j = z_{\omega,i}^j - h_{\omega,i}^j$ if and only if $z_{\omega,i}^j \geq \lceil h_{\omega,i}^j \rceil$.

Case II. $d_{\omega,i}^j = h_{\omega,i}^j - z_{\omega,i}^j$: This case will happen if and only if $h_{\omega,i}^j - z_{\omega,i}^j \geq z_{\omega,i}^j - h_{\omega,i}^j$ and $h_{\omega,i}^j - z_{\omega,i}^j \geq (1 - 2\mu_{\omega,i}^j)(z_{\omega,i}^j - \lfloor h_{\omega,i}^j \rfloor) + \mu_{\omega,i}^j$, which are equivalent to $z_{\omega,i}^j \leq h_{\omega,i}^j$ and $z_{\omega,i}^j \leq \lfloor h_{\omega,i}^j \rfloor$, respectively, as $\mu_{\omega,i}^j \leq 1$. Therefore, $d_{\omega,i}^j = h_{\omega,i}^j - z_{\omega,i}^j$ if and only if $z_{\omega,i}^j \leq \lfloor h_{\omega,i}^j \rfloor$.

Case III. $d_{\omega,i}^j = (1 - 2\mu_{\omega,i}^j)(z_{\omega,i}^j - \lfloor h_{\omega,i}^j \rfloor) + \mu_{\omega,i}^j$: This case will happen if and only if $(1 - 2\mu_{\omega,i}^j)(z_{\omega,i}^j - \lfloor h_{\omega,i}^j \rfloor) + \mu_{\omega,i}^j \geq h_{\omega,i}^j - z_{\omega,i}^j$ and $(1 - 2\mu_{\omega,i}^j)(z_{\omega,i}^j - \lfloor h_{\omega,i}^j \rfloor) + \mu_{\omega,i}^j \geq z_{\omega,i}^j - h_{\omega,i}^j$, which are equivalent to $z_{\omega,i}^j \geq \lfloor h_{\omega,i}^j \rfloor$ and $z_{\omega,i}^j \leq \lceil h_{\omega,i}^j \rceil$, respectively. Therefore, $d_{\omega,i}^j = (1 - 2\mu_{\omega,i}^j)(z_{\omega,i}^j - \lfloor h_{\omega,i}^j \rfloor) + \mu_{\omega,i}^j$ if and only if $\lfloor h_{\omega,i}^j \rfloor \leq z_{\omega,i}^j \leq \lceil h_{\omega,i}^j \rceil$.

For each $j \in J$, let $\mathcal{I} := \{1, \dots, m_2\}$ be partitioned into the disjoint sets \mathcal{I}_1^j , \mathcal{I}_2^j , and \mathcal{I}_3^j , i.e. $\mathcal{I} = \mathcal{I}_1^j \cup \mathcal{I}_2^j \cup \mathcal{I}_3^j$, such that $\mathcal{I}_1^j := \{i \in \mathcal{I} : d_{\omega,i}^j = z_{\omega,i}^j - h_{\omega,i}^j\}$, $\mathcal{I}_2^j := \{i \in \mathcal{I} : d_{\omega,i}^j = h_{\omega,i}^j - z_{\omega,i}^j\}$, and $\mathcal{I}_3^j := \{i \in \mathcal{I} : d_{\omega,i}^j = (1 - 2\mu_{\omega,i}^j)(z_{\omega,i}^j - \lfloor h_{\omega,i}^j \rfloor) + \mu_{\omega,i}^j\}$.

Therefore, in the light of the above discussed cases, we can define $\mathcal{K}_\omega^4(x)$ as

$$\mathcal{K}_\omega^4(x) = \left\{ (y_\omega, d_\omega) \in \mathbb{R}^{q|J|} \times \mathbb{R}_+^{m_2|J|+|J|} : W_\omega y_\omega \geq r_\omega - T_\omega x, \right. \\ e_{\omega,i}^j y_\omega^j \geq \lceil h_{\omega,i}^j \rceil - f_{\omega,i}^j x, \quad d_{\omega,i}^j = e_{\omega,i}^j y_\omega^j - (h_{\omega,i}^j - f_{\omega,i}^j x), \quad i \in \mathcal{I}_1^j, j \in J, \\ e_{\omega,i}^j y_\omega^j \leq \lfloor h_{\omega,i}^j \rfloor - f_{\omega,i}^j x, \quad d_{\omega,i}^j = (h_{\omega,i}^j - f_{\omega,i}^j x) - e_{\omega,i}^j y_\omega^j, \quad i \in \mathcal{I}_2^j, j \in J, \\ \lfloor h_{\omega,i}^j \rfloor - f_{\omega,i}^j x \leq e_{\omega,i}^j y_\omega^j \leq \lceil h_{\omega,i}^j \rceil - f_{\omega,i}^j x, \quad i \in \mathcal{I}_3^j, j \in J, \\ \left. d_{\omega,i}^j = (1 - 2\mu_{\omega,i}^j) (e_{\omega,i}^j y_\omega^j - \lfloor h_{\omega,i}^j \rfloor + f_{\omega,i}^j x) + \mu_{\omega,i}^j, \quad i \in \mathcal{I}_3^j, j \in J \right\}.$$

Let $(\hat{y}_\omega, \hat{d}_\omega)$ be an extreme point of $\text{Proj}_{y_\omega, d_1, \dots, d_{|\Omega|}}(\mathcal{K}_\omega^4(x))$ for a given $x \in X$, which is on the intersection of $|J|(q + m_2)$ constraints of $\mathcal{K}_\omega^4(x)$ such that the matrix defining these constraints is nonsingular. Since the polyhedron $\mathcal{K}_\omega^4(x)$ already has $m_2|J|$ equality constraints, we need a combination of at least $q|J|$ defining inequalities of $\mathcal{K}_\omega^4(x)$ to be binding at the point $(\hat{y}_\omega, \hat{d}_\omega)$. Let the constraints $w_{\omega,i} y_\omega \geq r_{\omega,i} - t_{\omega,i} x$ for $i \in \tau_0$, $e_{\omega,i}^j y_\omega^j \geq \lceil h_{\omega,i}^j \rceil - f_{\omega,i}^j x$, for $i \in \tau_1^j, j \in J_1$, and $e_{\omega,i}^j y_\omega^j \leq \lfloor h_{\omega,i}^j \rfloor - f_{\omega,i}^j x$ for $i \in \tau_2^j, j \in J_2$ be binding at the point $(\hat{y}_\omega, \hat{d}_\omega)$ where $w_{\omega,i}$, $r_{\omega,i}$, and $t_{\omega,i}$ denote i th row of matrix/vector W_ω , r_ω , and T_ω , respectively, and τ_0 , $\tau_1^j, j \in J_1 \subseteq J$, and $\tau_2^j, j \in J_2 \subseteq J$, are subsets of $\{1, \dots, m_2\}$ such that $|\tau_0| + \sum_{j \in J_1} |\tau_1^j| + \sum_{j \in J_2} |\tau_2^j| = q|J|$. Then, \hat{y}_ω satisfies the following system of equations:

$$w_{\omega,i} \hat{y}_\omega = r_{\omega,i} - t_{\omega,i} x, \quad i \in \tau_0, \quad (3.61)$$

$$e_{\omega,i}^j \hat{y}_\omega^j = \lceil h_{\omega,i}^j \rceil - f_{\omega,i}^j x, \quad i \in \tau_1^j, j \in J_1, \quad (3.62)$$

$$e_{\omega,i}^j \hat{y}_\omega^j = \lfloor h_{\omega,i}^j \rfloor - f_{\omega,i}^j x, \quad i \in \tau_2^j, j \in J_2, \quad (3.63)$$

which in compact form is written as $\Pi_\omega \hat{y}_\omega = \pi_\omega(x)$, where Π_ω is a submatrix of

$$\begin{bmatrix} W_\omega \\ E_\omega \end{bmatrix} = \begin{bmatrix} W_\omega^1 & \cdots & W_\omega^{|J|} \\ E_\omega^1 & 0 & 0 \\ 0 & \ddots & 0 \\ 0 & 0 & E_\omega^{|J|} \end{bmatrix}.$$

According to condition (i), if W_ω and E_ω^j are network flow matrices, i.e., each row of these matrices represents arc in a network and each column corresponds to node, then $\begin{bmatrix} W_\omega \\ E_\omega \end{bmatrix}$ is equivalent to adding arcs in a digraph, which is still a network flow matrix and is TU ([112]). Thus, Π_ω is also TU. Similarly, for condition (ii) when E_ω^j for $j \in J$ are TU matrices, which implies E_ω is TU, and $W_\omega = \mathbf{I}_{m_3}$ (or $W_\omega = \mathbf{0}$), Π_ω is a TU matrix.

Also, since each component of the vector $\pi_\omega(x)$, i.e., $r_{\omega,i} - t_{\omega,i}x$, $\lceil h_{\omega,i}^j \rceil - f_{\omega,i}^j x$, or $\lfloor h_{\omega,i}^j \rfloor - f_{\omega,i}^j x$, is integral, \hat{y}_ω is integral. Hence, all bounded faces of $\mathcal{K}_\omega^3(x)$ have extreme point $(\hat{y}_\omega, \hat{d}_\omega)$ in $\text{Proj}_{y_\omega, d_1, \dots, d_{|J|}}(\mathcal{K}_\omega^3(x))$ space with integral \hat{y}_ω and since $\mathcal{K}_\omega^3(x)$ is a subset of the continuous relaxation of $\mathcal{K}_\omega^1(x)$, $\mathcal{K}_\omega^3(x) \subseteq \text{conv}(\mathcal{K}_\omega^1(x))$ for all $x \in X$. Therefore, we have $\mathcal{K}_\omega^3(x) = \text{conv}(\mathcal{K}_\omega^1(x))$.

Finally because of Theorem 3.7, $\text{conv}(\mathcal{K}_\omega^1(x)) \cap \mathcal{K}_\omega^2(x) \subseteq \mathcal{K}_\omega^3(x) \cap \mathcal{K}_\omega^2(x)$ where $\mathcal{K}_\omega^2(x) := \{(y_\omega, d_\omega) \in \mathbb{R}^{q|J|} \times \mathbb{R}_+^{m_2|J|+|J|} : \|d_\omega^j\|_p \leq d_{\omega,0}^j, j \in J\}$, provides the convex hull (for $p = 1$) or an approximation (for $p \geq 2$) for $\mathcal{K}_\omega(x)$. In other words, we obtain the convex hull (for $p = 1$) or an approximation (for $p \geq 2$) of $\mathcal{K}_\omega(x)$ by

adding $m_2 \times |J|$ number of linear inequalities:

$$d_{\omega,i}^j \geq (1 - 2\mu_{\omega,i}^j) (e_{\omega,i}^j y_{\omega}^j - \lfloor h_{\omega,i}^j \rfloor + f_{\omega,i}^j) + \mu_{\omega,i}^j, i = 1, \dots, m_2, j \in J, \quad (3.64)$$

to the continuous relaxation of $\mathcal{K}_{\omega}(x)$. Moreover, $\mathcal{K}_{\omega}^3(x) \cap \mathcal{K}_{\omega}^2(x)$ when projected to $(y_{\omega}, d_{\omega,0})$ space gives the convex hull (for $p = 1$) or an approximation (for $p \geq 2$) of the feasible region of $\overline{\mathcal{Q}}_{\omega}(x)$, i.e.

$$\left\{ (y_{\omega}, d_{\omega,0}) \in \mathbb{R}^{|J|} \times \mathbb{R}_+^{|J|} : (3.49), (3.50), \text{ and } \left\| \overline{E}_{\omega,l}^j y_{\omega}^j + \overline{F}_{\omega,l}^j x - \overline{h}_{\omega,l}^j \right\|_p \leq d_{\omega,0}^j, l \in \mathcal{L}, j \in J \right\},$$

where the i th row of $\overline{E}_{\omega,l}^j y_{\omega}^j + \overline{F}_{\omega,l}^j x - \overline{h}_{\omega,l}^j$ is either $e_{\omega,i}^j y_{\omega}^j + f_{\omega,i}^j x - h_{\omega,i}^j$ or $(1 - 2\mu_{\omega,i}^j) (e_{\omega,i}^j y_{\omega}^j - \lfloor h_{\omega,i}^j \rfloor + f_{\omega,i}^j x) + \mu_{\omega,i}^j$. This completes the proof. \square

3.6.2 Scenario-Based Cuts for Extensive Formulation of Structured TSS-CMIPs

We consider extensive formulation of structured TSS-CMIPs introduced in the previous section and present partial convex hull for them using Theorems 3.8-3.12 and Corollary 3.10; the proofs are provided in Appendix A.3. Note that for $\hat{x} \in X$ and $\omega \in \Omega$, $\overline{\mathcal{K}}_{\omega}(\hat{x}) = Proj_{x=\hat{x}, y_{\omega}, d_{\omega}}(\overline{\mathcal{P}})$ and $\overline{\mathcal{K}}_{tight}^{\omega}(\hat{x}) = Proj_{x=\hat{x}, y_{\omega}, d_{\omega}}(\overline{\mathcal{P}}_{pch})$.

Corollary 3.13. *Let*

$$\overline{\mathcal{P}} := \left\{ \sqrt{(y_{\omega,1} + f_{\omega} x - h_{\omega})^2 + (y_{\omega,2})^2} \leq d_{\omega,0}, \omega \in \Omega \right. \quad (3.65)$$

$$x \in X, y_{\omega,1} \in \mathbb{Z}, y_{\omega,2} \in \mathbb{R}_+, d_{\omega,0} \in \mathbb{R}_+, \quad \omega \in \Omega \Big\}.$$

For each nonempty set $\Gamma \subseteq \Omega$, a partial convex hull of $\bar{\mathcal{P}}$ is given by

$$\bar{\mathcal{P}}_{pch} := \left\{ (x, y_{\omega,1}, y_{\omega,2}, d_{\omega,0}) \in X \times \mathbb{R} \times \mathbb{R}_+^2 : (3.65) \text{ and} \right. \\ \left. \sqrt{((1 - 2\mu_{\omega})(y_{\omega,1} + f_{\omega}x - h_{\omega}) + \mu_{\omega})^2 + (y_{\omega,2})^2} \leq d_{\omega,0}, \quad \omega \in \Omega \right\},$$

where $\mu_{\omega} = h_{\omega} - \lfloor h_{\omega} \rfloor$.

Corollary 3.14. *Let*

$$\bar{\mathcal{P}} := \left\{ (x, \{y_{\omega}, d_{\omega,0}\}_{\omega \in \Omega}) \in X \times \mathbb{Z}^{|\Omega| \times |J|} \times \mathbb{R}_+^{|\Omega| \times |J|} : T_{\omega}x + W_{\omega}y_{\omega} \geq r_{\omega}, \omega \in \Omega, \right. \\ \left. \|\mathbf{1}y_{\omega}^j + F_{\omega}^jx - h_{\omega}^j\|_p \leq d_{\omega,0}^j, \quad j \in J, \omega \in \Omega \right\},$$

where W_{ω} is a TU matrix. For each nonempty set $\Gamma \subseteq \Omega$, a partial convex hull of $\bar{\mathcal{P}}$ with $p = 1$ is given by

$$\bar{\mathcal{P}}_{pch} := \left\{ (x, \{y_{\omega}, d_{\omega,0}\}_{\omega \in \Omega}) \in X \times (\mathbb{Z}^{|\Omega| - |\Gamma|} \times \mathbb{R}^{|\Gamma|})^{|J|} \times \mathbb{R}_+^{|\Omega| \times |J|} : \right. \\ T_{\omega}x + W_{\omega}y_{\omega} \geq r_{\omega}, \quad \omega \in \Omega, \\ \|\mathbf{1}y_{\omega}^j + F_{\omega}^jx - h_{\omega}^j\|_p \leq d_{\omega,0}^j, \quad j \in J, \omega \in \Omega, \\ \left. \|\bar{E}_{\omega,l}^j y_{\omega}^j + \bar{F}_{\omega,l}^j x - \bar{h}_{\omega,l}^j\|_p \leq d_{\omega,0}^j, \quad l \in \mathcal{L}, j \in J, \omega \in \Gamma \right\},$$

where the i th row of $\bar{E}_{\omega,l}^j y_{\omega}^j + \bar{F}_{\omega,l}^j x - \bar{h}_{\omega,l}^j$ is either $y_{\omega}^j + f_{\omega,i}^j x - h_{\omega,i}^j$ or $(1 - 2\mu_{\omega,i}^j)(y_{\omega}^j - \lfloor h_{\omega,i}^j \rfloor + f_{\omega,i}^j x) + \mu_{\omega,i}^j$, and $\mu_{\omega,i}^j = h_{\omega,i}^j - \lfloor h_{\omega,i}^j \rfloor$.

Corollary 3.15. *Let*

$$\begin{aligned} \bar{\mathcal{P}} &:= \left\{ (x, \{y_\omega, d_{\omega,0}\}_{\omega \in \Omega}) \in X \times \mathbb{Z}^{q|\Omega| \times |J|} \times \mathbb{R}_+^{|\Omega| \times |J|} : \right. \\ &\quad T_\omega x + W_\omega y_\omega \geq r_\omega, \omega \in \Omega, \\ &\quad \left. \left\| E_\omega^j y_\omega^j + F_\omega^j x - h_\omega^j \right\|_p \leq d_{\omega,0}^j, j \in J, \omega \in \Omega \right\}, \end{aligned}$$

such that either of following conditions is satisfied:

- (i) E_ω^j , $j \in J$, and W_ω are network flow matrices;
- (ii) E_ω^j , $j \in J$ are TU matrices, and $W_\omega = \mathbf{I}_{m_3}$ or $W_\omega = \mathbf{0}$.

For each nonempty set $\Gamma \subseteq \Omega$, a partial convex hull of $\bar{\mathcal{P}}$ with $p = 1$ is given by

$$\begin{aligned} \bar{\mathcal{P}}_{pch} &:= \left\{ (x, \{y_\omega, d_{\omega,0}\}_{\omega \in \Omega}) \in X \times (\mathbb{Z}^{|\Omega| - |\Gamma|} \times \mathbb{R}^{|\Gamma|})^{q \times |J|} \times \mathbb{R}_+^{|\Omega| \times |J|} : \right. \\ &\quad T_\omega x + W_\omega y_\omega \geq r_\omega, \omega \in \Omega, \\ &\quad \left\| E_\omega^j y_\omega^j + F_\omega^j x - h_\omega^j \right\|_p \leq d_{\omega,0}^j, j \in J, \omega \in \Omega, \\ &\quad \left. \left\| \bar{E}_{\omega,l}^j y_\omega^j + \bar{F}_{\omega,l}^j x - \bar{h}_{\omega,l}^j \right\|_p \leq d_{\omega,0}^j, l \in \mathcal{L}, j \in J, \omega \in \Gamma \right\}, \end{aligned}$$

where the i th row of $\bar{E}_{\omega,l}^j y_\omega^j + \bar{F}_{\omega,l}^j x - \bar{h}_{\omega,l}^j$ is either $e_{\omega,i}^j y_\omega^j + f_{\omega,i}^j x - h_{\omega,i}^j$ or $(1 - 2\mu_{\omega,i}^j)(e_{\omega,i}^j y_\omega^j - \lfloor h_{\omega,i}^j \rfloor + f_{\omega,i}^j x) + \mu_{\omega,i}^j$, and $\mu_{\omega,i}^j = h_{\omega,i}^j - \lfloor h_{\omega,i}^j \rfloor$.

3.6.3 Tight Second Stage Formulation and Partial Convex Hull for the Extensive Formulation of MM-SFLP-S

We also provide tight second stage formulation for MM-SFLP-S (introduced in Section 3.1.3) and partial convex hull for the extensive formulation of the MM-SFLP-S. To do so, we first reformulate the second stage problem (3.12)-(3.14) using additional continuous variables (as discussed in Section 3.4) to get

$$Q_\omega(x, z, u) = \min \sum_{i \in P} w_{inv}^i \left(\sum_{k=1}^n \alpha_k x_{ik} + u_i - \sum_{j \in P'} (z_{ij} + y_\omega^{ij}) \right) + w_{sc} \sum_{j \in P'} \sum_{i \in P} t_{ij} y_{ij}^\omega + w_{pen} d_{\omega,0} \quad (3.66)$$

$$\text{s.t. } \left| \sum_{i \in P} (y_\omega^{ij} + z_{ij}) - \zeta_\omega^j \right| \leq d_{\omega,j}, \quad \text{for } j \in P', \quad (3.67)$$

$$\sum_{j \in P'} |d_{\omega,j}| \leq d_{\omega,0}, \quad d_{\omega,j} \geq 0, \quad j \in P', \quad (3.13), (3.14) \text{ hold.} \quad (3.68)$$

Corollary 3.16. *Let $\mathcal{Y}_\omega(x, z, u) := \{y_\omega : (3.67) - (3.68)\}$. For each $(x, z, u) \in \mathcal{X}$ and $\omega \in \Omega$, the convex hull of $\mathcal{Y}_\omega(x, z, u)$ is obtained by adding the following scenario-based conic MIR cuts to the continuous relaxation of $\mathcal{Y}_\omega(x, z, u)$:*

$$(1 - 2\zeta_\omega^j + 2\lfloor \zeta_\omega^j \rfloor) \left(\sum_{i \in P} y_{ij}^\omega - \lfloor \zeta_\omega^j \rfloor + \sum_{i \in P} z_{ij} \right) + \zeta_\omega^j - \lfloor \zeta_\omega^j \rfloor \leq d_{\omega,j}, \text{ for all } j \in P'. \quad (3.69)$$

Moreover, the addition of the foregoing cuts in $(x, z, u, y_\omega, d_\omega)$ space to the extensive formulation of the MM-SFLP-S provides a partial convex hull (with no integrality restrictions on y_ω integer variables) for the feasible region of the extensive

formulation.

Proof. Observe that the coefficient matrix associated with $y_\omega^j := (y_\omega^{1j}, y_\omega^{2j}, \dots, y_\omega^{|P|j})$ variables in constraint (3.67) is a network flow matrix. Likewise, the coefficient matrix associated with y_ω variables in constraint (3.13) is a network flow matrix. Therefore, we utilize Theorem 3.12(i) and Corollary 3.15(i) to derive convex hull of $\mathcal{Y}_\omega(x, z, u)$ for each $(x, z, u) \in \mathcal{X}$ and partial convex hull (with no integrality restrictions on y_ω variables) for the extensive formulation of the MM-SFLP-S, respectively, by adding the scenario-based conic MIR cuts,

$$(1 - 2\zeta_\omega^j + 2[\zeta_\omega^j]) \left(\sum_{i \in P} y_{ij}^\omega - [\zeta_\omega^j] + \sum_{i \in P} z_{ij} \right) + \zeta_\omega^j - [\zeta_\omega^j] \leq d_{\omega,j}, \text{ for all } j \in P',$$

to the continuous relaxation of \mathcal{Y}_ω and the extensive formulation, respectively. \square

Remark 3.17. The scenario-based cuts (3.69) in $(x, z, u, y_\omega, d_\omega)$ space are valid for the extensive formulation of MM-DRFLP-S, i.e.,

$$\begin{aligned} \min \quad & \sum_{i \in P} \sum_{k=1}^n c_i^k x_{ik} + \sum_{i \in P} \sum_{j \in P'} t_{ij} z_{ij} + \sum_{i \in P} g_i u_i + \theta \\ \text{s.t.} \quad & \sum_{\omega \in \Omega} \bar{p}_\omega f(x, z, u, y_\omega, d_\omega) \leq \theta, \quad \text{for all } \{\bar{p}\}_{\omega \in \Omega} \in \mathfrak{P}, \\ & (x, z, u) \in \mathcal{X}, \quad (3.67) - (3.68) \quad \text{for all } \omega \in \Omega, \end{aligned} \quad (3.70)$$

where the affine function

$$\begin{aligned} f(x, z, u, y_\omega, d_\omega) := & \sum_{i \in P} w_{inv}^i \left(\sum_{k=1}^n \alpha_k x_{ik} + u_i - \sum_{j \in P'} (z_{ij} + y_\omega^{ij}) \right) \\ & + w_{sc} \sum_{j \in P'} \sum_{i \in P} t_{ij} y_{ij}^\omega + w_{pen} d_{\omega,0}. \end{aligned}$$

3.7 Computational Experiments

We perform computational experiments to evaluate the effectiveness of adding scenario-based cuts (a priori) for solving MM-SFLP-S and MM-DRFLP-S (introduced in Section 3.1.3), and structured TSS-CMIP test and TSDR-CMIP instances. We describe generation of the test instances in Sections 3.7.1 and 3.7.2, and present our computational results in Section 3.7.3. For MM-SFLP-S and structured TSS-CMIP instances, we assume that all scenarios have same probability, i.e., $\bar{p}_\omega = 1/|\Omega|$ for all $\omega \in \Omega$. In contrast, for MM-DRFLP-S and structured TSDR-CMIP instances, we consider a finite set of distributions \mathfrak{P} with $|\mathfrak{P}| \in \{5, 10, 25, 50\}$. We generate the probability distributions for each ambiguity set as follows. For a probability distribution with $|\Omega|$ scenarios, we randomly draw $|\Omega|$ numbers, i.e., RN_ω for $\omega \in \Omega$, between $[0, 10000]$, and the probability of scenario ω is calculated as $\bar{p}_\omega = \frac{RN_\omega}{\sum_{\omega \in \Omega} RN_\omega}$.

3.7.1 Generation of MM-SFLP-S and MM-DRFLP-S Test Instances

We utilize “capacitated warehouse location problem” instances from J.E. Beasley OR-Library [21] where a set $P := \{1, \dots, 16\}$ of facilities, a set $P' := \{1, \dots, 50\}$ of retailers, and transportation cost t_{ij} for each $i \in P$ and $j \in P'$ are given. However, unlike instance in this library where demand $\mu \in \mathbb{R}_+^{|P'|}$ is assumed to be deterministic, we consider uncertain demand which follows a normal distribution with μ (provided in the library) as mean and variance is randomly drawn from a uniform distribution, i.e., $uniform[0.1\mu, 0.3\mu]$. Moreover, instead of assuming

that each facility has machines of fixed capacities, we consider n different types of machines with different capacities ($n \in \{2, 4\}$ for our experiments). Unlike the warehouse location problem, the MM-SFLP-S and MM-DRFLP-S also allow subcontracting and last minute order options, and its objective is to minimize the total machines' installation cost, transportation cost, subcontracting cost, and the expected (second-stage) transportation, inventory, and penalty costs associated with the last minute ordering after a realization of uncertain demand. We generate the aforementioned cost parameters as follows: the subcontract cost is 4 per unit, i.e., $g_i = 4$ for all i , the inventory cost is 0.35 per unit, i.e., $w_{inv}^i = 0.35$, for all i , the last minute order cost is 3 times the transportation cost t_{ij} , i.e., $w_{sc} = 3$, and the demand penalty is set to 100 per unit, i.e., $w_{pen} = 100$. The capacity of modules and their installation costs, (α_k, c_i^k) , belong to the set $\{(1000, 2700), (4000, 9000), (10000, 18000), (16000, 25000)\}$. We allow at most 200 subcontract items, i.e., $r = 2000$, and the maximum number of modules at each facility is at most 4, i.e., $s_i = 4$ for $i \in P$.

3.7.2 Generation of Structured TSS-CMIP Test Instances

For our computational experiments, we consider the extensive formulation of reformulated TSS-CMIP with $p = 1$ or $p = 2$, and structured CMIPs in the second stage (as discussed in previous section), i.e. either $E_\omega^j = \mathbf{I}$ (an identity matrix) or E_ω^j is a randomly generated deterministic network flow matrix for $j \in J$, and W_ω is a deterministic network flow matrix for all $\omega \in \Omega$. Specifically, we generate network flow matrices as follows. First, we randomly generate two graph edge vectors $v_1, v_2 \in \mathbb{Z}_+^{m'}$, where m' is the number of rows of desired matrix. For any

element in v_1 and v_2 , i.e., v_1^i and v_2^i for $1 \leq i \leq m'$, we have $v_1^i, v_2^i \leq n'$ and $v_1^i \neq v_2^i$, where n' is the number of columns of desired matrix. Here, v_1 and v_2 are vectors of index of graph nodes. We create an undirected graph with these m' node pairs using MATLAB function `graph(v1, v2)`. This function specifies (v_1^i, v_2^i) for $1 \leq i \leq m'$ as an edge, and generates a graph with m' edges and \hat{n} ($\hat{n} \leq n'$) nodes, where $\hat{n} = \max\{v_1^1, \dots, v_1^{m'}, v_2^1, \dots, v_2^{m'}\}$. We obtain the network flow matrix of size $m' \times \hat{n}$ corresponding to this graph and set the remaining $n' - \hat{n}$ columns to $\mathbf{0}$, thereby providing a network flow matrix of desired size. For each structured TSS-CMIP with $p = 2$ and only integer variables in the second stage, we generate two sets of random instances: instances from the first problem set are motivated from the Stochastic Integer Programming Library (SIPLIB) TSS-MILP instances [3], in particular stochastic server location problem (SSLP) and stochastic multiple binary knapsack problem (SMBKP) instances, whereas for the second problem set, we consider instances with larger number of scenarios (up to 10,000). More specifically, in the first problem set, we generate random instances with similar problem size as of SSLP and SMBKP instances but with uncertain cost-coefficients, technology matrix, F_ω^j , h_ω^j and right-hand-side.

Likewise for TSS-CMIPs with $p = 1$, we consider instances with network flow E_ω^j matrix for all $j \in J$ and larger number of scenarios (up to 50,000). In Tables 3.1, 3.2, and 3.3, we provide details of problem categories for different types of structured second-stage CMIPs, i.e., E_ω^j is an identity matrix or any network flow matrix, used for our experiments. We denote the number of linear constraints and number of integer variables by $\#LCon$ and $\#IVar$, respectively, in each stage. We use $\#PCCon$ and $\#p-OCcon$ to denote the number of polyhedral conic constraints

(3.19) or number of rows in E_{ω}^j , and number of p -order conic constraints (3.20), respectively, in the second stage.

Table 3.1: Details of TSS-CMIP Instances with $p = 1$ and E_{ω}^j is network flow matrix

Instance Category	Stage I		Stage II			
	#LCon	#IVar	#LCon	#IVar	#PCCon	# p -OCon
SCMIP.25.50.5	10	25	20	50	25	5
SCMIP.50.100.5	25	50	40	100	50	5
SCMIP.100.150.5	75	100	50	150	70	5
SCMIP.5.10.5	50	5	2	10	3	5

Table 3.2: Details of TSS-CMIP Instances with $p = 2$ and $E_{\omega}^j = \mathbf{I}$

Problem Set	Instance Category	Stage I		Stage II			
		#LCon	#IVar	#LCon	#IVar	#PCCon	# p -OCon
I	SCMIP.5.125.1	1	5	30	125	125	1
	SCMIP.10.500.1	1	10	60	500	500	1
	SCMIP.15.675.1	1	15	60	675	675	1
	SCMIP.20.800.1	1	20	60	800	800	1
	SCMIP.240.120.1	50	240	5	120	120	1
II	SCMIP.5.10.1	5	5	5	10	10	1
	SCMIP.10.10.1	5	10	10	10	10	1

Table 3.3: Details of TSS-CMIP Instances with $p = 2$ and E_{ω}^j is network flow matrix

Problem Set	Instance Category	Stage I		Stage II			
		#LCon	#IVar	#LCon	#IVar	#PCCon	# p -OCon
I	SCMIP.5.125.3	1	5	30	125	100	3
	SCMIP.10.500.3	1	10	60	500	300	3
	SCMIP.15.675.3	1	15	60	675	400	3
	SCMIP.240.120.3	50	240	5	120	100	3
II	SCMIP.10.25.3	5	10	10	25	10	3
	SCMIP.10.50.3	5	10	20	50	25	3
	SCMIP.10.75.3	5	10	20	75	35	3
	SCMIP.25.50.3	10	25	20	50	25	3
	SCMIP.25.100.3	10	25	20	100	80	3

We use SCMIP. α . β . λ to denote our instance category in Tables 3.1, 3.2, and 3.3,

where α is the number of integer variables in the first stage, β is the number of integer variables in the second stage, and λ is the number of p -order conic constraints in the second stage. Note that in Table 3.2, #PCCon is the same as #IVar in the second stage as E_ω^j is an identity matrix. For each instance category, we generate instances as follow: we draw c from $uniform[0, 10]$, A, b from $uniform[0, 100]$, r_ω, T_ω from $integer\ uniform[-100, 100]$, F_ω^j from $integer\ uniform[-10, 10]$, h_ω^j from $uniform[-10, 10]$. Moreover, for instance categories in Table 3.2, we let $g_\omega = \mathbf{0}$ and $\hat{g}_\omega^j = 1$ for $\omega \in \Omega$, $j \in J$, while for instance categories in Tables 3.1 and 3.3, g_ω is randomly generated from $uniform[-1, 1]$ and \hat{g}_ω^j is randomly generated from $uniform[-10, 10]$. Since y_ω^j is an unrestricted variable and $g_\omega \in [-1, 1]$ for $j \in J$ and $\omega \in \Omega$, we observed that many randomly generated TSS-CMIP instances have unbounded solution values. Therefore, in order to obtain finite optimal solution values, we impose an upper bound of 100 and a lower bound of -100 on each y_ω^j variable. Note that when $E_\omega^j = \mathbf{I}$, the number of integer variables in the second stage, i.e., q , is same as number of polyhedral conic constraints, i.e., m_2 . Whereas for instance categories in Table 3.1 and 3.3, E_ω^j is not a square matrix. These instances will be available at computational Operations Research exchange (cORe) <https://core.isrd.isi.edu/> and GitHub page of the authors.

3.7.3 Computational Framework

In this section, we evaluate the effectiveness of our scenario-based cuts by performing computational experiments on instances belonging to the aforementioned instance categories with different number of scenarios. The results of our experi-

ments are presented in Tables 3.4, 3.6, 3.7, and 3.9. Each row in Tables 3.6 and 3.7 reports the average over five randomly generated instances corresponding to the instance category in Table 3.1 and 3.2, respectively, while each row in Tables 3.4 and 3.9 report the average over three randomly generated (relatively harder) instances belonging to MM-SFLP-S and instance category in Table 3.3, respectively. For instances in Table 3.1, we perform three experiments: NO-SCUT, WITH-SCUTS, and BD-WITH-SCUTS. While for instances in Table 3.2, 3.3 and 3.4, we only perform the first two experiments. In NO-SCUT, we solve the reformulated extensive formulation of the problem using CPLEX 12.70 with its default settings, without adding our scenario-based cuts. (In order to improve the performance of CPLEX, we substitute unrestricted variable y_ω^j by $y_\omega^{j+} - y_\omega^{j-}$ in our experiments, where $y_\omega^{j+}, y_\omega^{j-} \geq 0$ for $j \in J, \omega \in \Omega$.) Whereas in WITH-SCUTS, we add our scenario-based linear cuts (provided in Theorem 3.12 or derived through reformulation of $\overline{\mathcal{P}}_{pch}$ in Corollary 3.15 for $\Gamma = \Omega$), a priori to the reformulated extensive formulation of the problem instance, relax the integrality constraints of second stage integer variables, and use CPLEX 12.70 with its default settings to solve it. In BD-WITH-SCUTS for TSS-CMIP with $p = 1$, we first convexify the second stage problem by adding our parametric cuts (provided in Theorem 3.12), and then solve it using Benders' decomposition routine of CPLEX 12.70. For NO-SCUT and WITH-SCUTS, we allow presolve option in CPLEX 12.70; while for BD-WITH-SCUTS, we turn it off. All experiments are performed on a 8-core Xeon 2.4 GHz machine with 24 GB RAM running with Windows 10.

In Tables 3.4, 3.5, 3.6, 3.7 and 3.9, we report following statistics: number of integer variables in the extensive formulation with(out) scenario-based cuts ($\#IVar$),

number of linear constraints in the extensive formulation without our scenario-based cuts ($\#LCon$), and the number of linear scenario-based cuts added in the the extensive formulation ($\#LCuts$). Also, we denote the total time taken to solve TSS-CMIP and TSDR-CMIP instances without and with our scenario-based cuts in extensive formulation by T-EF and T-EFC, respectively, and the percentage of integrality gap closed by a priori addition of scenario-based cuts by $ImprG\% = 100 \times (V_{pcut} - V_{cp}) / (V_{mip} - V_{cp})$, where V_{pcut} , V_{cp} , and V_{mip} denote the optimal objective value of continuous relaxation of extensive formulation with our scenario-based cuts, continuous relaxation of extensive formulation without our scenario-based cuts, and original formulation, respectively. In Table 3.6, T-BDC denotes the time taken to solve TSS-CMIP with $p = 1$ and linear programming equivalent of the second stage CMIP, using Benders' decomposition routine of CPLEX. We use TL to notify that CPLEX cannot solve the corresponding instance within 3 hours time limit and OM to notify that our system ran out of 24 GB memory when solving this instance. Instances for which we could not obtain the optimal value due to TL or OM, we put - in column $ImprG\%$.

Computational results for MM-SFLP-S and MM-DRFLP-S instances.

In Table 3.4, we observe that by adding the scenario-based conic MIR cuts a priori, the number of integer variables ($\#IVar$) is significantly reduced for MM-SFLP-S instances. The average gap closed by the scenario-based cuts is 98%. Without the scenario-based cuts, only 8 out of 24 MM-SFLP-S instances can be solved by CPLEX within the time limit. In contrast, after adding the cuts, 10 out of 16 foregoing unsolved instances are solved in 2576 seconds (on average). After

adding the scenario-based cuts, CPLEX took lesser time to solve 6 out of above 8 instances, i.e., 1681 seconds on average. Whereas it took 2201 seconds (on average) for CPLEX to solve these instances without the cuts.

Table 3.4: Results of Computational Experiments for the MM-SFLP-S Instances

Instance Category	$ \Omega $	NO-SCUT			WITH-SCUTs			
		#IVar	#LCon	T-EF	#IVar	#LCuts	T-EFC	ImprG%
$\alpha_1 = 1000$ $\alpha_2 = 4000$	100	80944	11633	72.8	944	5000	52	98
	500	400944	58033	1173	944	25000	885	98
	750	600944	87033	TL	944	37500	2125	98
	1000	800944	116033	4913	944	50000	3633	98
$\alpha_1 = 1000$ $\alpha_2 = 16000$	100	80944	11633	TL	944	5000	145.1	89
	500	400944	58033	TL	944	25000	3513	90
	750	600944	87033	TL	944	37500	TL	90
	1000	800944	116033	TL	944	50000	TL	-
$\alpha_1 = 1000$ $\alpha_2 = 4000$ $\alpha_3 = 10000$ $\alpha_4 = 16000$	100	81072	11633	TL	1072	5000	360	92
	500	401072	58033	6329	1072	25000	8645	92
	750	601072	87033	TL	1072	37500	TL	-
	1000	801072	116033	TL	1072	50000	TL	-

In Table 3.5, we observe that by adding scenario-based conic MIR cuts a priori to the extensive formulation of MM-DRFLP-S, the average gap closed is 93.3%. Without these cuts, CPLEX could not solve any of the 36 MM-DRFLP-S instances within the time limit. In contrast, after adding the cuts, all these instances can be solved in 1145 seconds (on average). Recall that MM-SFLP-S is equivalent to MM-DRFLP-S with $|\mathfrak{P}| = 1$, therefore as expected, the time taken to solve MM-DRFLP-S instances in Table 3.5 is more than the time taken to solve MM-SFLP-S instances in Table 3.4 with $|\Omega| = 100$.

Table 3.5: Results of Computational Experiments for the MM-DRFLP-S Instances

Instance Category	$ \Omega $	$ \mathfrak{R} $	NO-SCUT	WITH-SCUTs		
			T-EF	#LCuts	T-EFC	ImprG%
$\alpha_1 = 1000$ $\alpha_2 = 4000$	100	5	TL	5000	180	98.1
	100	10	TL	5000	235	97.9
	100	25	TL	5000	474	98.1
	100	50	TL	5000	904	97.9
$\alpha_1 = 1000$ $\alpha_2 = 16000$	100	5	TL	5000	777	90.1
	100	10	TL	5000	744	90.1
	100	25	TL	5000	959	89.9
	100	50	TL	5000	1666	89.9
$\alpha_1 = 1000$ $\alpha_2 = 4000$ $\alpha_3 = 10000$ $\alpha_4 = 16000$	100	5	TL	5000	1601	92.2
	100	10	TL	5000	1944	91.9
	100	25	TL	5000	1252	91.7
	100	50	TL	5000	3008	91.9

Computational results for TSS-CMIPs where $p = 1$ and E_{ω}^j are network flow matrices for all $j \in J$.

In Table 3.6, we observe that by adding scenario-based cuts a priori, the number of integer variables ($\#I\text{Var}$) is significantly reduced. Without our scenario-based cuts, CPLEX with its default settings took 800 seconds (on average) to solve the extensive formulation of the TSS-CMIP instances where $p = 1$ and E_{ω}^j , $j \in J$, are network flow matrices. However, by adding our cuts, CPLEX took 143 seconds (on average) to solve the extensive formulation of these instances, and reduced the time by up to 25 times and 4.6 times (on average). Our scenario-based cuts closed the integrality gap by almost 100%. It is worth noting that even though we disabled presolve when using Benders decomposition routine, for instance category SCMIP.5.10.5, T-BDC is on average 79.83% of T-EF.

Table 3.6: Results of Computational Experiments for TSS-CMIPs with $p = 1$ and E_{ω}^j for all $j \in J$ are network flow matrices

Instance Category	$ \Omega $	NO-SCUT			WITH-SCUTS				
		#IVar	#LCon	T-EF	#IVar	#PCuts	T-EFC	T-BDC	ImprG%
SCMIP.25.50.5	500	315025	387510	27.15	25	62500	6.78	48.49	99.64
SCMIP.25.50.5	1000	630025	775010	77.93	25	125000	15.75	107.17	99.87
SCMIP.25.50.5	2000	1260025	1550010	176.92	25	250000	32.50	307.69	99.99
SCMIP.25.50.5	5000	3150025	3875010	791.69	25	625000	88.98	1039	100
SCMIP.50.100.5	500	637550	772525	62.01	50	125000	23.20	349.77	99.36
SCMIP.50.100.5	1000	1275050	1545025	134.25	50	250000	48.10	1839	99.37
SCMIP.50.100.5	2000	2550050	3090025	391.09	50	500000	103.11	2726	99.76
SCMIP.50.100.5	5000	6375050	7725025	1855.79	50	1250000	317.54	TL	99.98
SCMIP.100.150.5	500	927600	1127575	101.45	100	175000	54.58	270.60	100
SCMIP.100.150.5	1000	1855100	2255075	213.53	100	350000	118.31	830.07	100
SCMIP.100.150.5	2000	3710100	4510075	632.55	100	700000	262.46	TL	100
SCMIP.100.150.5	5000	9275100	11275075	3169.87	100	1750000	988.21	TL	100
SCMIP.5.10.5	500	60005	68502	9.29	5	7500	0.89	3.12	100
SCMIP.5.10.5	2000	240005	274002	26.43	5	30000	3.93	18.08	100
SCMIP.5.10.5	10000	1200005	1370002	314.34	5	150000	36.74	180.51	100
SCMIP.5.10.5	50000	6000005	6850002	4829.52	5	750000	186.16	2355.55	100

Results for TSS-CMIPs and TSDR-CMIPs with $p = 2$ and $E_{\omega}^j = \mathbf{I}$.

For TSS-CMIP and TSDR-CMIPs with $p = 2$, adding our scenario-based cuts in the extensive formulation and relaxing integrality restrictions on second stage integer variables provide an approximation of the problem. Let the approximation ratio be defined by $R\% = 100 \times V_{approx}/V_{mip}$ where V_{approx} is the optimal objective value obtained from the experiment WITH-SCUTS (after adding scenario-based cuts in the extensive formulation and relaxing the integrality constraints on the second stage variables). We observe that the approximation ratio of all instances, with known V_{mip} , in Table 3.7 is greater than 99.99%, thereby demonstrating the strength of our scenario-based cuts. In other words, these cuts provide near-optimal solution for TSS-CMIPs with $p = 2$ and $E_{\omega}^j = \mathbf{I}$.

Now by comparing T-EF and T-EFC in Table 3.7, we observe that adding our

Table 3.7: Results of Computational Experiments for TSS-CMIPs with $p = 2$ and $E_{\omega}^j = \mathbf{I}$

Problem Set	Instance Category	$ \Omega $	NO-SCUT			WITH-SCUTS			
			#IVar	#LCon	T-EF	#IVar	#PCuts	T-EFC	ImprG%
I	SCMIP.5.125.1	50	12505	14001	32.14	5	6250	5.43	35.42
	SCMIP.5.125.1	100	25005	28001	282.90	5	40501	91.52	15.90
	SCMIP.10.500.1	50	50010	53001	TL	10	25000	148.22	-
	SCMIP.10.500.1	100	100010	106001	TL	10	50000	601.91	-
	SCMIP.10.500.1	500	500010	530001	TL	10	250000	TL	-
	SCMIP.15.625.1	5	6265	7051	27.41	15	3375	1.40	3.39
	SCMIP.15.625.1	10	12505	14101	56.19	15	6750	2.41	14.61
	SCMIP.15.625.1	15	18765	21151	115.88	15	10125	5.77	13.50
	SCMIP.15.625.1	50	62515	70501	TL	15	33750	550.10	-
	SCMIP.20.800.1	20	32020	33201	TL	20	16000	500.88	-
	SCMIP.20.800.1	50	80020	83001	TL	20	40000	4532.02	-
	SCMIP.240.120.1	20	5040	4905	9.29	240	2400	1.00	4.65
	SCMIP.240.120.1	50	12240	12255	51.94	240	6000	2.61	6.58
	II	SCMIP.5.10.1	50	1005	1255	4.26	5	500	0.67
SCMIP.5.10.1		100	2005	2505	6.30	5	1000	1.26	27.68
SCMIP.5.10.1		200	4005	5005	11.14	5	2000	2.07	27.69
SCMIP.5.10.1		500	10005	12505	29.29	5	5000	4.81	43.49
SCMIP.5.10.1		1000	20005	25005	67.35	5	10000	9.88	52.47
SCMIP.5.10.1		5000	100005	125005	284.43	5	50000	82.74	72.91
SCMIP.5.10.1		10000	200005	250005	TL	5	100000	218.72	-
SCMIP.10.10.1		50	1010	2005	0.46	10	500	0.69	0.35
SCMIP.10.10.1		100	2010	4005	0.79	10	1000	1.61	0.75
SCMIP.10.10.1		200	4010	8005	2.75	10	2000	2.31	2.2
SCMIP.10.10.1		500	10010	20005	4.34	10	5000	5.38	2.10
SCMIP.10.10.1		1000	20010	40005	13.07	10	10000	14.62	10.57
SCMIP.10.10.1		5000	100010	200005	502.44	10	50000	91.8	13.11
SCMIP.10.10.1		10000	200010	400005	1490.35	10	100000	288.16	27.55

scenario-based linear cuts (a priori) significantly reduces the time taken to solve the reformulated extensive formulation of the TSS-CMIP instances, using CPLEX with its default settings. More specifically, after adding our scenario-based cuts, CPLEX solved 132 out of 135 randomly generated instances within the time limit, except three instances of SCMIP.10.50.1 with 500 scenarios. Whereas, without our cuts, CPLEX could not solve 35 out of 135 TSS-CMIP instances within 3 hours time limit (32 instances) and allocated memory (3 instances), and took 148 seconds (on average) to solve the remaining 100 instances in comparison to 32 seconds (on average) after adding our cuts. Additionally, WITH-SCUTS took

22 minutes (on average) for 32 out of 35 (unsolvable) instances. Overall, for instances in Table 3.7, our scenario-based cuts closed the integrality gap by 19.1% (on average) for instances solved to optimality using NO-SCUT, and reduced the time taken to solve the TSS-CMIP instances by 5 times (on average).

In particular, for problem set I, WITH-SCUTS were performed at least 2 times and up to 19 times faster than NO-SCUT. Whereas for problem set II, WITH-SCUTS is 5 times (on average) and up to 39 times faster than NO-SCUT. It is interesting to observe that while by adding our scenario-based cuts, there is a trade-off between the decrease in the number of integer variables and increase in the number of constraints. For instances such as SCMIP 10.10.1 where $|\Omega| \in \{50, 100, 500, 1000\}$, WITH-SCUTS took marginally longer time than NO-SCUT. However, for instances with larger number of scenarios, WITH-SCUTS are notably faster than NO-SCUT.

In Table 3.8, we present results for distributionally robust versions of TSS-CMIPs instances with $p = 2$ and $E_{\omega}^j = \mathbf{I}$. Specifically, we consider three instance categories from Table 3.7 that were solved in a reasonable time by CPLEX even without adding scenario-based cuts and for $|\mathfrak{P}| = 1$. We generated three TSDR-CMIP instances for each category, i.e., SCMIP.15.625.1, SCMIP.240.120.3, and SCMIP.10.10.1, with fixed number of scenarios $|\Omega|$ and distributions in the ambiguity set $|\mathfrak{P}|$. We observe that CPLEX could not solve the reformulated extensive formulation of 4 out of 9 instances within a time limit of 3 hours. However, after adding the scenario-based linear cuts (a priori), CPLEX solved these instances within 286 seconds (on average). For the remaining instances, by comparing T-EF and T-EFC in Table 3.8, we again observe that adding the scenario-based linear cuts reduces the time taken to solve the instances by 446 times (on average).

Table 3.8: Results of Computational Experiments for TSDR-CMIPs with $p = 2$ and $E_{\omega}^j = \mathbf{I}$

Instance Category	Instance #	(Ω , \mathfrak{P})	NO-SCUT		WITH-SCUTS			
			#IVar	T-EF	#IVar	#PCuts	T-EFC	ImprG%
SCMIP.15.625.1	1	(3, 5)	3765	2562.99	15	2025	11.71	0.37
	2		3765	72.72	15	2025	3.97	0
	3		3765	80.52	15	2025	3.98	2.08
SCMIP.240.120.3	1	(20, 10)	5040	TL	240	2400	491.2	13.57
	2		5040	TL	240	2400	85.6	18.66
	3		5040	TL	240	2400	565.9	8.3
SCMIP.10.10.1	1	(100, 15)	2010	TL	10	1000	2.26	0.89
	2		2010	37.77	10	1000	2.68	0.71
	3		2010	8380.76	10	1000	2.61	1.14

Computational results for TSS-CMIPs with $p = 2$ where E_{ω}^j for $j \in J$ are network flow matrix.

The problem instances considered in Table 3.9 are much harder than problem instances considered in Table 3.7, primarily because of multiple conic constraints (3.20) corresponding to each scenario (as $|J| = 3$) and multiple integer variables in each constraint (3.19). Nonetheless, we again observe that the approximation ratio $R\%$ for all problem instances, with known V_{mip} , in Table 3.9 is greater than 99.99%. It is evident from column T-EF in Table 3.9 which shows that CPLEX 12.70 with its default settings could not solve reformulated extensive formulation of 50 out of 75 TSS-CMIP instances (without our scenario-based cuts) within a time limit of 3 hours and the allocated 24 GB RAM. In contrast, after adding our scenario-based cuts, we solved all 75 instances in 449.64 seconds (on average). For instances solved to optimality using NO-SCUT, our cuts closed the integrality gap by 47.29% (on average) and reduced the time taken to solve the TSS-CMIP instances by 10.32 times (on average). It is worth to note that even though ImprG% is small for some instances (i.e., SCMIP.15.625.3, SCMIP.240.120.3, and SCMIP.25.100.3 for

$|\Omega| \in \{50, 200\}$), CPLEX with its default settings (without scenario-based cuts) took longer time, at least 2.4 times and up to 18 times, to solve these instances, in comparison to solving them using CPLEX with our scenario-based cuts.

Table 3.9: Computational Results for TSS-CMIPs where $p = 2$ and E_{ω}^j for $j \in J$ are network flow matrices

Problem Set	Instance Category	$ \Omega $	NO-SCUT			WITH-SCUTS			
			#IVar	#LCon	T-EF	#IVar	#PCuts	T-EFC	ImprG%
I	SCMIP.5.125.3	50	37505	69001	TL	5	15000	22.9	-
	SCMIP.5.125.3	100	75005	138001	TL	5	30000	73.5	-
	SCMIP.10.500.3	50	150010	243001	TL	10	45000	330.1	-
	SCMIP.10.500.3	100	300010	486001	TL	10	90000	1742.5	-
	SCMIP.15.625.3	5	18765	31051	1069.5	15	6000	56.1	0.1
	SCMIP.15.625.3	10	37515	62101	TL	15	12000	162.7	-
	SCMIP.15.625.3	15	56265	93151	TL	15	18000	265.5	-
	SCMIP.240.120.3	20	14640	26505	TL	240	6000	46.3	-
	SCMIP.240.120.3	50	36240	66255	TL	240	15000	386.2	-
	II	SCMIP.10.25.3	50	7510	11005	10	10	1500	1.82
SCMIP.10.25.3		100	15010	22005	20.9	10	3000	4.44	63.9
SCMIP.10.25.3		200	30010	44005	40.9	10	6000	10.33	97.3
SCMIP.10.50.3		50	15010	23505	TL	10	3750	6.4	-
SCMIP.10.50.3		100	30010	47005	OM	10	7500	14.3	-
SCMIP.10.50.3		200	60010	94005	TL	10	15000	54.4	-
SCMIP.10.75.3		50	22510	34005	OM	10	5250	19.6	-
SCMIP.10.75.3		100	45010	68005	OM	10	10500	41.2	-
SCMIP.10.75.3		200	90010	136005	TL	10	21000	120.5	-
SCMIP.25.50.3		50	15025	23510	OM	25	3750	5.9	-
SCMIP.25.50.3		100	30025	47010	OM	25	7500	15.2	-
SCMIP.25.50.3		200	60025	94010	OM	25	15000	54.8	-
SCMIP.25.50.3		500	150025	235010	OM	25	37500	568.9	-
SCMIP.25.100.3		50	30025	55010	165.4	25	12000	49.1	3.7
SCMIP.25.100.3	200	120025	220010	OM	25	48000	2428.1	-	
SCMIP.25.100.3	500	300025	550010	OM	25	120000	4256.6	-	

3.8 Conclusion

We presented conditions under which the addition of scenario-based nonlinear cuts in the extensive formulation of TSS-CMIPs is sufficient to relax the integrality restrictions on the second stage integer variables without impacting the integrality

of the optimal solution of the TSS-CMIP. We introduce structured TSS-CMIPs and cuts for them which satisfy these conditions, thereby providing partial convex hull for them. We introduced TSS-CMIPs and TSDR-CMIPs with structured p -order CMIPs in the second stage, derived scenario-based conic MIR cuts for them, and proved that these cuts provide conic/linear programming equivalent or approximation for the second stage CMIPs with $p = 1$ or $p \geq 2$, respectively. We also introduced a multi-module capacitated stochastic facility location problem with subcontracting (MM-SFLP-S) and demonstrate the applicability of the foregoing results for solving this problem. We also computationally evaluated the effectiveness of the scenario-based cuts by considering instances of MM-SFLP-S, its distributionally robust variant, and structured TSS-CMIPs with polyhedral CMIPs and second-order CMIPs in the second stage, i.e. $p = 1$ and $p = 2$, respectively. Our computational results showed that adding scenario-based cuts to the extensive formulation significantly reduces the time taken to solve extensive formulation of TSS-CMIPs and TSDR-CMIPs compared to solving the same problem instances without these cuts, using CPLEX 12.70 with its default settings. Furthermore, we derived (partial) convex hull for new deterministic multi-constraint polyhedral conic mixed integer sets with multiple integer variables.

Chapter 4

Risk-Neutral and Risk-Averse

Transmission Switching for Load

Shed Recovery

4.1 Introduction

In order to handle the uncertainty in generation and demand encountered during the recovery process as discussed in Section 1.4, we present two stochastic transmission switching models to deal with these uncertain parameters, and one of them incorporates conditional value-at-risk to measure the risk level of unrecovered load shed.

Various scientific works have demonstrated that transmission line switching (TS) could engender numerous benefits as a corrective action including relieving line overloads [61, 101], mitigating voltage violations [11, 127, 134], mitigating flow violations [9], and recovering load shed (LS) following an emergency [45, 51]. It is also recognized as a promising mechanism for improving system reliability when facing critical contingencies [69]. In [76], the authors presented an application to transmission expansion planning, where TS was shown to improve the system

from both security and economic aspects. Schumacher et al. [131] solved a robust transmission expansion planning problem with demand uncertainty, where they allowed TS as a corrective action to relieve the impact of the uncertainty and line failure. Recently, Li and Hedman [90, 91] considered TS as a corrective action and utilized it in the energy management system to enhance flexibility in practice. Readers can refer to [69] for a thorough introduction of the standardized TS methodology, otherwise known as topology control. It is important to add that, before its standardization through mathematical models, TS had been performed by operators based on historical experience recorded in operations manuals (e.g., [122]). Nowadays, topology control is implemented in practice but only on a limited basis, partly on account of the continuing need for adequate decision-making tools to support it.

In last decade, researchers have been focusing on developing mathematical optimization models to determine the best TS actions to execute under various situations. O'Neill et al. [116] introduced a deterministic model that systematically applies TS into the transmission network and studied the economic benefits of optimal TS actions under appropriate market rules. On the other hand, Hedman et al. [70] not only considered the economic benefits of TS, but also its ability to maintain reliability and stability. The authors proposed a mixed integer program for N-1 DC optimal dispatch with TS, and showed that TS can reduce generation costs while ensuring N-1 reliability. Note that both O'Neill et al. [116] and Hedman et al. [70] embedded TS decisions as binary variables within the well-known DC optimal power flow problem (DCOPF) linear programming formulation [54] to minimize generation costs. Recently, Escobedo et al. [51] explored the concept of

load shed recovery (LSR) and proposed a static transmission switching model for the DC optimal load shedding recovery (DCOLSR) problem with deterministic demand. Their computational results showed that by reconfiguring the topology of the transmission network via TS, the resulting load shed from line and/or generator contingencies could be reduced significantly. In studies related to load shedding without TS [72, 73], the authors presented a multi-objective expansion planning model which minimizes the operational and investment cost, as well as a risk index (referred to as Expected Energy Not Served) by integrating wind farms into distribution networks. In their model, they proposed virtual power generation to handle load shedding at certain load centers.

In the majority of the aforementioned papers, it was assumed that all generators are conventional, and demand is a fixed known quantity. Nowadays, renewable energy generators are playing an important role in energy markets. These generators heavily depend on intermittent resources such as wind and solar, and thus their operation comes with high uncertainty. Moreover, out of various factors of uncertainties in power systems (see [139]), electric power demand is among the most important and difficult to forecast, especially during emergency conditions. These uncertainties result in uncertainty in the requirements of the system, which could impact the validity of decisions obtained from deterministic models in practice. Therefore, to make TS and LSR decision-making tools more effective in practice, it is important to address uncertainty from renewable generation and demand in today's power system problems.

Different methods, i.e., robust optimization and probabilistic approaches, have been applied in various situations to handle uncertainties in power systems. De-

hghanian and Kezunovic [44] studied the optimal transmission switching problem with uncertain load and renewable generation. They incorporated the two-point estimation method with deterministic DCOPF to handle uncertainties and approximate the probability distribution function of generation costs. Zhang and Li [150] studied both DCOPF and ACOPF with load uncertainty and utilized chance-constrained programming to handle uncertainty, which sought a balance between reliability and total cost efficiency of the power system. Summers et al. [140] formulated a stochastic DCOPF problem which minimizes the expected short-term operating cost. Rabiee et al. [124] proposed a stochastic model to minimize energy procurement costs in the DCOPF. They considered uncertainties in load, wind power generation, and energy price. They compared results of different models (e.g., two stage stochastic programming and stochastic programming with variance index and with conditional value-at-risk (CVaR)) and concluded that the risk-averse solution is more conservative, which leads to higher procurement costs. Phan and Ghosh [121] proposed a two-stage stochastic programming model to handle the generation uncertainty in ACOPF. Their model considered the power extracted from all conventional generators as the first stage, and the re-dispatch of generators following the realization of uncertainties as the second stage. López et al. [95] considered a stochastic generation and transmission expansion problem under risk to minimize the total cost. More specifically, they consider uncertainties in the demand, the equivalent availability of generating plants and transmission capacity factor of the transmission lines. They also used a mean-variance to measure the risk. Doostizadeh et al. [48] considered a chance-constrained DCOPF with joint uncertainties in load and wind. Mühlfordt et al. [110] proposed a solution approach for a generalized chance-constrained DCOPF defined using con-

tinuous random variables. For a comprehensive survey of the chance-constrained applications in power system, readers can refer to [56].

Handling demand uncertainty by minimizing the expected level of unmet demand over a set of representative probabilistic scenarios uniformly may not be acceptable to decision makers. That is, even if the expected level of unmet demand over the full set of scenarios is low, such a *risk-neutral* treatment does not eliminate the possibility that the prescribed solution could result in a high amount of unmet demand for a small number of these scenarios. Preventing the occurrence of such outcomes during severe emergencies is of vital importance. In other words, decision makers may be more *risk-averse*, in the sense that they need tools to avoid the worst scenarios, i.e., when realized demand deviates from the expected demand, potentially leading to an outcome with large unmet demand. Different from aforementioned work which concentrate primarily on economic objectives for normal operation conditions, this research considers an *emergency-related* objective to maximize the amount of load shed that can be recovered following contingency-triggered imbalances between supply and demand while incorporating uncertainty in the generation and demand profile. It is important to remark that minimizing total generation cost during severe disaster events could result in huge unmet demand. The unmet demand may cause the interruption in services of public facilities such as rescue stations, police stations, and hospitals, which will lead to more financial losses in the long run. Hence, minimizing unmet demand during emergencies is critical [50]. It is also important to point out that the focus of this research is different from research on black-start schemes, whose goal is to recover the power in the system without external energy sources. Our goal is to suggest

decisions that may help prevent or mitigate the effects of a blackout. The proposed method could support self-healing by recovering more shedded load during an emergency, as well as serve as an offline contingency analysis tool for aiding decision makers or TSOs to balance maximal gains and risk during the recovery process. A prospective application could be used to identify crucial elements in the system and corresponding corrective actions for maintaining effective and up-to-date operator manuals.

This research builds on the previous work of Escobedo et. at. [51] by proposing stochastic load shed recovery models (S-LSR) to handle the uncertainty of generation and demand, and incorporate CVaR for measuring the risk level of unrecovered load. No work in the existing literature has considered the uncertain generation and demand and the risk of unrecovered LS in DCOLSR. In deterministic models, data parameters are assumed to be fixed and known, whereas in reality, the parameters are mostly uncertain. Therefore, S-LSR seeks a solution which is feasible for different realizations of the parameter values, while optimizing the expected LSR over the sample space (the set of all possible values of the parameters) of the random variables associated with uncertain generation and demand. A decision maker utilizing the expectation of LSR is referred to as risk-neutral. In contrast, when facing serious disasters, it is reasonable to make more conservative decisions to avoid extreme scenarios of unmet demand. In this research, we also utilize CVaR measure within S-LSR so that a decision maker can avoid the scenarios with large unrecovered LS in the worst-case quantile.

The main contributions of this research are as follows:

- (i) We introduce two stochastic models to handle generation and demand uncer-

tainties. Our models not only minimize load shedding, but also incorporate the risk preference of decision makers using CVaR.

- (ii) We demonstrate the importance of our models, which consider uncertainties in DCOLSR, by comparing their optimal values to those of the deterministic model [51]. The computational results confirm that our stochastic models support the self-healing capabilities of a smart grid by recovering more load shed and can provide a more reliable topology.
- (iii) We perform analyses that support the usage of the proposed methodology as an offline contingency tool. For instance, the models can be configured to suggest a sequence of individual switching operations.

The rest of this chapter is organized as follows: In Section 4.2, we provide two models for S-LSR. In Section 4.3, we introduce the criterion to evaluate the proposed models and a deterministic mean-value model. We also present an example of a 6-bus system [76] to illustrate the significance of the stochastic models. In Section 4.4, we illustrate the computational setup and in Section 4.5, we provide computational results for IEEE 118-bus test case, IEEE 14-bus test case, and the 6-bus system [76]. We compare the impact of different contingencies, number of scenarios, risk coefficient, and analyze the decision making process. In Section 4.6, we conclude the work and discuss potential future research directions.

4.2 Stochastic Optimal Load Shed Recovery

In this section, we present stochastic optimization models to maximize LSR or equivalently minimize LS, using TS actions; these models are extensions of the deterministic DCOLSR model of Escobedo et al. [51]. In [51], it is assumed that all generators are conventional (i.e., nonrenewable) and the demand at each bus after an emergency situation is fixed to its normal state value. However, the use of renewable generation, whose generation depends on intermittent natural sources, is well established in the modern power grid. Moreover, during emergency conditions, demand is especially hard to forecast. Ignoring the uncertainty in load may lead to overloading or under-loading of lines [137]. In order to handle the uncertainty in renewable generation and demand, we propose two-stage stochastic programming models where uncertainty is defined using a random variable with known probability distribution. The first one is referred to as the risk-neutral model (denoted by RN-LSR), where the risk preference of the decision makers is not considered, while the second model specifies their risk preferences by incorporating CVaR for a more conservative decision (denoted by CVaR-LSR). For more details about general risk-neutral and risk-averse stochastic models, readers can refer to [27].

4.2.1 Risk-Neutral Stochastic DC Optimal Load Shed Recovery With Transmission Switching

Figure 4.1 demonstrates the decision making process of RN-LSR.

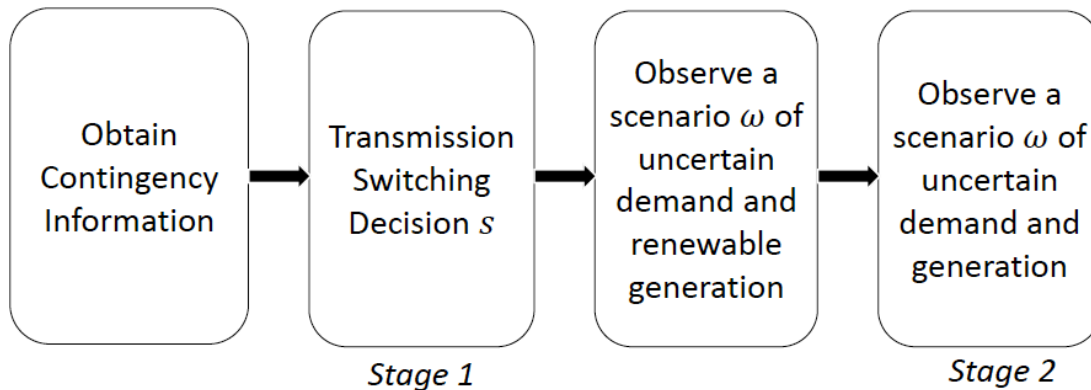


Figure 4.1: Decision making process for stochastic LSR.

Given a contingency, we make first-stage transmission-line switching decisions, called *here-and-now decisions*, without precise knowledge of the renewable generator outputs and demand at each bus after the occurrence of a contingency. Thereafter, when the renewable generation and demand are revealed in the future, we make operational decisions, referred to as *second-stage decisions*, which include adjusting bus phase-angles, conventional generator dispatch levels, and deciding power flow through each transmission line and unmet demand at each bus, with the goal to maximize LSR.

In other words, we seek a solution (i.e., corrective actions) that maximizes the expected value of the objective function (i.e., LSR) for the known probability distribution followed by the uncertain renewable generation and demand. Formally, given a set of generators G , a set of transmission lines K , a set of buses \mathcal{N} , a set of renewable generators ($\mathcal{G} \subseteq G$), and sets of out-of-service generators and out-of-service lines due to a contingency ($\dot{G} \subseteq G$ and $\dot{K} \subseteq K$, respectively), RN-LSR is

formulated as follows:

$$\max \left\{ \mathbb{E}_\xi[f(s, \omega)] : \sum_{k \in K} s_k \leq r, s \in \{0, 1\}^{|K|} \right\}, \quad (4.1)$$

where binary variable s_k , $k \in K$, denotes the switching action for line k made before the realization of uncertainty in renewable generation and demand, defined by random vector ξ with sample space Ω , are realized, and data parameter r denotes the switching limit, i.e., the maximum number of transmission line switches allowed. Problem (4.1) is referred to as the first-stage problem and we denote the set of first-stage feasible solutions, i.e., TS actions, by S . The objective is to maximize LSR associated with a given contingency (\dot{G}, \dot{K}) and therefore, we set $\mathbb{E}_\xi[f(s, \omega)] = LS_{\dot{G} \cup \dot{K}} - \mathbb{E}_\xi[Q(s, \omega)]$ where $LS_{\dot{G} \cup \dot{K}}$ (a constant for a given contingency) captures the total LS due to the contingency from the forecast demand without any corrective (TS or re-dispatching) operations, and $\mathbb{E}_\xi[Q(s, \omega)]$ provides the expected unmet demand for a given topology configuration (controlled by TS decisions s_k , $k \in K$). The latter is computed by solving the following linear programs, also referred to as the second-stage problems, for $(s, \omega) \in (S, \Omega)$:

$$Q(s, \omega) = \min \sum_{n \in N} u_n^\omega \quad (4.2)$$

Subject to:

$$\theta^{min} \leq \theta_n^\omega - \theta_m^\omega \leq \theta^{max}, \quad (m, n) \in K \quad (4.3a)$$

$$\sum_{\forall k(n, \dots)} P_k^\omega - \sum_{\forall k(\dots, n)} P_k^\omega + \sum_{\forall g(n) \in G} P_g^\omega = d_n^\omega - u_n^\omega, n \in N \quad (4.3b)$$

$$P_k^{min}(1 - s_k) \leq P_k^\omega \leq P_k^{max}(1 - s_k), \quad k \in \hat{K} \quad (4.3c)$$

$$B_k(\theta_n^\omega - \theta_m^\omega) - P_k^\omega + s_k M_k \geq 0, \quad k \in \widehat{K} \quad (4.3d)$$

$$B_k(\theta_n^\omega - \theta_m^\omega) - P_k^\omega - s_k M_k \leq 0, \quad k \in \widehat{K} \quad (4.3e)$$

$$P_k^{min} s_k \leq P_k^\omega \leq P_k^{max} s_k, \quad k \in \bar{K} \quad (4.3f)$$

$$B_k(\theta_n^\omega - \theta_m^\omega) - P_k^\omega + (1 - s_k) M_k \geq 0, \quad k \in \bar{K} \quad (4.3g)$$

$$B_k(\theta_n^\omega - \theta_m^\omega) - P_k^\omega - (1 - s_k) M_k \leq 0, \quad k \in \bar{K} \quad (4.3h)$$

$$P_g^{min} \leq P_g^\omega \leq P_g^{max}, \quad g \in G \setminus \{\dot{G} \cup \mathcal{G}\} \quad (4.3i)$$

$$P_g^\omega = \bar{P}_g^\omega, \quad g \in \mathcal{G} \quad (4.3j)$$

$$0 \leq u_n^\omega \leq d_n^\omega, \quad n \in \mathcal{N} \quad (4.3k)$$

$$P_k^\omega = 0, P_g^\omega = 0, \quad k \in \dot{K}, g \in \dot{G} \quad (4.3l)$$

where variable u_n^ω denotes the unmet demand at bus n for $n \in \mathcal{N}$. In Problem (4.2)-(4.3), the objective is to minimize the total unmet demand at all buses, u_n^ω for $n \in \mathcal{N}$, for a known realization of the stochastic (or uncertain) renewable generation and demand parameters at each bus, $\{\bar{P}_g^\omega\}_{g \in \mathcal{G}}$ and $\{d_n^\omega\}_{n \in \mathcal{N}}$ for $\omega \in \Omega$, and TS actions $s \in S$, while ensuring that the following constraints hold. Constraints (4.3a) set lower and upper limits on the difference between bus angles of adjacent buses for all lines $k \in K$ with incident nodes n and m . Constraints (4.3b) are node balance constraints, which ensure that the total power flow into a node/bus, $n \in \mathcal{N}$, including the power generation equals the total power flow out of the node, including the demand satisfied at that node. Notice that the first term $\sum_{\forall k(n, \dots)} P_k^\omega$ denotes total power flow into node n , the second term $\sum_{\forall k(\dots, n)} P_k^\omega$ denotes the total power flow out of node n , and the partial unfulfillment of demand d_n^ω at each bus, is allowed by introducing a non-negative continuous variable u_n^ω .

Constraints (4.3c) and (4.3f) set lower and upper limits on power flow through each transmission line $k \in K$. These constraints ensure that if a line k is in service before performing the TS operation, that is $k \in \widehat{K}$, and is set to be switched by the first-stage TS solution, i.e., $s_k = 1$ (or if a line k is out of service before performing the TS operations, that is $k \in \bar{K}$, and is not switched during TS actions, i.e., $s_k = 0$), then this line is open and thus does not allow any power flow. Otherwise, power flow is allowed through this line. Constraints (4.3d)-(4.3e) and (4.3g)-(4.3h) incorporate Kirchhoff's laws, where B_k is the susceptance of line $k \in K$ and M_k is large enough to ensure that the above constraints are satisfied regardless of the corresponding bus angles when a transmission line is switched to close and open state, respectively. Constraints (4.3i) set the lower and upper limits on power generated by conventional generators not impacted by the contingency $g \in G \setminus \{\dot{G} \cup \mathcal{G}\}$. Constraints (4.3j) set the output from renewable generators equal to the uncertain renewable generation parameter corresponding to scenario ω . Constraints (4.3k) make sure that the unmet demand at each bus $n \in \mathcal{N}$ does not exceed the demand at the bus. Constraints (4.3l) set power flow for lines and output for generators, respectively, impacted by the contingency to be 0. If a line is in contingency, we assume that there is no power flow through this line. Similarly, if a generator is in contingency, we assume that there is no output from that generator. Such a treatment is in line with other works in the literature (e.g., [10, 37, 70]).

4.2.2 Risk-Averse Stochastic DC Optimal Load Shed Recovery with Transmission Switching

In RN-LSR, the objective is to provide a topology configuration for a given contingency that maximizes the total expected LSR over the set of all possible realizations/scenarios of uncertain demand and generation. However, for a given contingency, it is possible that for some of the randomized scenarios, the unmet demand is extremely large while for the others it is extremely small, even though the total expected LSR is large, i.e., the unmet demand corresponding to each scenario is distributed with large variance. For such contingencies, power system operators (or decision makers) would likely opt for TS actions that avoid the risk of occurrence of outcomes with large unmet demand in certain scenarios, even if such TS actions may result in a slightly lower expected LSR. In this research, we also incorporate a risk measure, CVaR, into RN-LSR to specify the risk preference of the decision makers and avoid the risk of outcomes within the worst-case quantile.

Conditional Value-at-Risk

CVaR, also known as the mean excess loss or tail Value-at-Risk (VaR), is a popular function of risk measurement, which was first introduced by [126]. It has been widely applied in the finance industry [126] but used rather infrequently in the energy sector. Statistically, it represents the weighted average (i.e., expected value) of the losses for a given confidence interval of the distribution of total gain. Put otherwise, by optimizing CVaR, we minimize the risk of incurring huge losses.

Formally, CVaR is defined as follows [126],

$$\text{CVaR}_\alpha(X) = \mathbb{E}(X|X \geq \text{VaR}_\alpha(X))$$

where $\text{VaR}_\alpha(X)$ represents the expected worst loss of random variable X within a given confidence interval α . In this paper, since demand is assumed to have a known distribution, the corresponding outcome, i.e., unrecovered LS or unmet demand, also follows a certain distribution. We apply CVaR to measure the risk of outcomes in α -quantile by minimizing the expectation of unrecovered LS over this quantile.

Risk-averse Stochastic Formulation

We present a risk-averse two-stage stochastic programming model with CVaR which is defined as follows:

$$\min_{s \in \mathcal{S}} \left\{ \mathbb{E}_\xi[f(s, \omega)] + \lambda \times \text{CVaR}_\alpha(f(s, \omega)) \right\} \quad (4.4)$$

where $\text{CVaR}_\alpha(f(x, \omega))$ is the cost of risk, i.e., the expectation over the α -quantile of the distribution of outcomes $f(s, \omega)$ and λ denotes the exchange rate of the cost for risk. Here, $f(s, \omega)$ is defined the same as in RN-LSR for $s \in \mathcal{S}$ and $\omega \in \Omega$. For a finite sample space, i.e., $|\Omega| < \infty$, Noyan [114] presented a reformulation for general risk-averse two-stage stochastic linear programs where both stages have only continuous variables. We utilize this result to reformulate (4.4) and derive its

equivalent formulation as follows:

$$\begin{aligned} \max \quad & (1 + \lambda)LS_{\dot{G}\dot{U}\dot{K}} - \sum_{\omega \in \Omega} p_{\omega} \sum_{n \in N} u_n^{\omega} - \lambda\eta + \frac{\lambda}{1 - \alpha} \sum_{\omega \in \Omega} p_{\omega} z_{\omega} \\ \text{s.t.} \quad & z_{\omega} \geq \sum_{n \in N} u_n^{\omega} - \eta, \quad \omega \in \Omega \\ & (4.3a) - (4.3l) \text{ hold}, s \in \mathcal{S}, \eta \in \mathbb{R}, z_{\omega} \in \mathbb{R}, \omega \in \Omega. \end{aligned}$$

4.3 Evaluation of Stochastic Models for LSR

In this section, we present a criterion to evaluate RN-LSR and CVaR-LSR, in comparison to a deterministic mean-value (DMV) model for the S-LSR problem. The DMV model is a simple way to handle uncertainties in LSR problem. It corresponds to setting the deterministic DCOLSR model of Escobedo et al. [51] with fixed renewable generation and fixed demand parameters set to the mean of uncertain renewable generation and the mean of the uncertain demands, respectively, over all $\omega \in \Omega$. It is defined as follows:

$$\min \{LS_{\dot{G}\dot{U}\dot{K}} - Q(s, \mathbb{E}_{\xi}(\omega)) : s \in \mathcal{S}\}. \quad (4.5)$$

where $Q(\cdot, \cdot)$ is defined by (4.2). Let the optimal switching solution of above mean-value problem be \hat{s} . Even though this decision does not consider random variations of demand and generation, in reality, the decision makers will have to make the second-stage decisions (after the realization of uncertainties) based on \hat{s}

by solving:

$$f(\hat{s}, \omega) = \min LS_{G \cup K} - Q(\hat{s}, \omega) \quad (4.6)$$

for realized scenario $\omega \in \Omega$. Since we do not know which scenario will be realized, we calculate the expectation over all scenarios of the optimal value of the second stage problem, i.e., $\mathbb{E}_\xi[f(\hat{s}, \omega)]$, to evaluate the performance of \hat{s} . In general, compared to calculating the foregoing expectation, solving RN-LSR and CVaR-LSR takes longer time. The ensuing results help determine the trade-offs between computational time and LS provided by the S-LSR models proposed in this paper in addition to the deterministic problem.

4.3.1 Evaluation of Risk-Neutral LSR Solution

The concept of value of stochastic solution (VSS) is used to quantify the quality of an optimal solution of RN-LSR [27]. It measures the benefits of solving RN-LSR in comparison to the DMV problem and is calculated as follows:

$$VSS = \mathbb{E}_\xi[f(s, \omega)] - \mathbb{E}_\xi[f(\hat{s}, \omega)].$$

Since the optimal solution \hat{s} of the DMV model is a feasible solution for RN-LSR, VSS is always non-negative. If $VSS > 0$, the optimal solution of RN-LSR is strictly better, since it provides larger expected LSR. Otherwise, the optimal solutions of RN-LSR and DMV are of the same quality. We provide an illustrative example in the following section to demonstrate how to use VSS to evaluate RN-LSR solution.

4.3.2 An Illustrative Example: A 6-bus System

We give a simple example of a 6-bus system [76] given in Figure 4.2 to illustrate how the stochastic model, RN-LSR, performs better than the deterministic model DMV. In this case, we have 6 buses and 7 transmission lines, which are all in service. The mean base load of the system is 209 MW, and is distributed at the rate of 40%, 30%, and 30% among buses 3, 4, and 5, respectively. Line 3, 4, and 5 are switchable among all 7 transmission lines. Detailed specifications of the generators and transmission lines are given in [76].

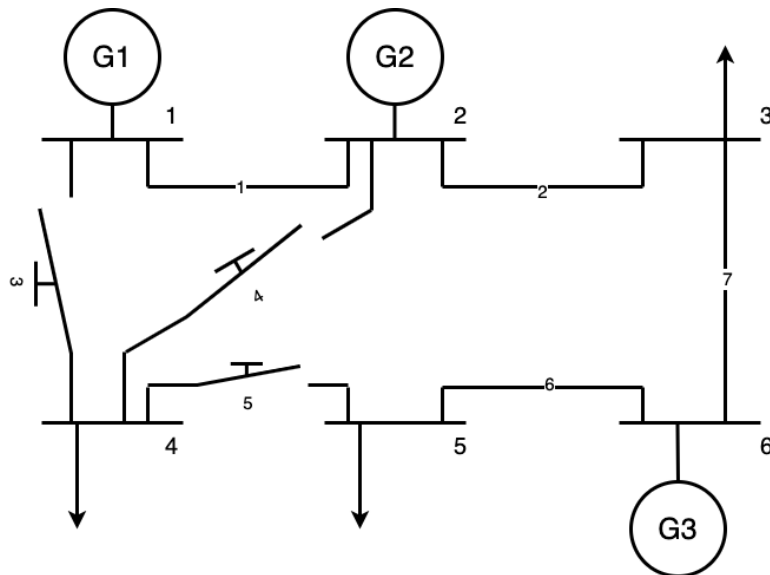


Figure 4.2: A 6-bus system.

We consider the case where line 5 is in contingency, and all generators are conventional. We assume that the demand at each bus follows a normal distribution with the mean given as above, i.e., 40% of 209 MW at bus 3, 30% of 209 MW at bus 4, and 30% of 209 MW at bus 5, and the standard deviation is 20% of each bus' average demand. Switching actions are made before the realization of the

demand at each bus. After the uncertainty is realized, other actions, i.e., adjusting phase-angles and conventional dispatch level, are performed to incorporate the impact of the switching actions. For this example, we assume that there are two possible demand scenarios, which are randomly drawn from the aforementioned normal distribution (see Table 4.1).

Table 4.1: Deterministic demand and two scenarios of stochastic demand for the 6-bus system (in MW)

scenario	bus 3	bus 4	bus 5
ω_1	89.11	66.45	65.98
ω_2	99.15	69.63	61.62
deterministic demand	83.6	62.7	62.7

We illustrate the first case where the ISO/TSO does not consider the uncertainty of demand. In this case, the ISO/TSO solves the DMV model, where the mean of the uncertain demand (or aforementioned deterministic demand as in [76]) is used as the fixed demand parameter in problem (??). This is equivalent to solving a one-scenario RN-LSR model with deterministic demand at each bus. The optimal switching action provided by the deterministic model is to switch off line 3. After obtaining the optimal switching actions, the TSO/ISO makes the other actions after the realization of the uncertain demand by solving (4.6). The expected load shedding of those two scenarios after performing the DMV optimal switching action, i.e., switch-off line 3, is 25.4 MW. Next, we consider the case where the TSO/ISO considers uncertainty in the model. Hence, a RN-LSR model with two scenarios is solved that gives the optimal switching action: switch-off line 4. The expected LS of those two scenarios after switching off line 4 is 21.3 MW. In summary, performing the optimal switching actions provided by the RN-LSR model recovers 4.1 MW more than the optimal switching actions provided by the

DMV model, i.e., $VSS = 4.1$ MW.

This small example demonstrates the importance of considering the uncertainty of demand in decision making. About 20% more LS is recovered by performing the optimal switching actions provided by RN-LSR model, in comparison to the DMV model.

4.3.3 Evaluation of Risk-Averse CVaR-LSR Solution

Although the expected LSR obtained by RN-LSR is theoretically superior to the total LSR obtained using CVaR-LSR, we cannot conclude that the solution of CVaR-LSR is “bad” compared to the solution of RN-LSR since the worst-case scenarios in α -quantile are avoided by solving CVaR-LSR (but this is not guaranteed with RN-LSR). Therefore, instead of comparing the optimal objective values, we compare the optimal solutions of these two stochastic models. If the optimal solutions of RN-LSR and CVaR-LSR coincide, then clearly the optimal solution of RN-LSR not only recovers the most LS, but also avoids the occurrence of outcomes with large unmet demand for certain scenarios. Otherwise, the solution of CVaR-LSR model is more conservative and it cannot recover as much LS as the solution of RN-LSR.

4.4 Computational Experiments

In this section, we discuss the scenario-generation process and the setup for our computational experiments, which were performed to evaluate the efficiency and

effectiveness of the proposed stochastic models, RN-LSR and CVaR-LSR.

4.4.1 Test Cases and Instance Generation

In this section, we discuss the scenario-generation process and the setup for our computational experiments, which were performed to evaluate the efficiency and effectiveness of the proposed stochastic models, RN-LSR and CVaR-LSR.

4.4.2 Test Cases and Instance Generation

The computational experiments consider three test cases:

IEEE 118-bus test case: We first consider a well known IEEE 118-bus test case that contains 19 generators and 186 transmission lines, to evaluate the impacts of stochastic demand during different outage events. For this test case, we assume all generators are conventional (i.e., nonrenewable). The total base load of IEEE 118-bus test case is 4519 MW.

IEEE 14-bus test case: Next, we consider the IEEE 14-bus test case, which contains 2 generators and 20 transmission lines with no transmission line power limit to test the effects of stochastic (renewable) generation and stochastic demand. We assume that there are two conventional generators and one renewable generator in the system. More specifically, at one node, we still have a conventional generator with capacity P_1 . At the other node, we have one conventional generator and one renewable generator. The capacity of this conventional generator is $0.5P_2$, where P_2 is the original gen-

eration capacity at that node. The renewable generation follows a uniform distribution defined over $[0, 0.5P_2]$. The total base load of IEEE 14-bus test case is 259 MW.

6-bus system: Finally, we consider the 6-bus system [76] discussed in Section 4.3.2. We consider two different types of generator set configurations: (a) 3 conventional generators; and (b) 3 conventional generators and an additional renewable generator at bus 1. Similar to the IEEE 14-bus test case, at bus 1, we assume that the capacity of the conventional generator is $0.5P_1$, where P_1 is the original generation capacity at bus 1, and the capacity of the renewable generator follows a uniform distribution defined over $[0, 0.5P_1]$. We follow the remaining settings as in [76].

For each generated instance for the IEEE 14-bus and 118-bus test cases, the demand $\{d_n^\omega\}_{n \in \mathcal{N}}$ is randomly drawn from a normal distribution with the original deterministic demand $\{d_n^0\}_{n \in \mathcal{N}}$ as the mean and 20% of the mean as the standard deviation. This is similar to the parameters chosen in [23], where the authors presented data of electric consumption during disasters for 41 countries. For each generated instance for 6-bus system, the demand is also drawn from a normal distribution, and we consider three instance categories with different standard deviation, i.e., 20%, 50% or 80% of the mean.

We follow the settings in [51], where the initial states of all non-faulty lines are closed and the emergency line and generator ratings are 125% of the normal ratings. Also, we apply the concept of the contingency list (CL) as in [51] to specify key contingencies considered in the test instances for our computational experiments. The CL is a collection of valid contingencies periodically examined by contingency

analysis programs which in practice contain all N-1 contingencies and a number of N-2 contingencies. The featured experiments consider a diverse selection of the latter type, specifically double generator failures, mixed generator and non-radial line failures, and double non-radial line failures, denoted by (G-2), (G-1+L-1), and (L-2), respectively. For experiments of IEEE 118-bus test case, we select fifteen contingencies in total from the foregoing contingency categories: five contingencies from G-2, five contingencies from G-1+L-1, and five contingencies from L-2. From our computational results, we observe that some of the aforementioned contingencies follow a similar trend. Hence, in section 4.5.1, we present results for only 5 out of the 15 contingencies. We refer readers to Table 4.2 for details, where each row lists a contingency and columns list its name, category, and components out of service. As an example, C.1 represents a contingency of type G-1+L-1, namely the outage of generator 14 and line 12. For experiments of IEEE 14-bus test case, we select four arbitrary L-2 contingencies: line 1 and line 2, line 4 and line 7, line 2 and line 5, and line 6 and line 18. For experiments of the 6-bus system, since it is a small (and not N-1 reliable) system, we consider all possible L-1 contingencies: single line failure and single generator failure. These contingencies were selected because, within each contingency category, they result in the highest LS before any generation re-dispatch and TS actions are executed and because generator re-dispatch alone (no TS) is insufficient to recover the associated unmet demand in full.

Table 4.2: A List of Contingencies for IEEE 118-bus Test Case

Name	Category	Components out of Service
C.1	G-1+L-1	Generator 14 and Line 12
C.2		Generator 13 and Line 43
C.3	G-2	Generator 13 and Generator 11
C.4		Generator 13 and Generator 1
C.5	L-2	Line 12 and Line 142

4.4.3 Experimental Framework

For each stochastic test instance, we perform five experiments: RN-LSR-DE, CVaR-LSR-DE, RN-LSR-BD, CVaR-LSR-BD, and DMV-B&C, each of which is represented by the name of the model and method applied to solve the model. In RN-LSR-DE and CVaR-LSR-DE, we solve the deterministic equivalent of RN-LSR and CVaR-LSR, respectively, i.e., large-scale block-angular structured mixed binary programs, using CPLEX 12.8, with its default settings. While in RN-LSR-BD and CVaR-LSR-BD we solve the RN-LSR and CVaR-LSR instances, respectively, using Benders' decomposition routine (BD) of CPLEX 12.8. Benders' decomposition is a popular technique for solving large-scale mixed integer programs and stochastic programs. It decomposes the original problem into master problem and smaller sized subproblems, and solves them iteratively by obtaining a lower bound approximation of the recourse function in each iteration. [39]. In DMV-B&C, we first utilize branch-and-cut routine of CPLEX 12.8 to obtain the optimal solution of DMV model, i.e., \hat{s} , and then we solve $f(\hat{s}, \omega)$ for $\omega \in \Omega$ and calculate $\mathbb{E}_\xi[f(\hat{s}, \omega)]$ as the optimal value. All experiments were performed on a 16-core Intel Xeon 3.2GHz machine with 32GB RAM running with Windows 10. The code was written in C++ using callable library of CPLEX 12.8. The time limit, which is

denoted as TL, was set to three hours for each experiment.

4.5 Results and Analysis

In this section, we report and analyze following statistics: time taken to solve RN-LSR-DE, CVaR-LSR-DE, RN-LSR-BD, and CVaR-LSR-BD, optimal LS (denoted by MinLS) by solving RN-LSR and CVaR-LSR, percentage of LSR , that is,

$$\%LSR = (LS_{\dot{G} \cup \dot{K}} - \text{MinLS}) / LS_{\dot{G} \cup \dot{K}} \times 100\%,$$

and VSS. For each $\dot{G} \cup \dot{K}$ in Table 4.2, the value of $LS_{\dot{G} \cup \dot{K}}$ was obtained from [51]. For the IEEE 14-bus and the 6-bus [76] test cases, we compute the value of $LS_{\dot{G} \cup \dot{K}}$ by solving the DMV model with mean demand and $r = 0$.

4.5.1 Computational Results for Risk-Neutral Stochastic LSR

We perform experiments on the IEEE 118-bus, IEEE 14-bus, and 6-bus test cases to evaluate the effectiveness of RN-LSR to handle generation and/or demand uncertainty. We first evaluate the effectiveness of the RN-LSR model to handle demand uncertainty after the occurrence of contingencies for the IEEE 118-bus test case considered in Table 4.2. For each row in Table 4.2, we perform experiments with different switching limits, i.e., $r \in \{2, 3, 4, 5\}$. We randomly generate five instances with 10 scenarios ($|\Omega| = 10$) for each contingency and each switching limit. We perform three experiments for each instance: RN-LSR-DE, RN-LSR-

BD, and DMV-B&C. The average of %LSR by RN-LSR model is plotted in Figure 4.3, and the average of VSS for these instances is in Figure 4.4. From Figure

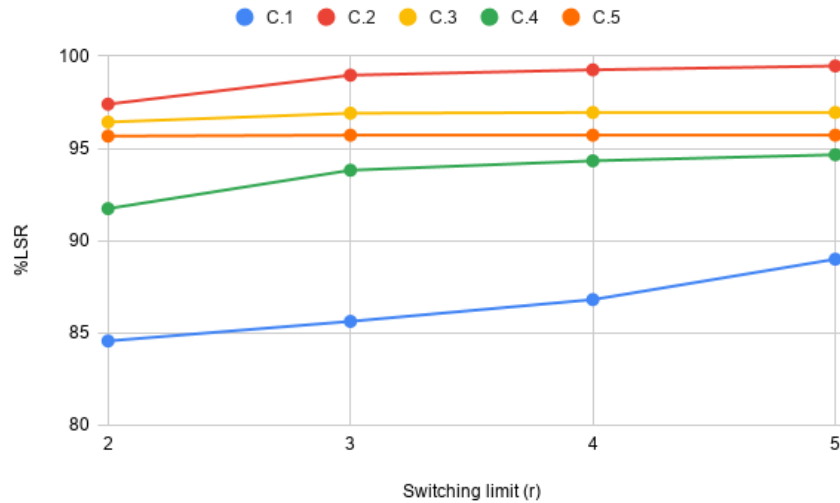


Figure 4.3: %LSR with different switching limits for IEEE 118-bus test case.

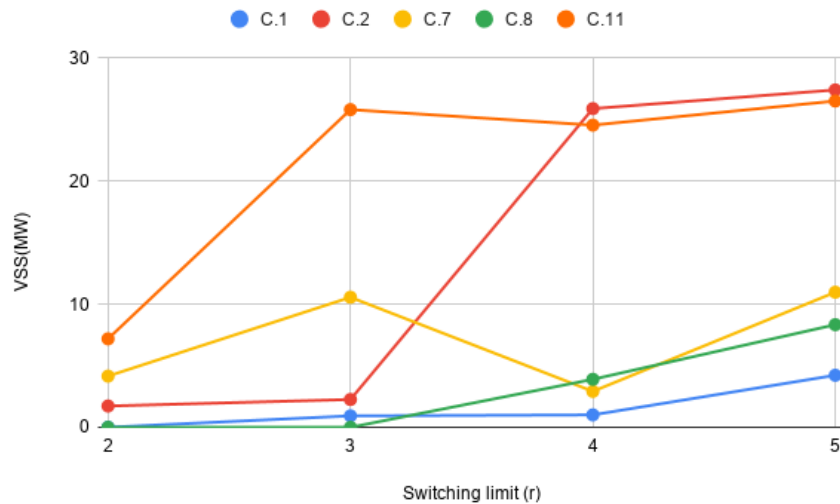


Figure 4.4: VSS for RN-LSR with different switching limits for IEEE 118-bus test case.

4.3 and 4.4, we observe that %LSR and VSS increase as the switching limit in-

creases for three out of five instance categories. In Figure 4.3, the percentage of LS recovered by performing optimal operations of RN-LSR ranges from 84.57% to 99.47% with an average of 94.3%, which implies a large portion of the LS incurred by the contingency is recovered by performing the optimal operations suggested by RN-LSR. In Figure 4.4, VSS is always positive. This implies that the optimal solution of RN-LSR model provides a better solution value compared with the LS obtained using the DMV model. Moreover, when switching more lines is permitted, RN-LSR provides a better solution for most cases. Recall that in Table 4.2, we only present five out of fifteen contingencies considered in our computational experiments, since the omitted results followed a similar trend.

Next, we evaluate the effectiveness of RN-LSR model to handle both generation and demand uncertainty after the occurrence of contingencies using instances obtained from IEEE 14-bus test case. For each of the four contingencies, we perform RN-LSR-DE and RN-LSR-BD experiments with different switching limits, i.e., $r \in \{1, 2, 3\}$ and different number of scenarios, i.e., $|\Omega| = \{100, 500, 1000\}$. We also perform DMV-B&C for these instances. In this case, increasing the switching limit (i.e., $r \geq 2$) does not necessarily increase the %LSR. This is because the total number of lines in this system is small. Switching off more lines may not be able to provide enough total load for the system. We present the result of time taken to solve RN-LSR and %LSR with $r = 1$ in Figure 4.5 and 4.6, respectively.

Since solving RN-LSR using BD is 6.2 times (on average) faster than solving its deterministic equivalent, we only provide the result of BD solution time in Figure 4.5. For instances with 100 scenarios, all instances can be solved within 3 seconds. The time taken by the BD solution method increases with the number of scenar-

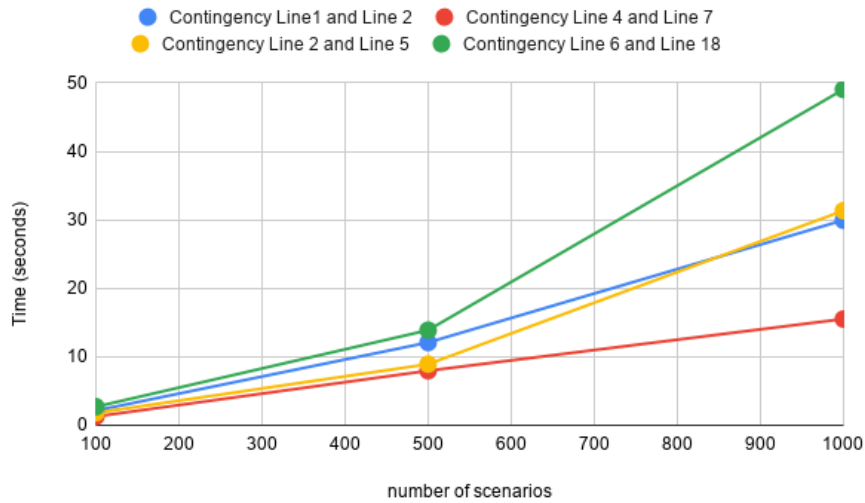


Figure 4.5: BD time with number of scenarios for IEEE 14-bus test case

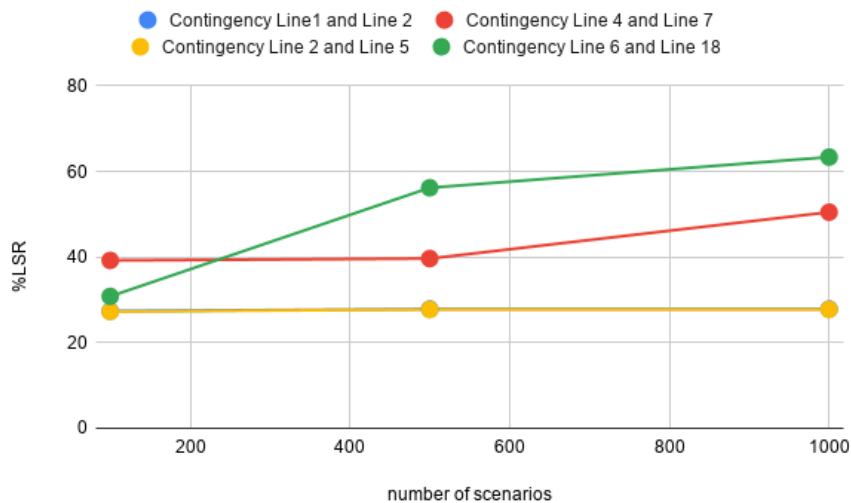


Figure 4.6: %LSR with number of scenarios for IEEE 14-bus test case

ios considered. Interestingly, even for instances with 1000 scenarios, 17 out of 20 instances can be solved within 50 seconds. In Figure 4.6, we evaluate the %LSR by switching at most one line for different number of scenarios. Note that the blue line and yellow line are almost overlapping with each other. We observe that

as the number of scenarios increases, %LSR significantly increases for 2 out of 4 contingencies. Moreover, the optimal switching action provided by experiments with different number of scenarios for the same contingency are identical. Hence, solving instances with 100 scenarios may be enough to obtain the optimal switching actions. From the above results, we conclude that our method can provide switching actions that recover more LS (compared with the deterministic framework) within few seconds for this system. Moreover, the VSS obtained from above 20 IEEE 14-bus test instances is up to 6 MW.

We also perform computational experiments for the randomly generated 6-bus test instances. Since our computational results of the 6-bus system follow the same trend as the example in Section 4.3.2, we omit the details of computational results for this test case. The VSS is 7 MW on average and up to 25 MW, more LS is recovered by performing the optimal switching actions provided by RN-LSR.

Our computational results confirm that RN-LSR is better than DMV, since it provides switching actions that recover more LS, leading to positive VSS and higher LSR than DMV. Our model can effectively handle problems with uncertainties from different sources, i.e., generation uncertainty and demand uncertainty. Moreover, switching one line may be enough for small power system; switching three or four lines seems reasonable for large power system in the sense that RN-LSR can be solved within 6000s and it recovers large portion of LS. Our method has significant impact on multiple test cases with differing tested uncertainty characteristics.

4.5.2 Computational Results of Risk-Averse CVaR-Based LSR

We consider the IEEE 118-bus test case for experiments in this section. To compare RN-LSR and CVaR-LSR models, we perform the second set of experiments on instances related to contingency C.5 from the (L-2) category, namely the outage of line 12 and line 152. Here, different values of confidence interval α and risk-coefficient λ are tested, with the number of scenarios of uncertain demand set to $|\Omega| = 200$ and the switching limit set to $r = 3$. In Table 4.3, we provide results of our computational experiments where each row in this table corresponds to a randomly generated test instance. Columns labeled as RN-Sol and CVaR-Sol provide the optimal TS operations (lines to be switched) provided by RN-LSR and CVaR-LSR, respectively. For example, the first row under RN-sol column indicates that switching line 154, line 157, and line 160 is an optimal solution for the RN-LSR instance associated to this row. The total LS after performing the optimal TS and re-dispatching operations of RN-LSR is reported in column labelled as MinLS. We observe that the total LS for RN-LSR and CVaR-LSR are the same but with different optimal solution for all the instances, except for one—in particular, for the instance with $\alpha = 0.85$ and $\lambda = 0.2$, the optimal value of CVaR-LSR is 3.52 MW less than that of RN-LSR. This demonstrates that CVaR-LSR optimal solutions not only avoid the outcomes with large LS, but also provide the least expected LSR (same as provided by RN-LSR) for most of the instances. In summary, after the failure of line 12 and line 152, an average of 96.31% of the LS is recovered by performing risk-averse TS and re-dispatching operations provided by CVaR-LSR.

Table 4.3: Results for Computational Experiments with Different Risk Coefficient and Confidence Interval

α	λ	Risk-Neutral LSR			Risk-Averse CVaR-Based LSR		
		RN-Sol	MinLS (in MW)	T-BD (in seconds)	CVaR-Sol	T-BD (in seconds)	%LSR
0.85	0.2	154 157 160	8.1	283	154 157 165	6301	96.7
	0.5	154 157 160	11.6	599	154 163 165	9722	95.3
	0.8	154 160 161	5.7	605	154 157 163	8732	97.7
	3	154 157 169	8.4	10^3	154 160 161	8949	96.6
	7	154 163 165	10.9	659	154 159 161	4959	95.6
	10	154 161 169	10.3	650	154 159 161	10^4	95.8
0.9	0.2	154 163 165	11.2	617	154 157 163	6615	95.5
	0.5	154 163 165	7.8	445	154 161 169	5983	96.8
	0.8	154 160 161	10.6	549	154 161 173	8509	95.7
	3	154 162 163	8.7	687	-	TL	-
	7	154 157 165	11.7	450	-	TL	-
	10	154 157 163	11	721	154 162 163	7497	95.6
0.95	0.2	154 161 162	8.2	483	139 154 161	5285	96.7
	0.5	154 160 161	7.7	545	154 159 161	9173	96.9
	0.8	154 161 173	7.3	778	154 157 169	7711	97.1
	3	154 161 169	10.6	364	154 157 169	9131	95.7
	7	132 154 157	6.8	582	73 154 161	5742	97.3
	10	154 161 162	7.6	531	-	TL	-

Columns labeled as T-BD provide the time taken (in seconds) to solve RN-LSR and CVaR-LSR instances using BD algorithm. RN-LSR-DE and CVaR-LSR-DE could not be solved within the three-hour time limit and, thus, their times are not reported; three instances of CVaR-LSR were similarly not solved via BD. RN-LSR instances and CVaR-LSR instances solved by the BD approach took on average 586 seconds and 7643 seconds, respectively. Put otherwise, solving RN-LSR using BD was 12 times faster than solving CVaR-LSR using BD.

The most important result from the above experiment is that the optimal TS operation of CVaR-LSR not only avoids the outcomes with large LS, the optimal LS provided by CVaR-LSR is almost the same as RN-LSR for most instances. How-

ever, the time taken to solve CVaR-LSR is longer than RN-LSR. Hence, decision makers should consider the trade-offs between the time taken to solve the problem and their risk preference when executing these TS operations.

4.5.3 Computational Results using Larger Number of Scenarios

We perform a third set of experiments on the IEEE 118-bus test case to evaluate the impact of increasing the number of scenarios on RN-LSR and CVaR-LSR and report results in Table 4.4. We denote an instance category by $C.\mu.r.\tau$ where $C.\mu$ is the contingency listed in Table 4.2, r is the switching limit, and τ is the number of scenarios ($|\Omega| \in \{200, 250, 300, 400\}$). For CVaR-LSR model, we set the risk-coefficient $\lambda = 7$, which represents the decision maker is risk-averse, and confidence interval $\alpha = 0.95$. Each row in Tables 4.4 corresponds to a randomly generated instance. Table 4.4 reports the optimal TS solution and MinLS provided by RN-LSR and CVaR-LSR. For instances that could not be solved within the time limit, the table reports the best known solution and upper bound, denoted by “*”; in case these are not known, “-” is used.

Using the BD algorithm, 23 of 24 RN-LSR instances were solved in 2091 seconds, and 12 of 24 CVaR-LSR instances were solved in 5926 seconds, on average. The average %LSR for solvable RN-LSR instances is 95%, and the RN-LSR and CVaR-LSR provide the same optimal TS solution for 9 out of 12 instances. For the remaining three instances, we observe that although CVaR-LSR solution increases LS (0.9 MW on average), it avoids the worst quantile of outcomes with high LS.

Table 4.4: Computational Results for RN-LSR and CVaR-LSR Models

Instance	Risk-Neutral LSR					Risk-Averse LSR		
	Sol	MinLS (in MW)	BD (in seconds)	VSS (in MW)	%LSR	Sol (in MW)	MinLS (in seconds)	BD
C.3.1.200	51	117.3	559	0	91	64	119.1	3662
	64	102.7	551	0.2	92.1	64	102.7	3423
C.3.1.300	51	91.6	665	0	93	64	92.5	8686
	51	100.8	901	0	92.3	64	100.8	8219
C.3.2.200	64 112	42.3	6123	5.6	96.8	115 141*	47.8*	TL
	64 112	38.3	5443	3.8	97	115 141*	42.1*	TL
C.3.2.250	64 112	40.9	7628	4.6	96.9	64 115*	71.8*	TL
	64 112	42.9	5911	5.6	96.7	51 115*	78.4*	TL
C.3.2.300	64 112	44.4	5515	3.8	96.6	51 115*	80.8*	TL
	64 112	48.6	5070	6.5	96.3	115 116*	55.1*	TL
C.3.2.400	-	-	TL	-	-	-	-	TL
	64 112	42.4	9626	5.9	96.7	51 115*	79.6*	TL
C.5.1.200	154	19.2	256	0	92.2	154	19.2	2023
	154	17.9	166	0	92.8	154	17.9	1906
C.5.1.400	154	15.5	519	0	93.7	154	15.5	6850
	154	16.4	456	0	93.4	154	16.4	7125
C.5.2.200	154 161	9.6	535	6.2	96.1	154 161	9.6	4587
	154 161	7.85	314	6.2	96.8	154 161	7.85	6184
C.5.2.250	154 161	10.4	580	6.5	95.8	154 161	10.4	8347
	154 161	10.57	568	7.1	95.7	154 161	10.57	10 ⁴
C.5.2.300	154 161	12.6	314	7.5	94.9	154 161*	12.6*	TL
	154 161	9.4	380	6.7	96.2	154 161*	9.4*	TL
C.5.2.400	154 161	9.9	370	6.9	96	134 154*	41.9*	TL
	154 161	7	715	6	97.2	154 161*	7*	TL

The most salient conclusion is that as the number of scenarios increases, the optimal solutions returned by RN-LSR and CVaR-LSR converge. This indicates that when number of scenarios is large enough, i.e., $|\Omega| = 200$, the optimal solution remains stable.

4.5.4 Practical Implications

We note that the proposed method does not provide a minute-to-minute specification for dealing with contingencies; rather, it provides effective topology modifications to be considered while preparing for the occurrence of such events and their

attendant uncertainties. In an attempt to help in providing operational recommendations, this subsection discusses separate procedures for generating a switching sequence that minimizes the load shedding and additional practical considerations.

In practice, operators may prefer to switch one line at a time, with sufficient time between switches to avoid engineering issues including transient stability (e.g., see [92]). Assuming each switching operation takes approximately 10-15 minutes [51], as many as five line switches could be putatively carried out within 90s minutes, i.e., the duration required by FERC to return the system to normal state and replenish reserves following a contingency [52]. This explains the choice of $r \leq 5$ for the experiments summarized in our computational experiments. A more stringent requirement by some TSOs (e.g., PJM [122]) states that the system must return to normal state within roughly 30 minutes [122]. Thus, we restrict $r \leq 3$ in the experiments associated with Tables 4.3 and 4.4. The LS decreases significantly from $r = 1$ to $r = 2$, and $VSS > 0$ for almost all instances with $r \geq 2$. This suggests that TSOs/ISOs should consider switching at least two lines, based on the optimal solution provided by experiments with $|\Omega| \geq 200$. If the stochastic risk-averse problem, CVaR-LSR, and the stochastic risk-neutral problem, RN-LSR, provide the same optimal solution, then this solution not only provides the most load shed recovery, but also avoids the worst case scenarios, and hence is a stable optimal solution. Moreover, our results may also provide the optimal sequence of switching, which minimizes the LS during switching operations. From our results in Section 4.4, we observe that for some instances, as r increases, the set of optimal solutions with switching limit $r - 1$, i.e., S_{r-1} , is a subset of the optimal solution with switching limit r , i.e., $S_{r-1} \subset S_r$. Thus, the optimal r -th switch is given by

$S_r \setminus S_{r-1}$. For the optimal solutions with some contingencies which do not have above properties, this methodology suggests operators to set $r = 1$ and solve RN-LSR or CVaR-LSR as desired up to a predetermined r_{\max} -times. The optimal TS solution provided by solving RN-LSR with $r = 1$ for r_{\max} -times is also a feasible solution to RN-LSR with $r = r_{\max}$, and it will also provide a switching sequence which minimizes the LS during switching operations.

In order to ensure that no islanding is caused by the executed changes to the network topology, the ISO/TSO can perform a post optimality analysis after obtaining the optimal switching action(s). One way to check whether the graph is connected is to do a breath-first search or depth-first search. If the final spanning tree contains all buses, then the graph/network is connected, i.e., there is no islanding issue. Otherwise, the ISO/TSO can restrict the previous switching action, resolve, and perform the post optimality analysis again, until a connected graph is found. The procedures suggested in [45, 51] can be performed to ensure the stability of the system. In particular, a multi-branch tree structure can be constructed to provide multiple possible topology control actions, which can be referenced in the case that a suggested action is deemed to pose stability risks.

The proposed methodology can be utilized as an offline contingency analysis tool to provide guidance for TSO/ISO to minimize load shedding during an emergency. Its benefits were illustrated via a limited selection of nontrivial contingencies involving the outage of two components. A wider selection could be tested offline to provide optimal TS operations that could supplement TSO operator manuals. Compared to previous deterministic LSR models, this method considers demand uncertainty and avoids the worst-case scenarios of large outages. Thus, it provides

more comprehensive and representative decision support for emergency situations.

4.6 Conclusion

We introduced stochastic risk-neutral and risk-averse transmission switching models for load shed recovery (LSR) under uncertain generation and demand. Our models provide the optimal transmission switching (TS) actions to perform after a contingency occurs but before the realization of uncertain renewable generation and demand, so that the expected LSR or the risk level measure of unrecovered LS is maximized. After the uncertainty is realized, other actions, such as adjusting the bus phase-angle, deciding output of the conventional generators, and transmission lines re-dispatch level, are performed to incorporate the effect of the optimal transmission switching actions. Compared to deterministic models that use only conventional generation and fix demand to the mean of uncertain demand over a number of scenarios, the stochastic models not only reduced expected LS, but also avoided the possible scenarios with extremely large LS. Most of the stochastic variants of the IEEE 118-, 14- and the 6-bus test cases were solved within a reasonable time. The percentage of LS that was recovered by TS operations and re-dispatching (suggested by the stochastic models) for the IEEE 118-bus test case ranges from 84.5% to 99%. Performing the transmission switching solution obtained from the RN-LSR model recovers 18 MW (on average) more shedded load compared with the TS based on the deterministic model [51] for IEEE 118-bus test case. Likewise, it recovers up to 6 MW more for IEEE 14-bus test case, and recovers 7 MW on average and up to 25 MW more for the 6-bus system, in comparison to the de-

terministic model. As the accompanying experiments and discussion evince, this method could recover more load shedding by performing transmission switching, and hence improve the self-healing capabilities of the smart grid. Moreover, this method can serve as an offline contingency analysis tool for large electrical network. Its outputs could help maximize the recovery of LS incurred by failures of generators and/or transmission lines effectively.

One possible direction of the future research could be to develop coordination strategies between different TSOs to incorporate TS actions and to develop policies to handle impact of TS in a region over other connected regions. Another future research direction could be the integration of simulation techniques to derive data-driven sample spaces for the random variables that are used to define uncertainty in the proposed stochastic models.

Chapter 5

Two-stage Stochastic Mixed-integer Quadratically Constrained Quadratic Programming

5.1 Introduction

We study two-stage stochastic mixed-integer quadratically constrained quadratic programs (TSS-MIQCQPs) with quadratic objectives in both stages and quadratic constraints in the second-stage problem. Different from existing research of TSS-MIQCQPs which only allows continuous or pure binary first-stage variables, our problem allows general integer variables in both stages. We utilize a scenario-based decomposition algorithm, i.e., dual decomposition, to solve such a problem. Additionally, we provide an open-source software implementation of our algorithm, thereby adding a new feature of an existing solver: Decomposition for Structured Programming (DSP), an open-source package developed by Kim and Zavala [80] for solving TSS-MILP at Argonne National Laboratory. In this chapter, we review

the literature related to TSS-MIQCQP and present dual decomposition approach to get a lower bound for TSS-MIQCQP. We also discuss architecture of DSP and introduce its new feature.

5.2 Literature Review: TSS-MIQCQP

In literature, different decomposition algorithms exist for solving variety of two-stage stochastic nonlinear programs (TSS-NLP) without discrete variables. Geoffrion [57] extends Benders' decomposition for two-stage stochastic linear programs [24] to the general structured programs with general convex constraints and objective functions, and referred to this approach as Generalized Benders Decomposition (GBD). Alzalg [5], Mehrotra and Ozevin [102] propose logarithmic barrier decomposition-based interior point methods to solve two-stage stochastic convex quadratic linear programs and two-stage stochastic convex quadratic second-order cone programs with quadratic terms in both first-stage and second-stage objective functions, respectively. Liu and Sen [93] study two-stage stochastic programs with non-coupling quadratic objectives in both first-stage and second-stage problems. They propose a stochastic decomposition to solve the aforementioned problems, and provide convergence analysis of their algorithm.

As to convex TSS-NLP with integer variables, different algorithms have been proposed to different types of problems. Mijangos [104] provides a branch-and-fixed coordination based algorithm which can only be used to solve two-stage stochastic programs with mixed-binary first-stage variables and continuous quadratic programs in the second-stage. Özaltın et al. [118] study two-stage stochastic quadratic

integer programs with only stochastic right-hand sides in the second stage along with deterministic quadratic objective functions, linear constraints, and only integer variables in both stages. They reformulate this problem using value functions for quadratic integer programs, and present a global branch-and-bound algorithm and a level-set approach to solve the problem. In [17], the authors study two-stage distributionally robust disjunctive programs with disjunctive constraints in both stages, and utilize the sequential convexification technique within L-shaped method. Li and Grossmann [85] study two-stage convex 0-1 mixed integer nonlinear stochastic programs, where the first stage and the second stage both have mixed binary variables and nonlinear constraints. They propose an improved L-shaped method, where the nonlinear constraints of the second-stage integer programs are outer approximated by a cut generating linear function [78], and both Lagrangian cuts and Benders' cuts are added to the master problem. However, their results do not guarantee finite convergence. Later, Li and Grossmann [86] propose a generalized Benders' decomposition-based branch-and-bound algorithm to solve the two-stage convex 0-1 mixed integer nonlinear stochastic programs, where the first stage and the second stage both have mixed binary variables and nonlinear constraints. They use the disjunctive programming technique [12] to reformulate the second stage feasible region into its disjunctive normal form, and then convexify the obtained disjunctive normal form to obtain the convex hull of the second stage feasible region. They solve the problem using GBD by branching on the first stage continuous variables and prove that their algorithm has finite ϵ -convergence. Luo and Mehrotra [100] study distributionally robust two-stage stochastic mixed-integer conic programs, where the first-stage variables are pure binary and the second-stage has mixed integer variables. They decompose the problem into sce-

nario subproblems, and use branch-and-cut algorithm to solve subproblems. They also generate optimality cuts using disjunctions in each scenario sub tree.

With respect to two-stage stochastic mixed-integer nonconvex program, Li et al. [89] study two-stage stochastic nonconvex mixed integer nonlinear problem with pure binary first-stage variables and mixed-integer second-stage variables along with nonconvex terms in the problem. They propose a nonconvex generalized Benders' Decomposition to solve such problems. Li et al. [87] propose an outer approximation algorithm which is based on a sample average approximation method to address two-stage stochastic nonconvex mixed integer nonlinear programs with any continuous or discrete probability distributions. The objective functions and constraints in both stage must be smooth, but could be nonconvex.

5.3 Dual Decomposition for TSS-MIQCQP

In this section, we present dual decomposition for TSS-MIQCQPs. The deterministic equivalent formulation of TSS-MIQCQPs (1.10) is:

$$z = \min \frac{1}{2}x^\top P^{xx}x + c^\top x + \sum_{\omega \in \Omega} p_\omega \left(\frac{1}{2}y_\omega^\top P_{\omega,0}^{yy}y_\omega + x^\top P_{\omega,0}^{xy}y_\omega + q_{\omega,0}^\top y_\omega \right) \quad (5.1a)$$

$$\text{s.t. } Ax \geq b, \quad (5.1b)$$

$$\frac{1}{2}[x; y_\omega]^\top P_{\omega,i} [x; y_\omega] + q_{\omega,i}^\top [x; y_\omega] + d_\omega^i \leq 0, \quad i = 1, \dots, I \quad (5.1c)$$

$$x \in X, y_\omega \in Y, \quad \omega \in \Omega. \quad (5.1d)$$

We first add auxiliary variables $x_{\omega_1}, x_{\omega_2}, \dots, x_{\omega_{|\Omega|}} \in X$ and constraints $x_{\omega_1} = x_{\omega_2} = \dots = x_{\omega_{|\Omega|}} = x$ in Problem (5.1):

$$z = \min \sum_{\omega \in \Omega} p_\omega \left(\frac{1}{2} x_\omega^\top P^{xx} x_\omega + c^\top x_\omega + \frac{1}{2} y_\omega^\top P_{\omega,0}^{yy} y_\omega + x_\omega^\top P_{\omega,0}^{xy} y_\omega + q_{\omega,0}^\top y_\omega \right) \quad (5.2a)$$

$$\text{s.t.} \quad \sum_{\omega \in \Omega} H_\omega x_\omega = 0, \quad (5.2b)$$

$$(x_\omega, y_\omega) \in G_\omega, \quad \omega \in \Omega, \quad (5.2c)$$

where for $\omega \in \Omega$, the scenario feasible set is defined as,

$$G_\omega = \left\{ (x_\omega, y_\omega) : Ax_\omega \geq b, \right. \\ \left. \frac{1}{2} \begin{bmatrix} x_\omega \\ y_\omega \end{bmatrix}^\top P_{\omega,i} \begin{bmatrix} x_\omega \\ y_\omega \end{bmatrix} + q_{\omega,i}^\top \begin{bmatrix} x_\omega \\ y_\omega \end{bmatrix} + d_\omega^i \leq 0, \quad i = 1, \dots, I, x_\omega \in X, y_\omega \in Y \right\}$$

The nonanticipativity constraint (5.2b) is the compact form of equations $x_{\omega_1} = x_{\omega_2} = \dots = x_{\omega_{|\Omega|}}$. We note that Problem (5.1) and (5.2) are equivalent. We obtain the Lagrangian dual function of Problem (5.2) by applying Lagrangian relaxation on nonanticipativity constraint (5.2b):

$$D(\lambda) = \min \sum_{\omega \in \Omega} \left(p_\omega \left(\frac{1}{2} x_\omega^\top P^{xx} x_\omega + c^\top x_\omega + \frac{1}{2} y_\omega^\top P_{\omega,0}^{yy} y_\omega + x_\omega^\top P_{\omega,0}^{xy} y_\omega + q_{\omega,0}^\top y_\omega \right) + \lambda^\top H_\omega x_\omega \right) \\ \text{s.t.} \quad (x_\omega, y_\omega) \in G_\omega, \quad \omega \in \Omega,$$

where $\lambda \in \mathbb{R}^{(|\Omega|-1)n}$ are the dual variables of nonanticipativity constraints (5.2b).

For a given λ , $D(\lambda) = \sum_{\omega \in \Omega} D_\omega(\lambda)$ for scenario $\omega \in \Omega$,

$$D_\omega(\lambda) = \min p_\omega \left(\frac{1}{2} x_\omega^\top P^{xx} x_\omega + c^\top x_\omega + \frac{1}{2} y_\omega^\top P_{\omega,0}^{yy} y_\omega + x_\omega^\top P_{\omega,0}^{xy} y_\omega + q_{\omega,0}^\top y_\omega \right) + \lambda^\top H_\omega x_\omega \quad (5.3a)$$

$$\begin{aligned}
& + \lambda^\top H_\omega x_\omega \\
\text{s.t. } & (x_\omega, y_\omega) \in G_\omega
\end{aligned} \tag{5.3b}$$

Our objective is to find the best lower bound of (5.1) by maximizing the Lagrangian dual problem over λ :

$$z \geq z_{LD} = \max_{\lambda} \sum_{\omega \in \Omega} D_\omega(\lambda) \tag{5.4}$$

We note that two-stage stochastic mixed integer linear programs (TSS-MILPs) is a special case of TSS-MIQCQPs by setting matrices P^{xx} , $P_{\omega,0}^{yy}$, $P_{\omega,0}^{xy}$, and $P_{\omega,i}$ for $i = 1, \dots, I$, $\omega \in \Omega$ to 0.

The dual decomposition algorithm for solving TSS-MIQCQPs are the same as the algorithm for TSS-MILP, i.e., Algorithm 1, except that in Line 4, we are solving Problem 5.3 instead of Problem (2.5b)-(2.5c).

5.4 An Open-source Package: Decomposition of Structured Programs (DSP)

In this section, we first briefly review the previous version of DSP, and then illustrate the new features of DSP.

5.4.1 DSP: Review

DSP, first developed by Kim and Zavala [80], is an open-source package for solving Stochastic Mixed-integer Linear Program (SMILP) by implementing serial and parallel implementations of different methods. It is objective-oriented and implemented in C++. DSP can specify problem instances written in SMPS, C code, MPS-DEC file, and Julia script. It implements several decomposition method, i.e., Benders decomposition, dual decomposition, and Dantzig Wolfe decomposition, and utilizes external solvers, i.e., CPLEX [41], OOQP, and SCIP, etc., to solve SMILP. In order to fulfill the aforementioned demands, the software design of DSP has different classes:

- *SolverInterface* class: DSP uses external MIP solvers to solve master problems and subproblems which are defined in the decomposition algorithms. This class provides a common interface between *OsiSolverInterface* and DSP to support the decomposition methods we implemented. *OsiSolverInterface* is *Open Solver Interface*, which provides interface for LP and MIP solvers. However, not all functions in each solver are implemented in *OsiSolverInterface*. In this class, we define new functions which are used in DSP but are not defined in *OsiSolverInterface*.
- *Model* class: The data structure of SMILP models is defined in *Model* class. Users can manage their models through other interface, i.e., SMPS, JuMP and C interface. For SMILP, an abstract class *StoModel* is used to define the general stochastic problems, while *TssModel* specifies the data structure for two-stage stochastic linear programs. There is also *DecModel* class to define

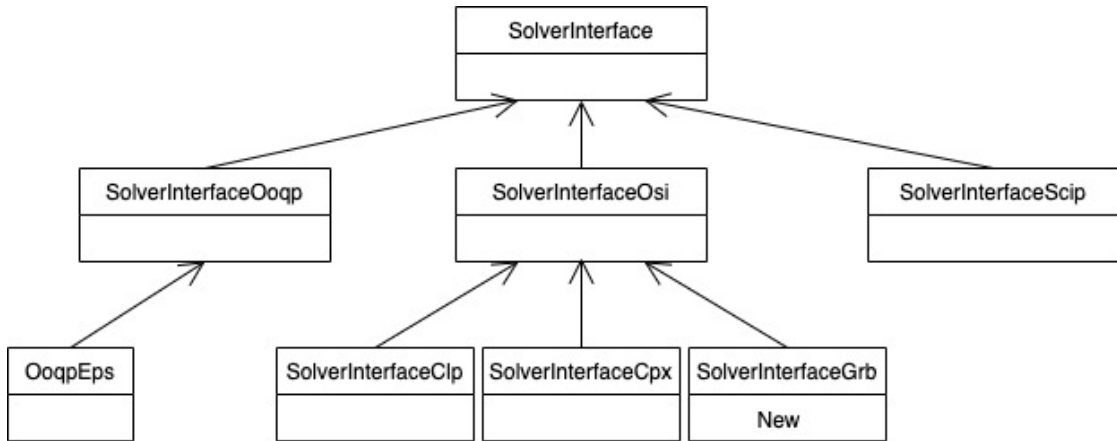


Figure 5.1: SolverInterface Class

the data structure which is used in decomposition algorithms.

- *Solver* class: *Solver* class is designed to implement different algorithms to solve SMILP models, which are built in *Model* class. Depending on different solution methods, there are four sub-classes in *Solver* class: Deterministic, Benders, DantzigWolfe, and DualDecomp.

5.4.2 Extension of DSP

We extend DSP to solve TSS-MIQPs by implementing decomposition algorithms, i.e., Benders decomposition, dual decomposition (as described in Section 5.3), and directly solving its deterministic equivalent formulation. We also add Gurobi [67] as an external solver in *SolverInterface* class. More specifically, we add additional external solver in *SolverInterface* class, modify the data structure in *Model* class, and extend the decomposition implementation in *Solver* class.

First, we extend DSP to support Gurobi for all decomposition method implemented in DSP for TSS-MILPs and TSS-MIQCPs, and create a new *SolverInterface* be-

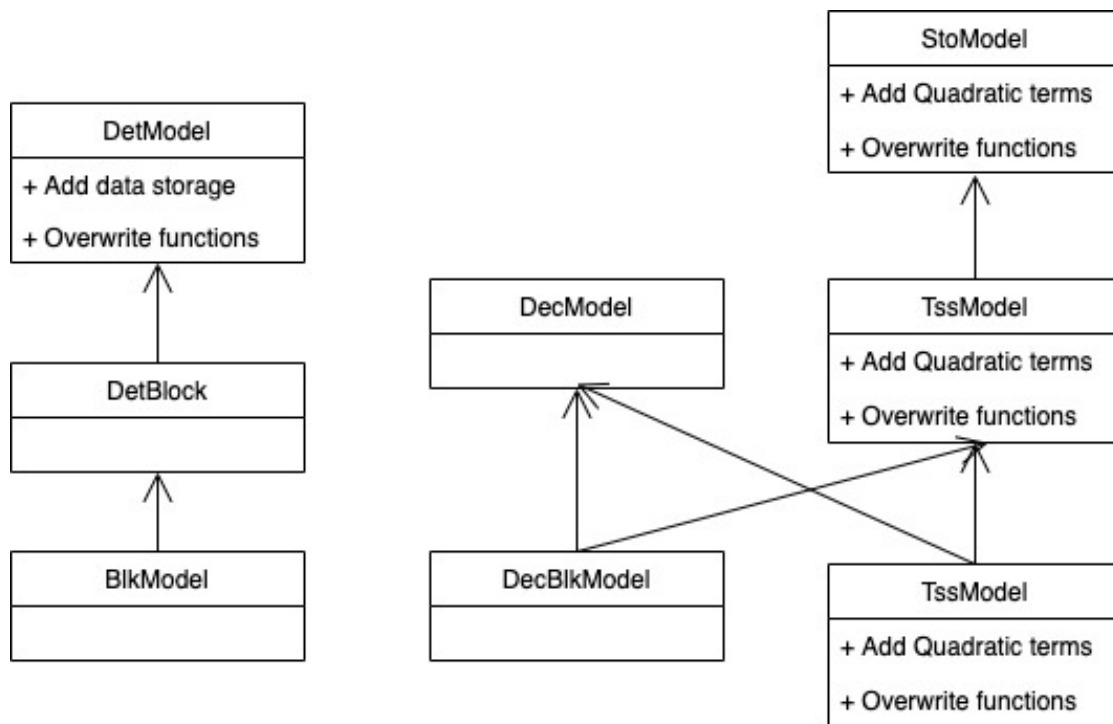


Figure 5.2: Model class.

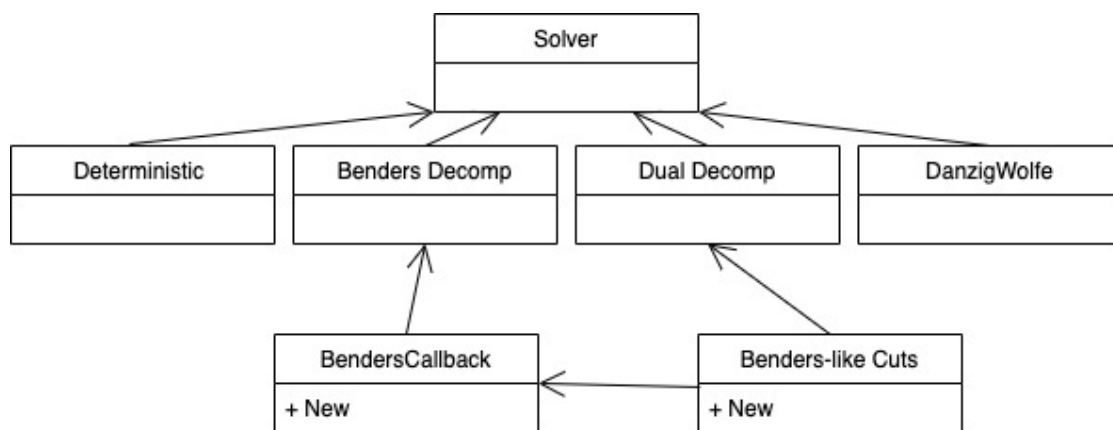


Figure 5.3: Solver Class

tween *OsiSolverInterface* and DSP for *Gurobi*, i.e., *DspOsiGrb*, for functions which are not previously defined in *OsiSolverInterface*.

Instead of deriving new *Model* class, we design the data structure and overwrite functions in *Model* class for TSS-MIQPs. More specifically, we extend the *StoModel* and *TssModel* class to store the data for quadratic terms using COIN-OR packages (*CoinPackedMatrix/CoinPackedVector*). For users' convenience, DSP accepts the quadratic terms written in coordinate format when reading the model through other interfaces.

We extend three among aforementioned four classes: *Deterministic*, *Benders*, and *DualDecomp*. In *Deterministic* class, we overwrite functions to load quadratic terms, and solve the deterministic equivalent of the stochastic model. Previously, DSP only supports *SCIP* as an external solver for *Benders* decomposition. We add a new class which provides generic callback structure for solving TSS-MIQP model. This new class allows *Benders* decomposition implementation to use the callback functions in *CPLEX* and *Gurobi* to add *Benders* cuts [57]. We note that *CPLEX* and *Gurobi* do not allow nonlinear cuts in callback functions, so we only add the linear form of *Benders* cuts.

5.5 Stochastic Quadratic Capacitated Facility Location Problem

To illustrate the importance of dual decomposition method for TSS-MIQCQP in DSP, we introduce a stochastic quadratic capacitated facility location problem

(SQCFL). We first provide a brief literature review for quadratic facility location problem, and then provide the computational experiment of SQCFL.

5.5.1 Literature of Quadratic Facility Location Problem

White [146] study a continuous unconstrained quadratic uncapacitated facility location problem (qUFL), whose objective is to minimize the total transportation cost. The transportation cost is calculated as the Euclidean distance between facilities. Later, Hajiaghayi et al. [68] study a facility location problem with general facility cost, which is an arbitrary function of the number of customers served by this facility. They also propose a greedy algorithm to solve the aforementioned problem with concave facility cost. Günlük and Linderoth [63, 64], Günlük et al. [66] consider another qUFL with mixed binary variables and its objective is to minimize the total installation cost and transportation cost. In their problem, one needs to decide the facility opening decision at each facility, as well as the fraction of demand satisfied by facilities. The transportation cost is proportional to the square of fraction of demand allocated to a facility. Fischetti et al. [53] propose a Benders decomposition for qUFL studied in [66]. They also derive so called “Generalized Benders Cuts” for qUFL.

Different from the aforementioned qUFL problems, which are all deterministic, we propose a stochastic quadratic multi-capacitated facility location problem (SQCFL), more specifically, multi-module capacitated stochastic facility location problem with quadratic transportation cost. In contrast of the qUFL considered in [66], where they do not have capacity constraint for each facility, we have multiply modules with different capacities that can be installed at each facility. In the

first-stage problem, the decision maker needs to decide the number of different modules to be installed at each facility, and the number of subcontracting items. After the uncertainty of demand is realized, the transportation decision is made in the second-stage problem. The problem is defined as follows. Given a set of possible facilities $M = \{1, \dots, m\}$, a set of customers $N = \{1, \dots, n\}$, quadratic transportation cost q_{ij} from facility $i \in M$ to customer $j \in N$, per unit holding cost v_i at facility $i \in M$, machines with capacity a_k for $k = 1, \dots, K$, which can be installed at facilities i with fixed cost c_{ik} , and subcontracting cost s_i per item with a fixed subcontracting cost g_i for $i \in M$. The SQCFPLP problem is defined as follows,

$$\min \sum_{i \in M} \sum_{k=1}^K c_{ik} x_{ik} + \sum_{i \in M} (s_i z_i + g_i \zeta_i) + \mathbb{E}_\xi(Q(x, \omega)) \quad (5.5)$$

$$\text{s.t. } \sum_{k=1}^K x_{ik} \leq f_i, \quad i \in M, \quad (5.6)$$

$$\sum_{i \in M} x_{ik} \leq e_k, \quad k = 1, \dots, K, \quad (5.7)$$

$$z_i \leq C\zeta_i, \quad i \in M, \quad (5.8)$$

$$x_{ik} \in \mathbb{Z}_+, z_i \in \mathbb{R}_+, \zeta_i \in \mathbb{Z}_+, \quad i \in M, j \in N, k = 1, \dots, K, \quad (5.9)$$

where x_{ik} is an integer variables denoting the number of machines with capacity a_k installed at facility i , z_i denotes the amount of commodity subcontracted by customer $i \in M$, which is not restricted to be integer. Since commodity must be shipped in packages in transportation, ζ_i is an integer variable denoting the amount of packages subcontracted at facility i . The objective (5.5) is to minimize

the total machines' installation cost, subcontracting cost, and expected second-stage cost, which includes the transportation cost and holding cost. Constraints (5.6) restrict the total number of machines installed at facility $i \in M$ to be at most f_i . Constraints (5.7) restrict the total number of machine with capacity a_k among all facilities to be at most e_k . The capacity for each subcontracting package is C , and constraints (5.8) restrict the number of subcontracting packages to hold all subcontracting commodity. Let $X = \{x : (5.6) \text{ and } (5.7) \text{ hold}\}$. For $x \in X$ and $\omega \in \Omega$, the recourse problem is defined as follows,

$$\min \sum_{i \in M} \sum_{j \in N} q_{ij} y_{\omega,ij}^2 + \sum_{i \in M} v_i s_{\omega,i} \quad (5.10)$$

$$\text{s.t. } \sum_{i \in M} y_{\omega,ij} \geq d_{\omega,j}, j \in N, \quad (5.11)$$

$$\sum_{j \in N} y_{\omega,ij} + s_{\omega,i} = \sum_{k=1}^K a_k x_{ik} + z_i, i \in M, \quad (5.12)$$

$$y_{\omega,ij} \in \mathbb{Z}_+, s_{\omega,i} \in \mathbb{R}_+, i \in M, j \in N \quad (5.13)$$

where $y_{\omega,ij}$ denotes the number of items transported from facility $i \in M$ to customer $j \in N$, and $s_{\omega,i}$ denotes the amount of holding commodity at each facility after the uncertain demand $d_{\omega,ij}$ is realized. The objective (5.10) is to minimize the total transportation cost and total holding cost at all facilities. Constraints (5.11) require that all demand at customer $j \in N$ must be satisfied by the sum of items transported from all facilities after the realization of uncertainties at that facility before the realization of uncertainties. Constraints (5.12) ensure the total items transported from facility i for $i \in M$ cannot exceed the total number of

commodity produced and subcontracted at that facility.

SQCFL can be applied in power system domain to model problems which include loss and voltage economic dispatch, and thermal generator cost [109]. One of the important applications for SQCFL model is optimal distributed generation placement (ODGP). The goal of ODGP is to find the best location to place a distributed generations, the best capacity of distributed generations to be installed at each location, minimize the total cost or total power loss. Such problem has been broadly studied in the power system domain ([6, 60, 71], etc.). In Ohm's law, the power loss on a transmission line is calculated by the resistance of this line multiply by the square of the current. Hence, in SQCFL model, x_{ik} decides whether to install distributed generation of type k at location i , and y_{ij} represents the current in each transmission line, and q_{ij} represents the resistance of that line. In the first stage, the objective is to minimize the total installation cost and the expected second-stage cost. In the second stage, we assume that the demand is uncertain, and there is a penalty for surplus generation after satisfying the demand. Therefore, SQCFL can be adapt to model ODGP by adding additional physical constraints from electrical power system. Readers may refer to [59] to more details.

5.5.2 Generation of SQCFL Test Instances

We utilize "capacitated warehouse location problem" instances from J.E. Beasley OR-Library with 16 potential facilities and 50 potential customers, i.e., $M = \{1, \dots, m\}$ with $m \leq 16$ and $N = \{1, \dots, n\}$ with $n \leq 50$, respectively. More specifically, we perform experiments with following number of facilities and customers: $(m, n) \in \{(8, 25), (8, 50), (16, 25), (16, 50)\}$. The transportation cost q_{ij}

for $i \in M$ and $j \in N$ is given. We also utilize the procedure to generate random instances in Bansal and Zhang [18], where the number of different types of modules K , a set of the capacity of modules and their installation costs $(\alpha_k, c_i^k) \in \{(1000, 2700), (10000, 18000)\}$, the subcontract cost s_i is a random number between $[3, 4]$ for $j \in N$ per unit, η_i is a random integer between $[100, 200]$, the inventory cost $v_i = 0.35$ for $i \in M$ per unit, the capacity for subcontracting package $C = 150$, the maximum number of modules at each facility $f_i = 2$ for $i \in M$, and maximum number of each module $e_1 = 5, e_2 = 1$. The probability for each scenario is randomly generated as follows: we first draw $|\Omega|$ random numbers num_ω for $\omega \in \Omega$ between $[0, 10000]$, and then calculate the probability of scenario ω as
$$p_\omega = \frac{num_\omega}{\sum_{\omega \in \Omega} num_\omega}.$$

5.5.3 Computational Framework of SQCFL Test Instances

For each instance in the SQCFL instance category, we perform two experiments, DEF, and DD. We use Gurobi [67] as the external solver in DSP for all experiments. In DEF, we solve the deterministic equivalent formulation of the problem using DSP. In DD, we solve the problem using dual decomposition. The time limit is 2000 seconds. We report the computational time in wall time for each experiments (T-DEF for DEF and T-DD for DD). The computational results for SQCFL is provided in Table 5.1. Each row is the average of five randomly generated instances. We observe that for instances in the first two instance categories, i.e., $\{m = 8, n = 25\}$ and $\{m = 8, n = 50\}$, DSP solves their DEF within 408 seconds (on average). By implementing the dual decomposition in DSP, these instances can be solved in 14 seconds (28 times faster than solving their DEF). For instances in

Table 5.1: Computational results of SQCFL random generated instances

Instance Category	$ \Omega $	First stage			Second stage				T-EF	T-DD
		#Cons	#Vars	#IntVars	#Cons	#Vars	#IntVars	#QVar		
m=8, n=25	50	18	32	24	1650	10400	10000	10000	86.3	34.0
	100	18	32	24	3300	20800	20000	20000	434.6	8.3
	200	18	32	24	6600	41600	40000	40000	1688.6	12.1
	400	18	32	24	13200	83200	80000	80000	TL	22.3
	600	18	32	24	19800	124800	120000	120000	TL	32.4
m=8, n=50	50	18	32	24	2900	20400	20000	20000	256.2	1.8
	100	18	32	24	5800	40800	40000	40000	8.3	9.3
	200	18	32	24	11600	81600	80000	80000	118.3	9.5
	400	18	32	24	23200	163200	160000	160000	263.5	15.0
	600	18	32	24	34800	244800	240000	240000	400.9	38.1
m=16, n=25	50	34	64	48	2050	20800	20000	20000	TL	4.7
	100	34	64	48	4100	41600	40000	40000	TL	10.5
	200	34	64	48	8200	83200	80000	80000	TL	15.8
	400	34	64	48	16400	166400	160000	160000	TL	30.0
	600	34	64	48	24600	249600	240000	240000	TL	52.4
m=16, n=50	50	34	64	48	3300	40800	40000	40000	TL	10.3
	100	34	64	48	6600	81600	80000	80000	TL	15.6
	200	34	64	48	13200	163200	160000	160000	TL	20.9
	400	34	64	48	26400	326400	320000	320000	TL	38.7
	600	34	64	48	39600	489600	480000	480000	TL	43.3

the last two instance categories, i.e., $\{m = 16, n = 25\}$ and $\{m = 16, n = 50\}$, DSP cannot solve their DEF within 2000 seconds time limit. Whereas by implementing DD, all instances are solved within 242.2 seconds (on average). Since the duality gap is huge ($> 70\%$) for all instances, we do not report it in the table. This is possibility because of the outer approximation for the master problem is not tight.

5.6 Conclusion

In this research, we present dual decomposition for solving TSS-MIQCQP, and perform computational experiments for stochastic quadratic capacitated facility location problem using DSP. We observe that by implementing dual decomposition for TSS-MIQCQP, the computational time is reduced by 28 times compared with

solving its deterministic equivalent formulation. However, the duality gap is still huge for all instances. Future research directions could be develop theory and algorithms to close the duality gap.

Chapter 6

Conclusion

In this dissertation, we introduced theoretical results and algorithms for two-stage stochastic mixed integer nonlinear programs, and presented their applications in facility location and power systems. From the theoretical aspect, we developed scenario-based valid inequalities and efficient algorithms for solving two-stage stochastic p -order conic mixed integer programs and two-stage stochastic quadratically constrained quadratic programs, respectively. From the application aspect, we studied two generalizations of stochastic facility location, and propose stochastic models for a power system application, i.e., stochastic load shed recovery.

In the first direction, we introduced two-stage stochastic p -order conic mixed integer programs (TSS-CMIPs) where the second stage problems have sum of l_p -norms in the objective functions along with integer variables. We provided sufficient conditions under which the addition of scenario-based (nonlinear) cuts in the extensive formulation of TSS-CMIPs is sufficient to relax the integrality restrictions on the second stage integer variables without impacting the integrality of the optimal solution of the TSS-CMIP. We introduced structured TSS-CMIPs and cuts for them which satisfy these conditions. We also presented TSS-CMIPs and their distributionally robust generalizations with structured CMIPs in the second stage, and derived scenario-based conic mixed integer rounding cuts for them. We proved

that these cuts provide conic/linear programming equivalent or approximation for the second stage CMIPs with $p = 1$ or $p \geq 2$, respectively. We introduced a multi-module capacitated stochastic facility location problem with subcontracting to demonstrate the applicability of the results for solving this problem. Extensive computational experiments were performed to highlight the efficiency of the scenario-based (nonlinear) cuts.

In the second direction, we proposed stochastic risk-neutral and risk-averse transmission switching models for load shed recovery to handle the uncertainty of renewable generation and demand, as well as incorporated CVaR to measure the risk level of the unrecovered load in the system. In our model, an optimal transmission switching decision was provided to perform after a contingency occurs but before the realization of uncertain renewable generation and demand, to maximize the expected LSR or the risk level measure of unrecovered LS. After the uncertainty is realized, other actions, i.e., adjusting the bus phase-angle, deciding the output of the conventional generators, and transmission lines re-dispatch level, are performed to incorporate the effect of the optimal transmission switching actions. Our computational results showed that our stochastic models reduced the expected load shed as well as avoided the possible scenarios with extremely large load shed. Our method can also serve as an offline contingency analysis tool for a electrical network to maximize the recovery of LS incurred by failures of generators and/or transmission lines effectively.

In the third direction, we proposed a dual decomposition of two-stage stochastic quadratically constrained quadratic programs (TSS-MIQCQPs). We also added new features to current open-source package DSP: we added Gurobi as an exter-

nal solver, added data structure for TSS-MIQCQPs, and implemented extensive formulation and dual decomposition for solving TSS-MIQCQPs. We introduced a stochastic quadratic facility location problem with mixed integer variables in both stages, and performed computational experiments on it. The computational results demonstrated that our proposed algorithm was computationally superior. One possible direction of future research could be minimizing the duality gap in dual decomposition.

Appendices

Appendix A

Appendix for Chapter 3

A.1 Proof of Theorem 3.8

Given $\omega_1 \in \Omega$, let

$$\text{conv}(\overline{\mathcal{K}}_{\omega_1}(x)) = \overline{\mathcal{K}}_{\text{tight}}^{\omega_1}(x) \quad (\text{A.1})$$

for all $x \in X$. Suppose that a point $(\hat{x}, \hat{y}_{\omega_1}, \dots, \hat{y}_{\omega_{|\Omega|}}, \hat{d}_{\omega_1,0}, \dots, \hat{d}_{\omega_{|\Omega|},0}) \in \overline{\mathcal{P}}$, which implies $(\hat{y}_{\omega_1}, \hat{d}_{\omega_1,0}) \in \overline{\mathcal{K}}_{\omega_1}(\hat{x})$ and because of assumption (A.1), $(\hat{y}_{\omega_1}, \hat{d}_{\omega_1,0}) \in \overline{\mathcal{K}}_{\text{tight}}^{\omega_1}(\hat{x})$. Since $(\hat{x}, \hat{y}_{\omega_1}, \dots, \hat{y}_{\omega_{|\Omega|}}, \hat{d}_{\omega_1,0}, \dots, \hat{d}_{\omega_{|\Omega|},0})$ satisfies all defining constraints of $\overline{\mathcal{P}}_{\text{pch},1}$, defined by

$$\begin{aligned} T_{\omega}x + W_{\omega}y_{\omega} &\geq r_{\omega}, & \omega \in \Omega, \\ \|E_{\omega}^j y_{\omega}^j + F_{\omega}^j x - h_{\omega}^j\|_p &\leq d_{\omega,0}^j, & j \in J, \omega \in \Omega, \\ \left\| \overline{E}_{\omega_1,l}^j y_{\omega_1}^j + \overline{F}_{\omega_1,l}^j x - \overline{h}_{\omega_1,l}^j \right\|_p &\leq \overline{d}_{\omega_1,0}^j, & l \in \mathcal{L}, j \in J, \\ x \in X, d \in \mathbb{R}_+^{J \times |\Omega|}, y_{\omega_1}^j &\in \mathbb{R}^q, & j \in J, \\ y_{\omega}^j &\in \mathbb{Z}^{q_1} \times \mathbb{R}^{q-q_1}, & j \in J, \omega \in \Omega \setminus \{\omega_1\}, \end{aligned}$$

the point $(\hat{x}, \hat{y}_{\omega_1}, \dots, \hat{y}_{\omega_{|\Omega|}}, \hat{d}_{\omega_1,0}, \dots, \hat{d}_{\omega_{|\Omega|},0}) \in \overline{\mathcal{P}}_{pch,1}$. Therefore,

$$\overline{\mathcal{P}} \subseteq \overline{\mathcal{P}}_{pch,1} \text{ and } conv(\overline{\mathcal{P}}) \subseteq conv(\overline{\mathcal{P}}_{pch,1}). \quad (\text{A.2})$$

Now suppose that a point $(\hat{x}, \hat{y}_{\omega_1}, \dots, \hat{y}_{\omega_{|\Omega|}}, \hat{d}_{\omega_1,0}, \dots, \hat{d}_{\omega_{|\Omega|},0}) \in \overline{\mathcal{P}}_{pch,1}$. Then point $(\hat{y}_{\omega_1}, \hat{d}_{\omega_1,0}) \in \overline{\mathcal{K}}_{tight}^{\omega_1}(\hat{x})$. Also, because of assumption (A.1), $(\hat{y}_{\omega_1}, \hat{d}_{\omega_1,0}) \in conv(\overline{\mathcal{K}}_{\omega_1}(\hat{x}))$, and hence this point can be written as convex combination of finite number of points, $\bar{\eta}_{\omega_1}^k \in \mathbb{R}^{q+|J|}$ for $k \in \{1, 2, \dots\}$, belonging to $\overline{\mathcal{K}}_{\omega_1}(\hat{x})$, i.e.,

$$(\hat{y}_{\omega_1}, \hat{d}_{\omega_1,0}) = \sum_k \lambda_k \bar{\eta}_{\omega_1}^k$$

where $\sum_k \lambda_k = 1$ and $\lambda_k \geq 0$ for all k . Since $(\hat{y}_{\omega}, \hat{d}_{\omega,0}) \in \overline{\mathcal{K}}_{\omega}(\hat{x})$ for $\omega \in \Omega \setminus \{\omega_1\}$ and $\bar{\eta}_{\omega_1}^k \in \overline{\mathcal{K}}_{\omega_1}(\hat{x})$,

$$(\hat{x}, \bar{\eta}_{\omega_1}^k, \hat{y}_{\omega_2}, \hat{d}_{\omega_2,0}, \dots, \hat{y}_{\omega_{|\Omega|}}, \hat{d}_{\omega_{|\Omega|},0}) \in \overline{\mathcal{P}}$$

for all k as $\overline{\mathcal{K}}_{\omega}(\hat{x}) = \text{Proj}_{x=\hat{x}, y_{\omega}, d_{\omega}}(\overline{\mathcal{P}})$ for all $\omega \in \Omega$. This implies

$$\left(\hat{x}, \sum_k \lambda_k \bar{\eta}_{\omega_1}^k = (\hat{y}_{\omega_1}, \hat{d}_{\omega_1,0}), \hat{y}_{\omega_2}, \hat{d}_{\omega_2,0}, \dots, \hat{y}_{\omega_{|\Omega|}}, \hat{d}_{\omega_{|\Omega|},0} \right) \in conv(\overline{\mathcal{P}}).$$

Hence,

$$\overline{\mathcal{P}}_{pch,1} \subseteq conv(\overline{\mathcal{P}}) \text{ and } conv(\overline{\mathcal{P}}_{pch,1}) \subseteq conv(\overline{\mathcal{P}}). \quad (\text{A.3})$$

From (A.2) and (A.3), we get

$$\bar{\mathcal{P}} \subseteq \bar{\mathcal{P}}_{pch,1} \subseteq \text{conv}(\bar{\mathcal{P}}) = \text{conv}(\bar{\mathcal{P}}_{pch,1})$$

which means $\bar{\mathcal{P}}_{pch,1}$ is a partial convex hull of $\bar{\mathcal{P}}$.

Next, we assume that $\text{conv}(\bar{\mathcal{K}}_{\omega_2}(x)) = \bar{\mathcal{K}}_{tight}^{\omega_2}(x)$ for all $x \in X$. Replacing $\bar{\mathcal{P}}$ by $\bar{\mathcal{P}}_{pch,1}$ and using the similar arguments above, we can prove that $\bar{\mathcal{P}}_{pch,2}$ is a partial convex hull of $\bar{\mathcal{P}}$ where

$$\begin{aligned} \bar{\mathcal{P}}_{pch,2} &:= \{T_\omega x + W_\omega y_\omega \geq r_\omega, & \omega \in \Omega, \\ &\|E_\omega^j y_\omega^j + F_\omega^j x - h_\omega^j\|_p \leq d_{\omega,0}^j, & j \in J, \omega \in \Omega \\ &\|E_{\omega_1,l}^j y_{\omega_1}^j + F_{\omega_1,l}^j x - \bar{h}_{\omega_1,l}^j\|_p \leq d_{\omega_1,0}^j, & l \in \mathcal{L}, j \in J, \\ &\|E_{\omega_2,l}^j y_{\omega_2}^j + F_{\omega_2,l}^j x - \bar{h}_{\omega_2,l}^j\|_p \leq d_{\omega_2,0}^j, & l \in \mathcal{L}, j \in J, \\ &x \in X, y_{\omega_1}^j \in \mathbb{R}^q, y_{\omega_2}^j \in \mathbb{R}^q, y_\omega^j \in \mathbb{Z}^{q_1} \times \mathbb{R}^{q-q_1}, j \in J, \omega \in \Omega \setminus \{\omega_1, \omega_2\}\}. \end{aligned}$$

We repeat the foregoing steps by replacing $\bar{\mathcal{P}}$ by $\bar{\mathcal{P}}_{pch,i}$ for $\omega_i, i = 2, \dots, |\Omega| - 1$. Meanwhile, for each step, we assume that $\text{conv}(\bar{\mathcal{K}}_{\omega_i}^1(x)) = \text{Proj}_y(\bar{\mathcal{K}}_{tight}^{\omega_i})$ for all $x \in X$. Finally, we have $\text{Proj}_{x,y,d}(\bar{\mathcal{P}}_{pch,|\Omega|}) = \text{Proj}_{x,y,d}(\bar{\mathcal{P}}_{pch})$ is a partial convex hull of $\bar{\mathcal{P}}$. This completes the proof.

A.2 Tight Second Stage Formulations for Structured TSS-CMIPs

A.2.1 Proof of Corollary 3.10

For $x \in X$ and $\omega \in \Omega$, by substituting $\sigma = y_{\omega,1} - f_{\omega}x \in \mathbb{Z}$, $\beta = h_{\omega}$, $v = y_{\omega,2} \in \mathbb{R}_+$ and $\rho_0 = d_{\omega,0} \in \mathbb{R}_+$ in the set \bar{Z} , we get $\bar{\mathcal{K}}_{\omega}(x)$. Hence according to Proposition 3.3, the convex hull of the feasible region of $\bar{\mathcal{Q}}_{\omega}(x)$, i.e., $\text{conv}(\bar{\mathcal{K}}_{\omega}(x))$, for all $x \in X$ can be obtained by adding inequality,

$$\sqrt{((1 - 2\mu_{\omega})(y_{\omega,1} + f_{\omega}x - h_{\omega}) + \mu_{\omega})^2 + (y_{\omega,2})^2} \leq d_{\omega,0},$$

to the continuous relaxation of $\bar{\mathcal{K}}_{\omega}(x)$. Furthermore, we reformulate $\text{conv}(\bar{\mathcal{K}}_{\omega}(x))$ in higher dimensional space by adding variables $d_{\omega,1}$ and $d_{\omega,2}$, and obtain

$$\left\{ (y_{\omega,1}, y_{\omega,2}, d_{\omega,1}, d_{\omega,2}, d_{\omega,0}) \in \mathbb{R} \times \mathbb{R}_+^4 : |y_{\omega,1} + f_{\omega}x - h_{\omega}| \leq d_{\omega,1}, \right. \\ \left. |y_{\omega,2}| \leq d_{\omega,2}, \sqrt{d_{\omega,1}^2 + d_{\omega,2}^2} \leq d_{\omega,0}, (1 - 2\mu_{\omega})(y_{\omega,1} - \lfloor h_{\omega} \rfloor + f_{\omega}x) + \mu_{\omega} \leq d_{\omega,1} \right\},$$

which is the convex hull of the feasible region of $\mathcal{Q}_{\omega}(x)$, i.e., $\text{conv}(\mathcal{K}_{\omega}(x))$.

A.3 Partial Convex Hull for Extensive Formulation of Structured TSS-CMIPs

A.3.1 Proof of Corollary 3.13

For $x \in X$ and $\omega \in \Gamma$, let

$$\bar{\mathcal{K}}_{tight}^\omega(x) = \left\{ (y_{\omega,1}, y_{\omega,2}, d_{\omega,0}) \in \mathbb{R} \times \mathbb{R}_+^2 : (3.65) \text{ and } \sqrt{((1 - 2\mu_\omega)(y_{\omega,1} + f_\omega x - h_\omega) + \mu_\omega)^2 + (y_{\omega,2})^2} \leq d_{\omega,0} \right\}.$$

From Corollary 3.10, we know that $\text{conv}(\bar{\mathcal{K}}_\omega(x)) = \bar{\mathcal{K}}_{tight}^\omega(x)$ for all $x \in X$ and $\omega \in \Gamma$. Hence, by utilizing Theorem 3.8, a partial convex hull of $\bar{\mathcal{P}}$ is given by $\bar{\mathcal{P}}_{pch}$.

A.3.2 Proof of Corollary 3.14

For $x \in X$ and $\omega \in \Gamma$, let

$$\bar{\mathcal{K}}_{tight}^\omega(x) = \left\{ (y_\omega, d_{\omega,0}) \in \mathbb{R} \times \mathbb{R}_+^{|\mathcal{J}|} : (3.29), (3.30), \text{ and } \left\| \bar{E}_{\omega,l}^j y_\omega^j + \bar{F}_{\omega,l}^j x - \bar{h}_{\omega,l}^j \right\|_p \leq d_{\omega,0}^j, l \in \mathcal{L}, j \in \mathcal{J} \right\},$$

where the i th row of $\bar{E}_{\omega,l}^j y_\omega^j + \bar{F}_{\omega,l}^j x - \bar{h}_{\omega,l}^j$ is either $y_\omega^j + f_{\omega,i}^j x - h_{\omega,i}^j$ or $(1 - 2\mu_{\omega,i}^j)(y_\omega^j - [h_{\omega,i}^j] + f_{\omega,i}^j x) + \mu_{\omega,i}^j$, and $\mu_{\omega,i}^j = h_{\omega,i}^j - [h_{\omega,i}^j]$. From Theorem 3.11, we know that $\text{conv}(\bar{\mathcal{K}}_\omega(x)) = \bar{\mathcal{K}}_{tight}^\omega(x)$ for all $x \in X$ and $\omega \in \Gamma$ when $p = 1$. Hence, by utilizing Theorem 3.8, it is clear that $\bar{\mathcal{P}}_{pch}$ is a partial convex hull of $\bar{\mathcal{P}}$.

A.3.3 Proof of Corollary 3.15

For $x \in X$ and $\omega \in \Gamma$, let

$$\bar{\mathcal{K}}_{tight}^\omega(x) = \left\{ (y_\omega, d_{\omega,0}) \in \mathbb{R}^q \times \mathbb{R}_+^{|J|} : (3.49) \text{ and } (3.50) \right. \\ \left. \left\| \bar{E}_{\omega,l}^j y_\omega^j + \bar{F}_{\omega,l}^j x - \bar{h}_{\omega,l}^j \right\|_p \leq d_{\omega,0}^j, \quad l \in \mathcal{L}, j \in J \right\},$$

where the i th row of $\bar{E}_{\omega,l}^j y_\omega^j + \bar{F}_{\omega,l}^j x - \bar{h}_{\omega,l}^j$ is either $e_{\omega,i}^j y_\omega^j + f_{\omega,i}^j x - h_{\omega,i}^j$ or $(1 - 2\mu_{\omega,i}^j)(e_{\omega,i}^j y_\omega^j - \lfloor h_{\omega,i}^j \rfloor + f_{\omega,i}^j x) + \mu_{\omega,i}^j$, and $\mu_{\omega,i}^j = h_{\omega,i}^j - \lfloor h_{\omega,i}^j \rfloor$. From Theorem 3.12, we know $\text{conv}(\bar{\mathcal{K}}_\omega(x)) = \bar{\mathcal{K}}_{tight}^\omega(x)$ for all $x \in X$ and $\omega \in \Gamma$ when $p = 1$. Hence, by utilizing Theorem 3.8, we can claim that $\bar{\mathcal{P}}_{pch}$ is a partial convex hull of $\bar{\mathcal{P}}$.

A.4 Deterministic Polyhedral Conic Mixed Integer Sets

Since this paper is focused on stochastic programming, we provide proofs of Theorems 3.11 and 3.12 in the manuscript, and utilize these results to provide the following proofs for Theorems 3.4-3.6 (which are important in their own right).

A.4.1 Proof of Theorem 3.4

In the proof of Theorem 3.11, by substituting W_ω , y_ω , $r_\omega - T_\omega x$, $f_{\omega,i}^j x - h_{\omega,i}^j$, $d_{\omega,1}^j, \dots, d_{\omega,m_2}^j$, for $j = 1, \dots, |J|$, by \mathcal{A} , σ , b , β_{ik} , and $\rho_1^k, \dots, \rho_m^k$, for $k = 1, \dots, K$, respectively, the set $\mathcal{K}_\omega^1(x)$ reduces to R_K^m . Additionally, $\text{conv}(\mathcal{K}_\omega^1(x)) = \text{conv}(R_K^m)$

reduces to the set defined as in Theorem 3.4.

A.4.2 Proof of Theorem 3.5

(a) In the proof of Theorem 3.12, we substitute W_ω , y_ω , $r_\omega - T_\omega x$, E_ω^j , $f_{\omega,i}^j x - h_{\omega,i}^j$, and $d_{\omega,i}^j$, for $i = 1, \dots, m_2$ and $j = 1, \dots, |J|$, by \mathcal{A} , σ , b , \mathcal{G}_k , β_{ik} , and ρ_i^k , for $i = 1, \dots, m$ and $k = 1, \dots, K$, respectively. This reduces the set $\mathcal{K}_\omega^1(x)$ to $S_K^{m,n}$ and $\text{conv}(\mathcal{K}_\omega^1(x)) = \text{conv}(S_K^{m,n})$ reduces to the set obtained by adding

$$\left(1 - 2\beta_{ik}^{(1)}\right) \left(\sum_{t=1}^n g_{kt}^i \sigma_{kt} - \lfloor \beta_{ik} \rfloor\right) + \beta_{ik}^{(1)} \leq \rho_i^k, \quad i = 1, \dots, m, k = 1, \dots, K,$$

to the continuous relaxation of $S_K^{m,n}$.

(b) We prove this result using Corollary 3.15 in which we set $|\Omega| = |\Gamma| = 1$ and $X = \mathbb{Z}^u$, and substitute variables x , y_ω^j , and $d_{\omega,0}^j$ for $j = 1, \dots, |J|$, by η , σ^k , and ρ_0^k for $k = 1, \dots, K$, respectively, and parameters T_ω , W_ω , r_ω , E_ω^j , F_ω^j , and h_ω^j by \mathcal{A}_1 , \mathcal{A}_2 , b , \mathcal{G}^k , \mathcal{C}^k , and β_k , respectively. Then similar to the previous proof, by reformulating $\overline{\mathcal{P}}$ and $\overline{\mathcal{P}}_{pch}$ using additional continuous variables ρ_i^k for $i = 1, \dots, m$, and $k = 1, \dots, K$ (as discussed in Section 3.4), we get $U_K^{m,n,u}$ and $U_{K,pch}^{m,n,u}$, respectively. Since $\overline{\mathcal{P}}_{pch}$ is a partial convex hull of $\overline{\mathcal{P}}$ according to Corollary 3.15, it is clear that $U_{K,pch}^{m,n,u}$ is a partial convex hull of $U_K^{m,n,u}$.

A.4.3 Proof of Theorem 3.6

This result can be easily proved using Corollary 3.14 in which we set $|\Omega| = |\Gamma| = 1$ and $X = \mathbb{Z}^u$, and substitute variables x , y_ω^j , and $d_{\omega,0}^j$ for $j = 1, \dots, |J|$, by η , σ^k ,

and ρ_0^k for $k = 1, \dots, K$, respectively, and parameters T_ω , W_ω , r_ω , F_ω^j , and h_ω^j by \mathcal{A}_1 , \mathcal{A}_2 , b , \mathcal{C}^k , and β_k , respectively. Then, by reformulating $\overline{\mathcal{P}}$ and $\overline{\mathcal{P}}_{pch}$ using additional continuous variables ρ_i^k for $i = 1, \dots, m$, and $k = 1, \dots, K$ (as discussed in Section 3.4), we get $T_K^{m,u}$ and $T_{K,pch}^{m,u}$, respectively. Since $\overline{\mathcal{P}}_{pch}$ is a partial convex hull of $\overline{\mathcal{P}}$ according to Corollary 3.14, it is clear that $T_{K,pch}^{m,u}$ is a partial convex hull of $T_K^{m,u}$.

Bibliography

- [1] Berkeley lab estimates sustained electric power interruptions cost the u.s. approximately \$44 billion annually – a 25% increase since 2006. <https://emp.lbl.gov/news/berkeley-lab-estimates-sustained-electric>.
- [2] Shabbir Ahmed, Mohit Tawarmalani, and Nikolaos V Sahinidis. A finite branch-and-bound algorithm for two-stage stochastic integer programs. *Mathematical Programming*, 100(2):355–377, 2004.
- [3] Shabbir Ahmed, Renan Garcia, Nan Kong, Lewis Ntaimo, Gyana Parija, F. Qiu, and Suvrajeet Sen. Siplib: A stochastic integer programming test problem library. <https://www2.isye.gatech.edu/~sahmed/siplib/>, 2015.
- [4] Farid Alizadeh and Donald Goldfarb. Second-order cone programming. *Mathematical programming*, 95(1):3–51, 2003.
- [5] Baha Alzalg. Decomposition-based interior point methods for stochastic quadratic second-order cone programming. *Applied Mathematics and Computation*, 249:1–18, 2014.
- [6] LD Arya, Atul Koshti, and SC Choube. Distributed generation planning using differential evolution accounting voltage stability consideration. *International journal of electrical power & energy systems*, 42(1):196–207, 2012.

- [7] Alper Atamtürk and Vishnu Narayanan. Conic mixed-integer rounding cuts. *Mathematical Programming*, 122(1):1–20, 2010.
- [8] Alper Atamtürk and Vishnu Narayanan. Lifting for conic mixed-integer programming. *Mathematical programming*, 126(2):351–363, 2011.
- [9] R Bacher and H Glavitsch. Network topology optimization with security constraints. *IEEE Transactions on Power Systems*, 1(4):103–111, 1986.
- [10] L. Bai, F. Li, T. Jiang, and H. Jia. Robust scheduling for wind integrated energy systems considering gas pipeline and power transmission $n-1$ contingencies. *IEEE Transactions on Power Systems*, 32(2):1582–1584, 2017.
- [11] Anastasios G Bakirtzis and AP Sakis Meliopoulos. Incorporation of switching operations in power system corrective control computations. *IEEE Transactions on Power Systems*, 2(3):669–675, 1987.
- [12] Egon Balas. Disjunctive programming: Properties of the convex hull of feasible points. *Discrete Applied Mathematics*, 89(1-3):3–44, 1998.
- [13] Manish Bansal. Facets for single module and multi-module capacitated lot-sizing problems without backlogging. *Discrete Applied Mathematics*, 255:117–141, 2019.
- [14] Manish Bansal and Kiavash Kianfar. n -step cycle inequalities: facets for continuous n -mixing set and strong cuts for multi-module capacitated lot-sizing problem. *Mathematical Programming*, 154:113–144, 2015.
- [15] Manish Bansal and Kiavash Kianfar. Facets for continuous multi-mixing set

- with general coefficients and bounded integer variables. *Discrete Optimization*, 26:1–25, 2017.
- [16] Manish Bansal and Kiavash Kianfar. n -step cycle inequalities: facets for continuous n -mixing set and strong cuts for multi-module capacitated lot-sizing problem. In Jon Lee and Jens Vygen, editors, *Integer Programming and Combinatorial Optimization*, Lecture Notes in Computer Science, 8494:102–113, June 2014.
- [17] Manish Bansal and Sanjay Mehrotra. On solving two-stage distributionally robust disjunctive programs with a general ambiguity set. *European Journal of Operational Research*, 2019.
- [18] Manish Bansal and Yingqiu Zhang. Scenario-based cuts for structured two-stage stochastic and distributionally robust p -order conic mixed integer programs. *Journal of Global Optimization*, January 2021. ISSN 1573-2916. doi: 10.1007/s10898-020-00986-w. URL <https://doi.org/10.1007/s10898-020-00986-w>.
- [19] Manish Bansal, Kuo-Ling Huang, and Sanjay Mehrotra. Tight second stage formulations in two-stage stochastic mixed integer programs. *SIAM Journal on Optimization*, 28(1):788–819, 2018.
- [20] Manish Bansal, Kuo-Ling Huang, and Sanjay Mehrotra. Decomposition algorithms for two-stage distributionally robust mixed binary programs. *SIAM Journal on Optimization*, 28(3):2360–2383, 2018.
- [21] J E Beasley. Or-library: Capacitated warehouse location. <http://people.brunel.ac.uk/~mastjjb/jeb/orlib/capinfo.html>, 1988.

- [22] Aharon Ben-Tal, Dick den Hertog, Anja De Waegenaere, Bertrand Melenberg, and Gijs Rennen. Robust Solutions of Optimization Problems Affected by Uncertain Probabilities. *Management Science*, 59(2):341–357, November 2012.
- [23] Nadia Benali and Kais Saidi. A robust analysis of the relationship between natural disasters, electricity and economic growth in 41 countries. *Journal of Economic Development*, 42(3):89–109, 2017.
- [24] J. F. Benders. Partitioning procedures for solving mixed-variables programming problems. *Numerische Mathematik*, 4(1):238–252, December 1962.
- [25] Dimitris Bertsimas and Ioana Popescu. Optimal inequalities in probability theory: A convex optimization approach. *SIAM Journal on Optimization*, 15(3):780–804, 2005.
- [26] Dimitris Bertsimas, Xuan Vinh Doan, Karthik Natarajan, and Chung-Piaw Teo. Models for minimax stochastic linear optimization problems with risk aversion. *Mathematics of Operations Research*, 35(3):580–602, 2010.
- [27] John R Birge and Francois Louveaux. *Introduction to stochastic programming*. Springer Science & Business Media, 2011.
- [28] Merve Bodur and James R Luedtke. Mixed-integer rounding enhanced benders decomposition for multiclass service-system staffing and scheduling with arrival rate uncertainty. *Management Science*, 63(7):2073–2091, 2016.
- [29] Merve Bodur, Sanjeeb Dash, Oktay Günlük , and James Luedtke. Strength-

- ened benders cuts for stochastic integer programs with continuous recourse. *INFORMS Journal on Computing*, 29(1):77–91, 2016.
- [30] Michèle Breton and Saeb El Hachem. Algorithms for the solution of stochastic dynamic minimax problems. *Computational Optimization and Applications*, 4(4):317–345, October 1995. ISSN 1573-2894.
- [31] Michèle Breton and Saeb El Hachem. A scenario aggregation algorithm for the solution of stochastic dynamic minimax problems. *Stochastics and Stochastic Reports*, 53(3-4):305–322, May 1995. ISSN 1045-1129.
- [32] Michael Bussieck. *Optimal Lines in Public Rail Transport*. PhD thesis, Dec 1998. URL https://publikationsserver.tu-braunschweig.de/receive/dbbs_mods_00001030.
- [33] Giuseppe C Calafiore. Ambiguous risk measures and optimal robust portfolios. *SIAM Journal on Optimization*, 18(3):853–877, 2007.
- [34] Richard J Campbell. Weather-related power outages and electric system resiliency. Technical report, Congr. Res. Serv., Washington, DC, USA, Aug. 2012.
- [35] Claus C Carøe and Rüdiger Schultz. Dual decomposition in stochastic integer programming. *Operations Research Letters*, 24(1-2):37–45, 1999.
- [36] Claus C Carøe and Jørgen Tind. A cutting-plane approach to mixed 0–1 stochastic integer programs. *European Journal of Operational Research*, 101(2):306–316, 1997.

- [37] R. L. Chen, A. Cohn, N. Fan, and A. Pinar. Contingency-risk informed power system design. *IEEE Transactions on Power Systems*, 29(5):2087–2096, 2014.
- [38] MT Claessens, Nico M van Dijk, and Peter J Zwaneveld. Cost optimal allocation of rail passenger lines. *European Journal of Operational Research*, 110(3):474–489, 1998.
- [39] Michele Conforti, Gérard Cornuéjols, Giacomo Zambelli, et al. *Integer programming*, volume 271. Springer.
- [40] William Cook, Ravindran Kannan, and Alexander Schrijver. Chvátal closures for mixed integer programming problems. *Mathematical Programming*, 47(1-3):155–174, 1990.
- [41] IBM ILOG Cplex. V12. 1: User’s manual for cplex. *International Business Machines Corporation*, 46(53):157, 2009.
- [42] XT Cui, XJ Zheng, SS Zhu, and XL Sun. Convex relaxations and miqcqp reformulations for a class of cardinality-constrained portfolio selection problems. *Journal of Global Optimization*, 56(4):1409–1423, 2013.
- [43] George B Dantzig. Linear programming under uncertainty. *Management Science*, pages 197–206, 1955.
- [44] Payman Dehghanian and Mladen Kezunovic. Probabilistic decision making for the bulk power system optimal topology control. *IEEE Transactions on Smart Grid*, 7(4):2071–2081, 2016.

- [45] Payman Dehghanian, Yaping Wang, Gurunath Gurralla, Erick Moreno-Centeno, and Mladen Kezunovic. Flexible implementation of power system corrective topology control. *Electric Power Systems Research*, 128:79–89, 2015.
- [46] Erick Delage and Yinyu Ye. Distributionally robust optimization under moment uncertainty with application to data-driven problems. *Operations Research*, 58:595–612, 2010.
- [47] Tao Ding, Rui Bo, Fangxing Li, and Hongbin Sun. A bi-level branch and bound method for economic dispatch with disjoint prohibited zones considering network losses. *IEEE Transactions on Power Systems*, 30(6):2841–2855, 2014.
- [48] Meysam Doostizadeh, Farrokh Aminifar, Hassan Ghasemi, and Hamid Lesani. Energy and reserve scheduling under wind power uncertainty: An adjustable interval approach. *IEEE Transactions on Smart Grid*, 7(6):2943–2952, 2016.
- [49] Jitka Dupačová. The minimax approach to stochastic programming and an illustrative application. *Stochastics: An International Journal of Probability and Stochastic Processes*, 20(1):73–88, 1987.
- [50] Erik Ela, Michael Milligan, and Brendan Kirby. Operating reserves and variable generation. Technical report, National Renewable Energy Lab.(NREL), Golden, CO (United States), 2011.
- [51] Adolfo R Escobedo, Erick Moreno-Centeno, and Kory W Hedman. Topology

- control for load shed recovery. *IEEE Transactions on Power Systems*, 29(2): 908–916, 2014.
- [52] *Disturbance Control Standard-Contingency Reserve for Recovery From a Balancing Contingency Event Reliability Standard*. Federal Energy Regulatory Commission, Feb 2017.
- [53] Matteo Fischetti, Ivana Ljubić, and Markus Sinnl. Redesigning benders decomposition for large-scale facility location. *Management Science*, 63(7): 2146–2162, 2017.
- [54] Emily B Fisher, Richard P O’Neill, and Michael C Ferris. Optimal transmission switching. *IEEE Transactions on Power Systems*, 23(3):1346–1355, 2008.
- [55] Dinakar Gade, Simge Kücükayavuz, and Suvrajeet Sen. Decomposition algorithms with parametric gomory cuts for two-stage stochastic integer programs. *Mathematical Programming*, pages 1–26, 2012.
- [56] Xinbo Geng and Le Xie. Data-driven decision making in power systems with probabilistic guarantees: Theory and applications of chance-constrained optimization. *Annual Reviews in Control*, 47:341–363, 2019.
- [57] Arthur M Geoffrion. Generalized benders decomposition. *Journal of optimization theory and applications*, 10(4):237–260, 1972.
- [58] Pflug Georg, Pichlera Alois, and Wozabalb David. The $1/n$ investment strategy is optimal under high model ambiguity. *Journal of Banking and Finance*, 36(2):410–417, 2012.

- [59] Pavlos S Georgilakis and Nikos D Hatziargyriou. Optimal distributed generation placement in power distribution networks: models, methods, and future research. *IEEE Transactions on power systems*, 28(3):3420–3428, 2013.
- [60] M Gomez-Gonzalez, A López, and F Jurado. Optimization of distributed generation systems using a new discrete pso and opf. *Electric power systems research*, 84(1):174–180, 2012.
- [61] Gianpietro Granelli, Mario Montagna, Fabio Zanellini, Paola Bresesti, Riccardo Vailati, and Mario Innorta. Optimal network reconfiguration for congestion management by deterministic and genetic algorithms. *Electric power systems research*, 76(6-7):549–556, 2006.
- [62] Oktay Günlük and Jeff Linderoth. Perspective reformulations of mixed integer nonlinear programs with indicator variables. *Mathematical Programming*, 124(1):183–205, Jul 2010. ISSN 1436-4646.
- [63] Oktay Günlük and Jeff Linderoth. Perspective reformulations of mixed integer nonlinear programs with indicator variables. *Mathematical programming*, 124(1):183–205, 2010.
- [64] Oktay Günlük and Jeff Linderoth. Perspective reformulation and applications. In *Mixed Integer Nonlinear Programming*, pages 61–89. Springer, 2012.
- [65] Oktay Günlük and Yves Pochet. Mixing mixed-integer inequalities. *Mathematical Programming*, 90(3):429–457, 2001. ISSN 0025-5610.

- [66] Oktay Günlük, Jon Lee, and Robert Weismantel. Minlp strengthening for separable convex quadratic transportation-cost ufl. 2007.
- [67] LLC Gurobi Optimization. Gurobi optimizer reference manual, 2020. URL <http://www.gurobi.com>.
- [68] M.T. Hajiaghayi, M. Mahdian, and V.S. Mirrokni. The facility location problem with general cost functions. *Networks*, 42:2003, 2002.
- [69] K. W. Hedman, S. S. Oren, and R. P. O’Neill. A review of transmission switching and network topology optimization. In *2011 IEEE Power and Energy Society General Meeting*, pages 1–7, July 2011. doi: 10.1109/PES.2011.6039857.
- [70] Kory W Hedman, Richard P O’Neill, Emily Bartholomew Fisher, and Shmuel S Oren. Optimal transmission switching with contingency analysis. *IEEE Transactions on Power Systems*, 24(3):1577–1586, 2009.
- [71] Duong Quoc Hung and Nadarajah Mithulananthan. Multiple distributed generator placement in primary distribution networks for loss reduction. *IEEE Transactions on industrial electronics*, 60(4):1700–1708, 2011.
- [72] Mohammad Sadegh Javadi, Mohsen Saniei, Habib Rajabi Mashhadi, and Guillermo Gutiérrez-Alcaraz. Multi-objective expansion planning approach: distant wind farms and limited energy resources integration. *IET Renewable Power Generation*, 7(6):652–668, 2013.
- [73] MS Javadi, M Saniei, and Habib Rajabi Mashhadi. An augmented nsga-ii technique with virtual database to solve the composite generation and trans-

- mission expansion planning problem. *Journal of Experimental & Theoretical Artificial Intelligence*, 26(2):211–234, 2014.
- [74] Ruiwei Jiang and Yongpei Guan. Risk-averse two-stage stochastic program with distributional ambiguity. *Operations Research*, 66(5):1390–1405, 2018.
- [75] James E Kelley, Jr. The cutting-plane method for solving convex programs. *Journal of the society for Industrial and Applied Mathematics*, 8(4):703–712, 1960.
- [76] Amin Khodaei, Mohammad Shahidehpour, and Saeed Kamalinia. Transmission switching in expansion planning. *IEEE Transactions on Power Systems*, 25(3):1722–1733, 2010.
- [77] Kiavash Kianfar and Yahya Fathi. Generalized mixed integer rounding inequalities: facets for infinite group polyhedra. *Mathematical Programming*, 120(2):313–346, 2009. ISSN 0025-5610.
- [78] Mustafa R Kılınç, Jeff Linderoth, and James Luedtke. Lift-and-project cuts for convex mixed integer nonlinear programs. *Mathematical Programming Computation*, 9(4):499–526, 2017.
- [79] Fatma Kılınç-Karzan. On minimal valid inequalities for mixed integer conic programs. *Mathematics of Operations Research*, 41(2):477–510, 2016.
- [80] Kibaek Kim and Victor M Zavala. Algorithmic innovations and software for the dual decomposition method applied to stochastic mixed-integer programs. *Mathematical Programming Computation*, 10(2):225–266, 2018.

- [81] Kibeak Kim and Sanjay Mehrotra. A two-stage stochastic integer programming approach to integrated staffing and scheduling with application to nurse management. *Operations Research*, 63(6):1431–1451, 2015.
- [82] Nan Kong, Andrew J Schaefer, and Brady Hunsaker. Two-stage integer programs with stochastic right-hand sides: a superadditive dual approach. *Mathematical Programming*, 108(2-3):275–296, 2006.
- [83] Simge Küçükyavuz and Suvrajeet Sen. *An Introduction to Two-Stage Stochastic Mixed-Integer Programming*, chapter 1, pages 1–27. 2017.
- [84] Gilbert Laporte and François V. Louveaux. The integer L-shaped method for stochastic integer programs with complete recourse. *Operations Research Letters*, 13(3):133–142, April 1993.
- [85] Can Li and Ignacio E Grossmann. An improved l-shaped method for two-stage convex 0-1 mixed integer nonlinear stochastic programs. *Computers & Chemical Engineering*, 112:165–179, 2018.
- [86] Can Li and Ignacio E Grossmann. A finite ϵ -convergence algorithm for two-stage stochastic convex nonlinear programs with mixed-binary first and second-stage variables. *Journal of Global Optimization*, 75(4):921–947, 2019.
- [87] Can Li, David E Bernal, Kevin C Furman, and Ignacio E Grossmann. Sample average approximation for stochastic nonconvex mixed integer nonlinear programming via outer approximation. 2019.
- [88] Qifeng Li. A tight sdp relaxation for miqcqp problems in power systems based on disjunctive programming. *arXiv preprint arXiv:1509.05141*, 2015.

- [89] Xiang Li, Asgeir Tomasgard, and Paul I Barton. Nonconvex generalized benders decomposition for stochastic separable mixed-integer nonlinear programs. *Journal of optimization theory and applications*, 151(3):425, 2011.
- [90] Xingpeng Li and Kory W Hedman. Enhanced energy management system with corrective transmission switching strategy—part i: Methodology. *IEEE Transactions on Power Systems*, 34(6):4490–4502, 2019.
- [91] Xingpeng Li and Kory W Hedman. Enhanced energy management system with corrective transmission switching strategy—part ii: Results and discussion. *IEEE Transactions on Power Systems*, 34(6):4503–4513, 2019.
- [92] Cong Liu, Jianhui Wang, and James Ostrowski. Static switching security in multi-period transmission switching. *IEEE Transactions on Power Systems*, 27(4):1850–1858, 2012.
- [93] Junyi Liu and Suvrajeet Sen. Asymptotic results of stochastic decomposition for two-stage stochastic quadratic programming. *SIAM Journal on Optimization*, 30(1):823–852, 2020.
- [94] Miguel Sousa Lobo, Lieven Vandenbergh, Stephen Boyd, and Hervé Lebret. Applications of second-order cone programming. *Linear Algebra and its Applications*, 284(1–3):193–228, November 1998.
- [95] Juan Alvarez López, Kumaraswamy Ponnambalam, and Víctor H Quintana. Generation and transmission expansion under risk using stochastic programming. *IEEE Transactions on Power Systems*, 22(3):1369–1378, 2007.
- [96] Robin Lougee-Heimer. The common optimization interface for operations

- research: Promoting open-source software in the operations research community. *IBM Journal of Research and Development*, 47(1):57–66, 2003.
- [97] David K. Love and Guzin Bayraksan. Phi-divergence constrained ambiguous stochastic programs for data-driven optimization. Technical report, Department of Integrated Systems Engineering, The Ohio State University, Columbus, Ohio, 2015. Available at http://www.optimization-online.org/DB_HTML/2016/03/5350.html.
- [98] Miles Lubin, Kipp Martin, Cosmin G Petra, and Burhaneddin Sandıkçı. On parallelizing dual decomposition in stochastic integer programming. *Operations Research Letters*, 41(3):252–258, 2013.
- [99] Guglielmo Lulli and Suvrajeet Sen. A branch-and-price algorithm for multi-stage stochastic integer programming with application to stochastic batch-sizing problems. *Management Science*, 50(6):786–796, 2004.
- [100] Fengqiao Luo and Sanjay Mehrotra. A decomposition method for distributionally-robust two-stage stochastic mixed-integer cone programs, 2019. available at <https://arxiv.org/abs/1911.08713>.
- [101] Abdulhalem A Mazi, Bruce F Wollenberg, and Morten H Hesse. Corrective control of power system flows by line and bus-bar switching. *IEEE Transactions on Power Systems*, 1(3):258–264, 1986.
- [102] Sanjay Mehrotra and M Gokhan Ozevin. Decomposition based interior point methods for two-stage stochastic convex quadratic programs with recourse. *Operations Research*, 57(4):964–974, 2009.

- [103] Sanjay Mehrotra and He Zhang. Models and algorithms for distributionally robust least squares problems. *Mathematical Programming*, 148(1–2):123–141, 2014.
- [104] Eugenio Mijangos. An algorithm for two-stage stochastic mixed-integer nonlinear convex problems. *Annals of Operations Research*, 235(1):581–598, 2015.
- [105] Andrew J. Miller and Laurence A. Wolsey. Tight formulations for some simple mixed integer programs and convex objective integer programs. *Mathematical Programming*, 98(1-3):73–88, September 2003.
- [106] Ruth Misener and Christodoulos A Floudas. Global optimization of mixed-integer quadratically-constrained quadratic programs (miqcqp) through piecewise-linear and edge-concave relaxations. *Mathematical Programming*, 136(1):155–182, 2012.
- [107] Sina Modaresi and Juan Pablo Vielma. Convex hull of two quadratic or a conic quadratic and a quadratic inequality. *Mathematical Programming*, 164(1-2):383–409, 2017.
- [108] Sina Modaresi, Mustafa R. Kilinc, and Juan Pablo Vielma. Split cuts and extended formulations for mixed integer conic quadratic programming. *Operations Research Letters*, 43(1):10 – 15, 2015.
- [109] James A Momoh, Rambabu Adapa, and ME El-Hawary. A review of selected optimal power flow literature to 1993. i. nonlinear and quadratic programming approaches. *IEEE transactions on power systems*, 14(1):96–104, 1999.

- [110] Tillmann Mühlpfordt, Timm Faulwasser, and Veit Hagenmeyer. A generalized framework for chance-constrained optimal power flow. *Sustainable Energy, Grids and Networks*, 16:231–242, 2018.
- [111] *A Systems View of the Modern Grid*. National Energy Technology Laboratory, 2007.
- [112] George L. Nemhauser and Laurence A. Wolsey. *Integer and Combinatorial Optimization*. Wiley-Interscience, New York, NY, USA, 1988.
- [113] George L. Nemhauser and Laurence A. Wolsey. A recursive procedure to generate all cuts for 0-1 mixed integer programs. *Mathematical Programming*, 46(1-3):379–390, 1990.
- [114] Nilay Noyan. Risk-averse two-stage stochastic programming with an application to disaster management. *Computers & Operations Research*, 39(3): 541–559, 2012.
- [115] Lewis Ntaimo. Disjunctive decomposition for two-stage stochastic mixed-binary programs with random recourse. *Operations Research*, 58(1):229–243, July 2009.
- [116] Richard P O’Neill, Ross Baldick, Udi Helman, Michael H Rothkopf, and William Stewart. Dispatchable transmission in rto markets. *IEEE Transactions on Power Systems*, 20(1):171–179, 2005.
- [117] Osman Y. Ozaltin, Oleg A. Prokopyev, and Andrew J. Schaefer. Two-stage quadratic integer programs with stochastic right-hand sides. 133(1):121–158, 2012.

- [118] Osman Y Özaltın, Oleg A Prokopyev, and Andrew J Schaefer. Two-stage quadratic integer programs with stochastic right-hand sides. *Mathematical programming*, 133(1-2):121–158, 2012.
- [119] Georg Pflug and David Wozabal. Ambiguity in portfolio selection. *Quantitative Finance*, 7(4):435–442, 2007.
- [120] Viet Pham, Carl Laird, and Mahmoud El-Halwagi. Convex hull discretization approach to the global optimization of pooling problems. *Industrial & Engineering Chemistry Research*, 48(4):1973–1979, 2009.
- [121] Dzung Phan and Soumyadip Ghosh. Two-stage stochastic optimization for optimal power flow under renewable generation uncertainty. *ACM Transactions on Modeling and Computer Simulation (TOMACS)*, 24(1):2, 2014.
- [122] PJM. *Manual 3: transmission Operations Section 5: Index and Operating Procedures for PJM RTO Operation, 54th edition*, Dec. 10. 2018.
- [123] András Prékopa. *Stochastic programming*, volume 324. Springer Science & Business Media, 2013.
- [124] Abbas Rabiee, Seyed Masoud Mohseni-Bonab, Tahereh Soltani, and Leila Bayat. A risk-based two-stage stochastic optimal power flow considering the impact of multiple operational uncertainties. *Journal of Energy Management and Technology*, 1(1):30–42, 2017.
- [125] Morten Riis and Kim Allan Andersen. Applying the minimax criterion in stochastic recourse programs. *European Journal of Operational Research*, 165(3):569–584, September 2005.

- [126] R. Tyrrell Rockafellar and Stanislav Uryasev. Optimization of conditional value-at-risk. *Journal of Risk*, 2:21–41, 2000.
- [127] J. G. Rolim and L. J. B. Machado. A study of the use of corrective switching in transmission systems. *IEEE Transactions on Power Systems*, 14(1):336–341, Feb 1999. ISSN 0885-8950. doi: 10.1109/59.744552.
- [128] Sujeevraja Sanjeevi, Sina Masihabadi, and Kiavash Kianfar. Using cuts for mixed integer knapsack sets to generate cuts for mixed integer polyhedral conic sets. *Mathematical Programming*, 159(1):571–583, 2016.
- [129] Herbert E Scarf. A min-max solution of an inventory problem. In *Studies in the Mathematical Theory of Inventory and Production*, chapter 12, pages 201–209. 1958.
- [130] Rüdiger Schultz, Leen Stougie, and Maarten H Van Der Vlerk. Solving stochastic programs with integer recourse by enumeration: A framework using gröbner basis. *Mathematical Programming*, 83(1-3):229–252, 1998.
- [131] Kathryn M Schumacher, Richard Li-Yang Chen, and Amy EM Cohn. Transmission expansion with smart switching under demand uncertainty and line failures. *Energy Systems*, 8(3):549–580, 2017.
- [132] Suvrajeet Sen and Julia L Hige. The C^3 theorem and a D^2 algorithm for large scale stochastic mixed-integer programming: set convexification. *Mathematical Programming*, 104(1):1–20, 2005.
- [133] Suvrajeet Sen and Hanif D Sherali. Decomposition with branch-and-cut ap-

- proaches for two-stage stochastic mixed-integer programming. *Mathematical Programming*, 106(2):203–223, 2006.
- [134] Wei Shao and Vijay Vittal. Corrective switching algorithm for relieving overloads and voltage violations. *IEEE Transactions on Power Systems*, 20(4):1877–1885, 2005.
- [135] Hanif D Sherali and Barbara MP Fraticelli. A modification of benders’ decomposition algorithm for discrete subproblems: An approach for stochastic programs with integer recourse. *Journal of Global Optimization*, 22(1-4):319–342, 2002.
- [136] Hanif D Sherali and Xiaomei Zhu. On solving discrete two-stage stochastic programs having mixed-integer first-and second-stage variables. *Mathematical Programming*, 108(2-3):597–616, 2006.
- [137] Pavee Siriruk. *Cournot Competition under Uncertainty in Power Markets*. PhD thesis, Dept. ISE, Auburn Univ, 2009.
- [138] Lawrence V Snyder. Facility location under uncertainty: a review. *IIE transactions*, 38(7):547–564, 2006.
- [139] Alireza Soroudi and Turaj Amraee. Decision making under uncertainty in energy systems: State of the art. *Renewable and Sustainable Energy Reviews*, 28:376–384, 2013.
- [140] Tyler Summers, Joseph Warrington, Manfred Morari, and John Lygeros. Stochastic optimal power flow based on conditional value at risk and dis-

- tributional robustness. *International Journal of Electrical Power & Energy Systems*, 72:116–125, 2015.
- [141] Tyler Summers, Joseph Warrington, Manfred Morari, and John Lygeros. Stochastic optimal power flow based on conditional value at risk and distributional robustness. *International Journal of Electrical Power & Energy Systems*, 72:116–125, 2015.
- [142] Alexander Vinel and Pavlo Krokhmal. On valid inequalities for mixed integer p-order cone programming. *Journal of Optimization Theory and Applications*, 160(2):439–456, 2014.
- [143] Mathieu Van Vyve. The continuous mixing polyhedron. *Mathematics of Operations Research*, 30(2):441–452, May 2005. ISSN 0364-765X.
- [144] Zizhuo Wang, Peter W. Glynn, and Yinyu Ye. Likelihood robust optimization for data-driven problems. *Computational Management Science*, 13(2):241–261, April 2016.
- [145] Adrian Werner, Kristin Tolstad Uggen, Marte Fodstad, Arnt-Gunnar Lium, and Ruud Egging. Stochastic mixed-integer programming for integrated portfolio planning in the lng supply chain. *The Energy Journal*, 35(1), 2014.
- [146] John A. White. A quadratic facility location problem. *A I I E Transactions*, 3(2):156–157, 1971. doi: 10.1080/05695557108974799. URL <https://doi.org/10.1080/05695557108974799>.
- [147] L. A Wolsey. *Integer Programming*. Wiley, New York, USA, 1998.

- [148] David. Wozabal. A framework for optimization under ambiguity. *Annals of Operations Research*, 193(1):21–47, 2012.
- [149] Ihsan Yanikoğlu and Dick den Hertog. Safe Approximations of Ambiguous Chance Constraints Using Historical Data. *INFORMS Journal on Computing*, 25(4):666–681, November 2012.
- [150] Hui Zhang and Pu Li. Chance constrained programming for optimal power flow under uncertainty. *IEEE Transactions on Power Systems*, 26(4):2417–2424, 2011.
- [151] Chaoyue Zhao and Yongpei Guan. Data-driven risk-averse two-stage stochastic program with ζ -structure probability metrics, 2015. Available at http://www.optimization-online.org/DB_HTML/2015/07/5014.html.
- [152] Mehmet Tolga Çezik and Garud Iyengar. Cuts for mixed 0-1 conic programming. *Mathematical Programming*, 104(1):179–202, 2005.